Univerzita Karlova v Praze
1. lékařská fakulta

Studijní obor: Biochemie a patobiochemie

Ing. Renata Koníčková

Antiproliferační účinky produktů katabolické dráhy hemu

Antiproliferative effects of heme catabolic pathway´s products

Disertační práce

Vedoucí závěrečné práce/školitel:
Prof. MUDr. Libor Vítek, Ph.D, MBA

Praha, 2014

Prohlášení:

Prohlašuji, že jsem závěrečnou práci zpracovala samostatně a že jsem řádně uvedla a citovala všechny použité prameny a literaturu. Současně prohlašuji, že práce nebyla využita k získání jiného nebo stejného titulu.

Souhlasím s trvalým uložením elektronické verze mé práce v databázi systému meziuniverzitního projektu Theses.cz za účelem soustavné kontroly podobnosti kvalifikačních prací.

V Praze, 16.09.2014

Renata Koníčková

Podpis

Identifikační záznam:

KONÍČKOVÁ, Renata. *Antiproliferační účinky produktů katabolické dráhy hemu. [Antiproliferative effects of heme catabolic pathway´s products].* Praha, 2014. 96 s. Disertační práce. Univerzita Karlova v Praze, 1. lékařská fakulta, Ústav lékařské biochemie a laboratorní diagnostiky. Vítek, Libor.

Abstrakt

Předkládaná práce se zabývá metabolismem hemu s hlavním zaměřením na žlučové pigmenty. Data z posledních let ukazují, že bilirubin není jen pouhým odpadním produktem katabolické dráhy hemu, ale že vykazuje řadu významných biologických vlastností, včetně účinků antiproliferačních. Metabolismus bilirubinu však není doposud zcela poznán, což brání posoudit i jeho potenciální působení protinádorové. Cílem předkládané disertační práce bylo tedy osvětlit některé metabolické aspekty katabolické dráhy hemu, se zřetelem na antiproliferační vlastnosti jejích produktů.

Vzhledem k faktu, že bilirubin významně ovlivňuje kancerogenezi tlustého střeva, zabývali jsme se nejprve dosud ne příliš známými aspekty metabolismu bilirubinu střevními bakteriemi. Dále jsme studovali neurotoxické účinky bilirubinu na zvířecím modelu hyperbilirubinemických Gunnových potkanů - distribuci v mozku a odbourávání za patologických podmínek, jako jsou např. novorozenecká žloutenka či Criglerův-Najjarův syndrom. Zabývali jsme se možným zlepšením dosavadní léčby závažných nekonjugovaných hyperbilirubinemií a to zvýšením účinků fototerapie podáváním sérového albuminu. Hlavním důvodem těchto studií byla skutečnost, že mechanismy neurotoxických účinků bilirubinu jsou povětšinou shodné s mechanismy, kterými se bilirubin uplatňuje v inhibici nádorového růstu. Zkoumali jsme dále protinádorové účinky dalšího významného produktu katabolické dráhy hemu - oxidu uhelnatého. Tetrapyrolová struktura žlučových pigmentů patří v přírodě k evolučně zachovalým strukturním motivům. Právě tento fakt nás přivedl ke studiu kyanobakteriálních a rostlinných tetrapyrolových sloučenin, u kterých jsme antioxidační a protinádorové účinky také prokázali.

Klíčová slova: Žlučové pigmenty, bilirubin, fykobiliny, chlorofyl, tetrapyroly, metabolismus hemu, hyperbilirubinemie.

Abstract

Presented work is focused on heme metabolism with the main interest in bile pigments. Recent data indicate that bilirubin is not only a waste product of the heme catabolic pathway, but also emphasize its important biological impacts, including possible antiproliferative effects. Until today metabolism of bilirubin has not been completely elucidated, which has prevented detailed evaluation of its potential anticancer action. The aim of this study was to clarify some aspects of heme catabolism with respect for antiproliferative properties of its products.

Based on the fact that bilirubin potently affects carcinogenesis of the intestine, we initially investigated not properly known bilirubin metabolism by intestinal bacteria. We studied bilirubin neurotoxic effects in hyperbilirubinemic Gunn rats - its distribution in the brain tissue and its degradation during pathological conditions, such as severe newborn jaundice or Crigler-Najjar syndrome. Possible approaches to improve the treatment of severe unconjugated hyperbilirubinemias, combination of the phototherapy and human albumin administration were also investigated. The main reason of these studies was the fact that mechanisms of neurotoxic effects of bilirubin are predominantly identical with those, by which bilirubin inhibits cancer cells growth. We were also concerned with anticancer impact of other important heme catabolic pathway´s product, which is carbon monoxide. The evolutionary conserved tetrapyrrolic structure of human bile pigments led us to study biological effects of cyanobacterial and plant tetrapyrroles as well, for which important antioxidant and anticancer activities were proved.

Keywords: Bile pigments, bilirubin, phycobilins, chlorophyll, tetrapyrroles, heme metabolism, hyperbilirubinemias.

Acknowledgements

I would like to thank my supervisor Prof. MUDr. Libor Vítek, Ph.D, MBA, that enabled me the work on this project and was very supportive especially in successful ending of my work. Many thanks belong to our coworkers Doc. RNDr. Ladislav Lešetický, CSc and RNDr. Martin Štícha and to my lab collegues or rather friends, to Mgr. Alena Jirásková Ph.D., Ing. Iva Subhanová Ph.D., MUDr. Martin Leníček Ph.D., Ing. Jaroslav Zelenka Ph.D., MUDr. Lucie Muchová Ph.D., Mgr. Aleš Dvořák, Ing. Miro Hindoš and Mgr. Jana Vaníková for their support, help, sharing experience and valuable feedback.

Very significant acknowledgement belongs to my boyfriend and family, that were very helpful and always supportive, without their help and patience I would not be able to finish my PhD study.

This work was supported by grants GAUK 52210 and SVV 260032-2014 given by the Charles University in Prague.

Content

1 Literature review

1.1 Heme catabolic pathway - from heme to urobilinoids

Heme degradation is an important pathway implemented in iron homeostasis since almost all iron is incorporated into heme-containing proteins. The major products of the heme catabolic pathway in the intravascular compartment are biologically active molecules including iron, carbon monoxide (CO), biliverdin (BV) and unconjugated bilirubin (UCB). In the healthy adult, the daily production is approximately 4 mg of UCB/kg body weight (Berk, Howe et al. 1969). The main source of heme in the human body is hemoglobin from the senescent or damaged red blood cells. Other heme sources include myoglobin, as well as heme-containing enzymes.

1.1.1 Heme and its cleavage by heme oxygenase

Heme is a cyclic tetrapyrrolic compound known also as protoporphyrin IX that binds iron in its center (Fig.1). The number IX follows the classical nomenclature and describes the order of substituents (methyl, vinyl, propionyl) on the tetrapyrrole ring. Protoporhyrin IX belongs to the very common porphyrins in Nature. Molecule of heme is capable of free radicals generating in reactions primarily related to the central iron atom (Fig.2); on the other hand protective impact of heme is connected to its degradation by heme oxygenase (HMOX, EC 1.14.99.3) (see below). Heme is an essential molecule for life under aerobic condition. Organisms on our planet have developed the way how to use big benefits of heme, how to survive in oxygen atmosphere and of course how to protect themselves before damaging power of heme. This is governed by tight control of the heme cellular levels with fine balance between its biosynthesis and degradation. Heme as a prosthetic group is a part of many proteins, hemoproteins, which have various vital functions based mainly on electron transfer or gaseous molecule storage and transport. These proteins include hemoglobin, myoglobin, cytochromes, catalase, guanylate cyclase, nitric oxide synthase, etc. Heme plays an important role in the control of protein synthesis and cell differentiation (Ponka 1999). It has been shown that free heme increases deleterious reactive oxygen species (ROS) production with various toxic effects (Ryter and Tyrrell 2000), e.g. inhibition of enzymatic activities (Floyd and Carney 1993), biological membrane damage through lipoperoxide production (Schmitt, Frezzatti et al. 1993), oxidation of nucleic acids (Aft and Mueller 1983) or cell lysis (Meshnick, Chang et al. 1977).

The first rate-limiting step in heme degradation, which is opening of the heme tetrapyrrolic cycle, is catalyzed by microsomal enzyme HMOX and yields to equimolar quantities of CO, ferrous iron and BV (Fig. 1). This reaction, that occurs mainly in the reticuloendothelial system, requires three molecules of oxygen, NAD(P)H and NADPH hemoprotein reductase (EC 1.6.2.4).

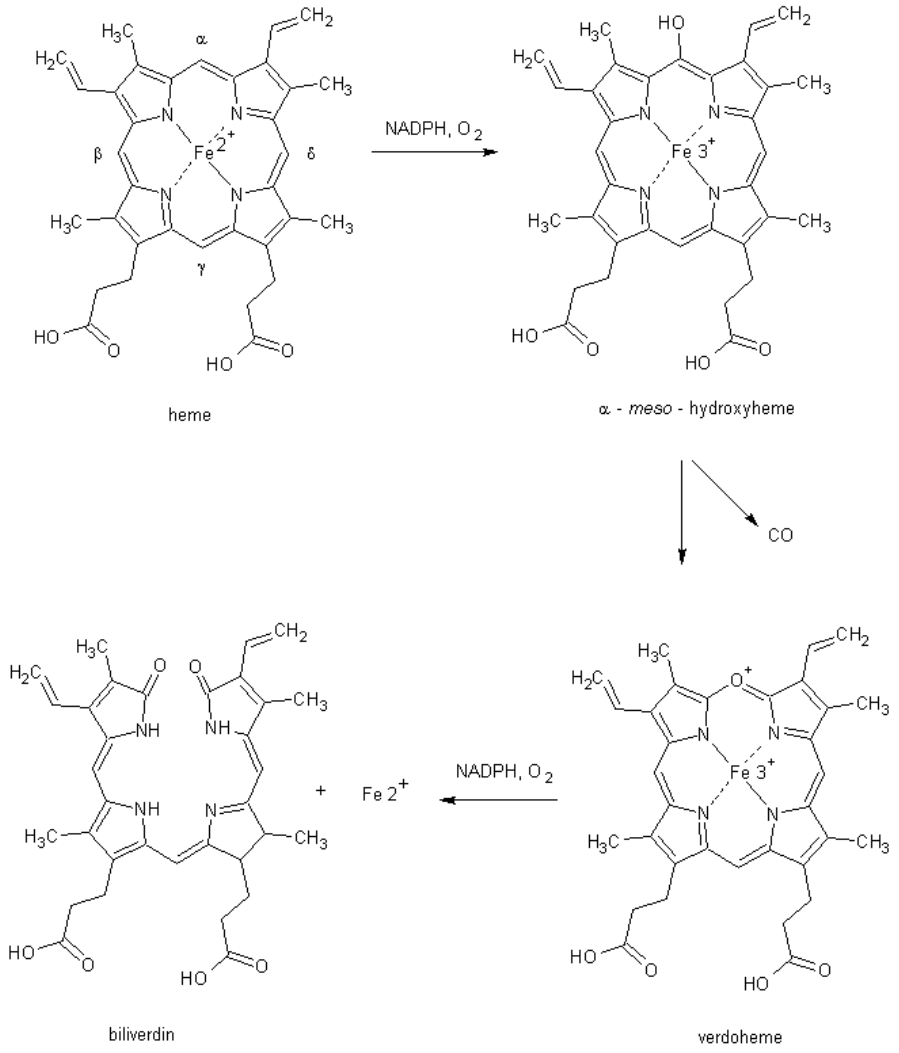

Fig. 1. Cleavage of heme by heme oxygenase

The α-meso carbon bridge of heme is specifically cleaved, oxygen atoms are incorporated into the carbonyl groups of pyrroles´ rings, the alpha carbon is converted to CO, BV IXα is formed, central iron is released and kept in a reduced state Fe^{2+} by NAD(P)H reductase.

In case the heme molecule is needed as a substrate for the anabolic pathway, HMOX most likely does not cleave heme just for its elimination from the body, but rather uses it as a

source of important bioactive molecules (ferrous iron, CO, BV) with impact on cellular functions (Foresti, Green et al. 2004), as described below.

HMOX expression is a phylogenetically well conserved protein indicating its physiological importance. HMOX has been detected in prokaryotic bacteria, plants, fungi, as well as mammals (Lee 1995, Muramoto, Kohchi et al. 1999). The HMOX is essential for human life, as its deficiency results in death (Kawashima, Oda et al. 2002, Radhakrishnan, Yadav et al. 2011). HMOX consists of two isoenzymes HMOX1 and HMOX2 (Braggins, Trakshel et al. 1986). HMOX1 is believed to be the most inducible enzyme in the human body (Maines 1997, Otterbein and Choi 2000) and it is one of the most important enzymes in the enzymatic antioxidant defense system. On contrary, HMOX2 expression is relatively constant. However, elevated HMOX1 expression was detected in several pathological conditions (Wagener, Volk et al. 2003), which could be one of the protective feedbacks of the body. It has been shown that HMOX1 induction has protective effect against ischemia/reperfusion injury (Amersi, Buelow et al. 1999), oxidative stress (Yang, Quan et al. 1999), inflammation (Willoughby, Moore et al. 2000), transplant rejection (Sato, Balla et al. 2001), or apoptosis (Inguaggiato, Gonzalez-Michaca et al. 2001). HMOX1 is therefore considered as a potent cytoprotective agent. The precise mechanisms are not completely clear and require further investigation.

Iron is a transition metal. It is essential for the organism as a biological catalyst and required for growth. Under physiological conditions, iron must be constantly bound to specific molecules to stay in a non-toxic and soluble form. If not, iron can catalyze the production of ROS that can be highly toxic (Eaton and Qian 2002), *via* a process known as Fenton reaction (Fig.2). In recent years, many studies focused on the role of iron in cell proliferation and carcinogenesis. It seems that cancer cells require larger amount of iron than normal proliferating cells. Based on this fact, one of the anticancer treatment strategies is based on iron chelating agents (Richardson, Kalinowski et al. 2009).

$$\mathbf{Fe\ (II+) + H_2O_2 \rightarrow Fe\ (III+) + OH^{\cdot} + OH^{-}}$$

Fig.2. Fenton reaction

Ferrous ion is oxidized by hydrogen peroxide to form ferric ion and very reactive hydroxyl radical and hydroxide ion. Products of Fenton reaction have strong oxidative properties and can cause damage to different biological molecules like DNA, proteins, or lipids.

CO is a colorless, odorless and tasteless gas. However, CO is also an essential signaling molecule, high concentrations are, nevertheless, toxic to humans; exposure to CO concentrations of 1600 ppm causes headache, tachycardia, dizziness, and nausea within 20 minutes and death in less than 2 hours (Hardy and Thom 1994). The main reason for CO toxicity is its very strong affinity (approximately 200 times higher compared to oxygen) to hemoglobin (Townsend and Maynard 2002).This results in decrease of oxygen delivery to the tissues, suffocation and death (Wagener, Volk et al. 2003). CO, nitric oxide (NO) and hydrogen sulfide (H_2S) belongs to family of small endogenous gaseous transmitters, that are naturally produced in the body (Wang 2002). These small gas molecules have some mutual biological effects acting predominantly as vasoactive substances (Furchgott and Jothianandan 1991, Telezhkin, Brazier et al. 2009). CO has various other beneficial effects, such as anti-inflammatory (Otterbein, Bach et al. 2000), apoptosis-modulating (Brouard, Otterbein et al. 2000), anti-atherogenic (Otterbein, Zuckerbraun et al. 2003), anti-proliferative (Peyton, Reyna et al. 2002) and cytoprotective effects (Otterbein, Mantell et al. 1999, Zuckerbraun, Billiar et al. 2003). On the molecular level, CO is an activator of soluble guanylate cyclase resulting in vessel relaxation (Furchgott and Jothianandan 1991) or mitogen activated protein kinase (MAPK) pathway, that is connected with anti-inflammatory impact (Otterbein, Bach et al. 2000). Because of the CO potential toxicity and possible overdose during inhalation, the CO-releasing molecules (CORMs) have been developed with the aim to liberate CO directly to biological tissues (Motterlini, Clark et al. 2002).

BV is a green, relatively water-soluble, and non-toxic molecule that represents the final product of the heme catabolic pathway in the systemic circulation of the lower vertebrates (birds or fish). It is also present in egg shells of the large bird species, such as Emus (Zhao, Xu et al. 2006). Chemical structures of UCB and BV look seemingly very similar. BV as compared with UCB has „just“ one additional double bond at the C10 atom, however, this difference accounts for UCB unique chemical properties.

1.1.2 Bilirubin, its formation, hepatic biotransformation, biliary secretion, enterohepatic circulation and intestinal metabolism

Molecule of BV is a substrate for cytosolic enzyme biliverdin reductase (BLVRA, EC 1.3.1.24). BLVRA is a unique protein having a dual pH cofactor dependent activity profile (Kutty and Maines 1981), uses either NADH in acidic pH or NADPH under basic condition. BLVRA is evolutionary well conserved and surprisingly, it is not exclusive to mammals. It can be found commonly in Nature (Xu and Ding 2003, Maines 2005) or even in lower organisms, such as cyanobacteria (Schluchter and Glazer 1997). BLVRA functions in the cells are arguably unmatched by any single protein. It has a unique serin/threonin/tyrosine kinase activity, works as a scaffold protein (Gibbs, Tudor et al. 2012), a transcription factor, an intracellular transporter, or gene regulator, and plays a major role in the glucose uptake (Lerner-Marmarosh, Shen et al. 2005) and the stress response. BLVRA is importantly involved in the cell signaling.

BLVRA is responsible for reduction on the middle methine carbon of BV IXα and the initial relatively polar green compound changes to non-polar yellow pigment UCB IXα (Fig.3).

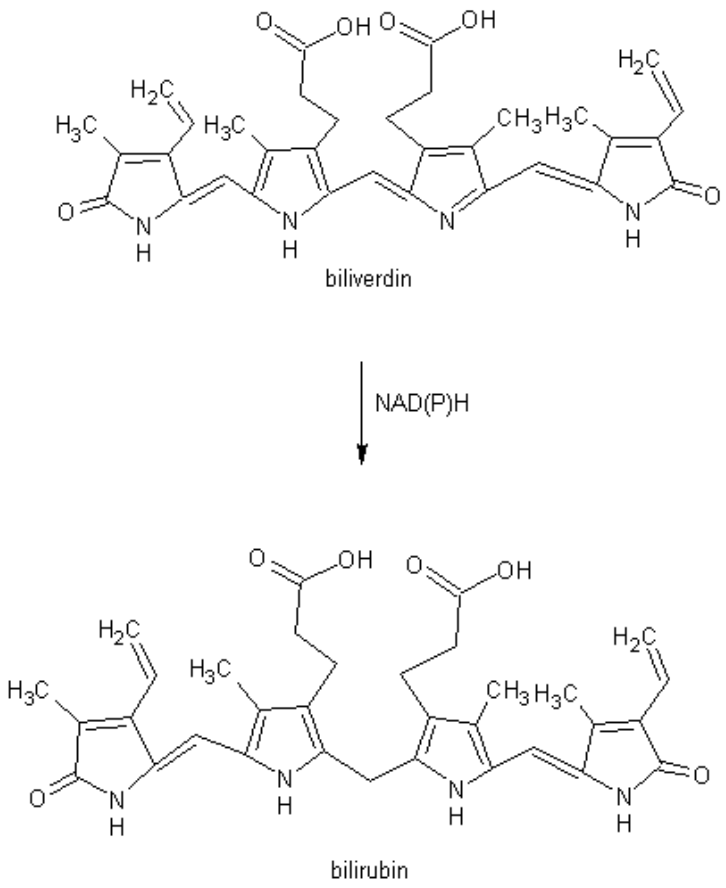

Fig. 3. Biliverdin reduction

Central methine bridge of BV is reduced by biliverdin reductase to UCB.

For decades, UCB was viewed only as a waste, potentially toxic product of the heme catabolic pathway, particularly for the central nervous system (Vitek 2012). In 1987, UCB was re-discovered as an important antioxidant that prevents lipid peroxidation (Stocker, Yamamoto et al. 1987). Later on, UCB was recognized as a major antioxidant in blood (Frei, Stocker et al. 1988) and mildly elevated concentrations of UCB in the bloodstream have been convincingly demonstrated to be associated with lower risk of cardiovascular disease, diabetes, metabolic syndrome, and cancer (Vitek 2012).

UCB occurs mainly in mammals (McDonagh, Palma et al. 1981), but surprisingly, it can be found in plants as well (Pirone, Quirke et al. 2009). From the chemical point of view, it is a poorly water-soluble and easily oxidisable compound. The system of conjugated bonds is "interrupted" on the central carbon (C10), where a single bond is present. This single bond enables rotation of two dipyrrolic halves of the UCB molecule with formation of six intramolecular hydrogen bonds (Fig.4), that make from UCB a non-polar substance.

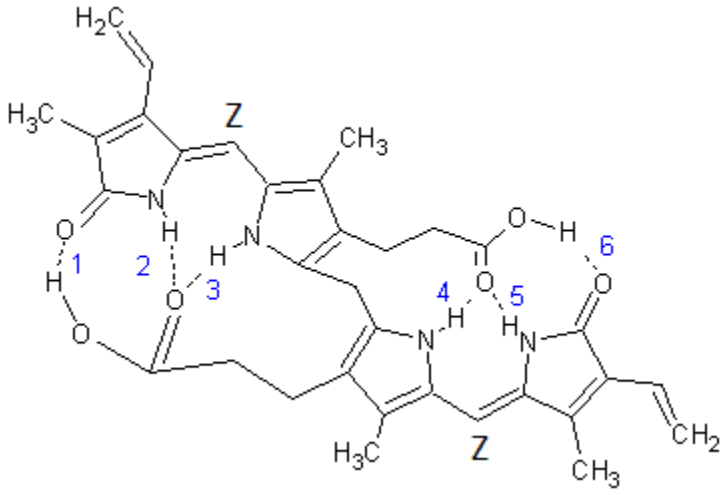

Fig. 4. Structure of 4Z,15Z-bilirubin IXα

Molecule of predominantly naturally occurring 4Z,15Z-bilirubin IXα isomer with its six intramolecular hydrogen bonds (numbered in blue). Other UCB stereoisomers, such as 4E,15Z-UCB IXα, or other isomers, like UCB IXβ, IXϒ, and IXδ are not capable of intramolecular hydrogen bonding. UCB IXβ, IXϒ, and IXδ may occur during nonenzymatic cleavage of protoporphyrin IX with further reduction by one of the four biliverdin reductase isoforms (Yamaguchi, Komoda et al. 1994). UCB isomers IXβ, IXϒ, and IXδ are water soluble and can be found in the fetal bile (Onishi, Isobe et al. 1980, Yamaguchi and Nakajima 1995).

The polarity of UCB is crucial and plays an important role in subsequent metabolism. Majority of bilirubin in the bloodstream is tightly bound to albumin, the main transport protein in human plasma. Binding of two UCB molecules on albumin is believed to involve ion pairing, hydrogen bonding, and π-interaction between albumin´s amino acid side chains and the pigment. The binding is strong enough to prevent UCB excretion into urine. Albumin-bound UCB protects the protein itself against peroxyl radical-mediated damage and also prevents albumin-bound fatty acids from oxidation (R. Stocker et al., 1987). Furthermore, because approximately 60% of human albumin is located in the extravascular space (Rothschild, Bauman et al. 1955), antioxidant activity of albumin-bound UCB is not limited only to the bloodstream. Only less than 0.01% of UCB is not bound to any plasma proteins or lipoproteins, this UCB fraction is known as free bilirubin (Bf) (Vitek and Ostrow 2009). Bf is intensively studied and it is believed to be responsible for most of biological

effects of UCB. Bf diffuses through the membranes and protects the cells against oxidative stress, oxidative damage with strong impact on the cell signaling. Bf levels are important – UCB toxicity may occur when they overcome the aqueous solubility of UCB (which is 70 nM) (Ostrow, Pascolo et al. 2003). Bf can be a ligand for aryl hydrocarbon receptor (AhR) acting as an important transcription factor. Bf can activate AhR, which may lead to increased transcription of P450 monooxygenases (Cyp), as described in jaundiced Gunn rats (Kapitulnik and Gonzalez 1993). In turn, Cyp oxidize UCB to more polar metabolites easily secreted into bile. Cyp can even participate in UCB elimination like cellular defense against high Bf levels (Sinal and Bend 1997).

It was discovered that drugs with higher affinity to UCB binding sites on albumin can displace the pigment and cause severe elevation of Bf. This was first described in 1950s, when sulfisoxazole-treated newborns developed kernicterus in the presence of relatively low plasma bilirubin levels (Harris, Lucey et al. 1958). The importance of Bf for pathophysiology of bilirubin encephalopathy was highlighted by Ahlfors et al. by the observation that auditory brainstem response screening, a quantifiable method to evaluate the bilirubin-induced neurotoxicity, correlates with Bf rather than with total bilirubin concentration in the blood (Ahlfors, Amin et al. 2009).

Albumin-bound UCB is carried to the liver and enters hepatocyte sinusoidal membrane probably through passive diffusion or *via* active transport mediated by OATPs (Organic Anion Transport Polypeptides) (van de Steeg, Stranecky et al. 2012). In hepatocytes as other non-polar substances, bilirubin is bound to intracellular transporting proteins and subsequently conjugated with glucuronic acid by bilirubin UDP-glucuronosyl transferase (UGT1A1, EC 2.4.1.17), a membrane bound enzyme located in the endoplasmatic reticulum, to form bilirubin mono- and bis-glucuronoside (Tukey and Strassburg 2000). This conjugation dramatically changes bilirubin properties and makes it a polar substance that is actively secreted into bile by canalicular multidrug resistance-related polypeptide (2), a member of the adenosine triphosphate (ATP)-binding cassette (ABC) family of transporters. At the sinusoidal membrane, a substantial fraction of conjugated bilirubin is secreted by MRP3 into the blood and reuptaken by sinusoidal membrane–bound transporters OATP1B1 and OATP1B3 back into the liver. It is suggested that MRP3 and OATP1Bs transporters form a

sinusoidal liver-to-blood cycle which mediates shifting of bilirubin and other substrates from periportal to centrizonal hepatocytes (van de Steeg, Stranecky et al. 2012, Sticova and Jirsa 2013). From the liver, conjugated bilirubin is transported into duodenum *via* bile duct system. In the digestive tract the intestinal bacteria cleave off glucuronic acid from conjugated bilirubin by β-glucuronidase (EC 3.2.1.31) (Fig. 5). Nevertheless, β-glucuronidase occurs also in the bile duct epithelium, enterocytes, hepatocytes or breast milk.

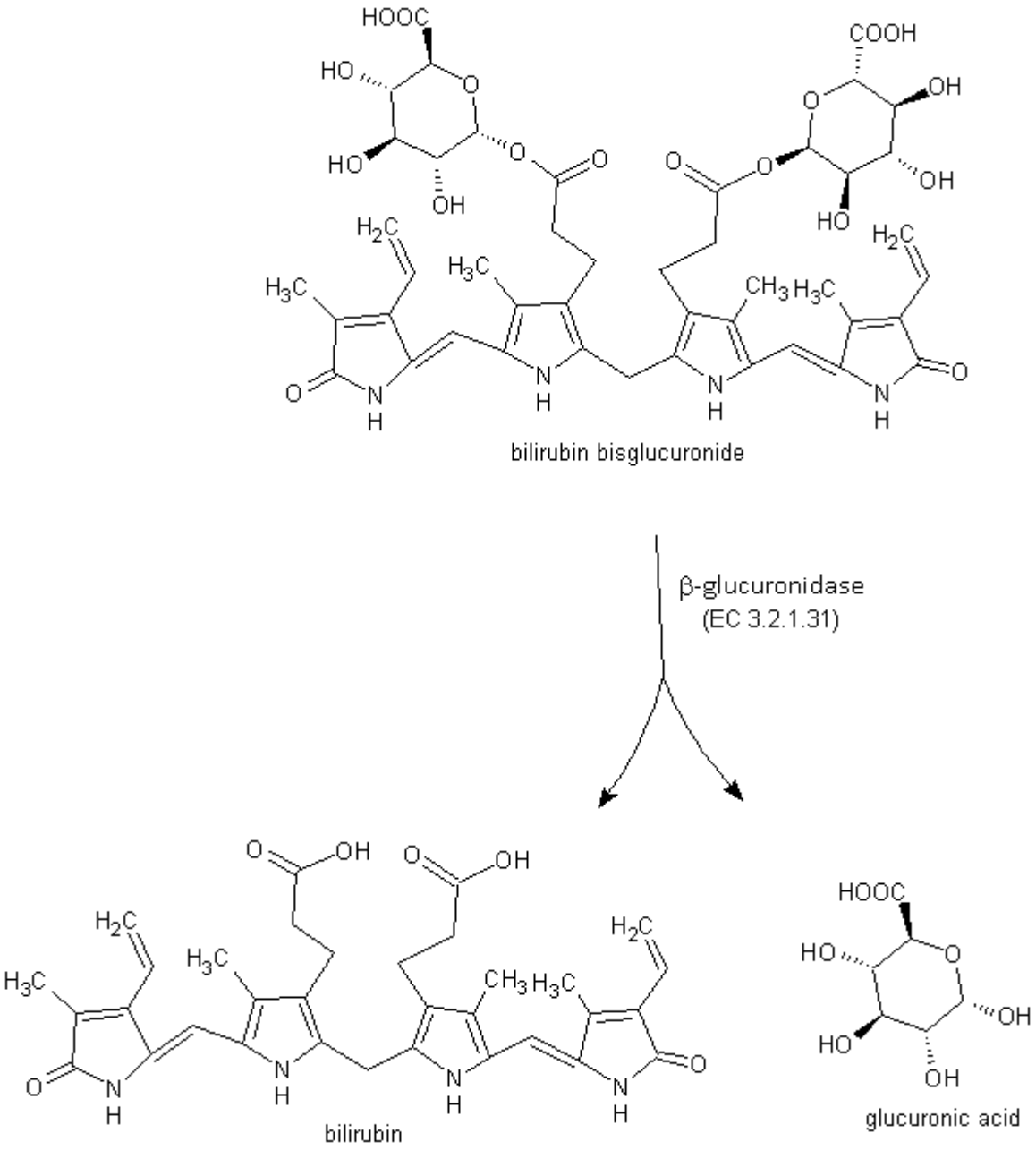

Fig.5. Cleavage of glucuronic acid from bilirubin bis-glucuronoside

Some UCB portion can be reabsorbed and under specific conditions can even enter systemic circulation (so-called enterosystemic circulation of bilirubin), and may thus lead to mild elevation of serum bilirubin levels. Bilirubin transported *via* portal vein to the liver is reconjugated and resecreted into the bile and passed again into the intestine. In the gut, a substantial proportion of UCB is reduced by intestinal microflora to non-toxic and relatively polar substances called urobilinoids (Fig. 6), which are mostly urobilinogen and stercobilinogen with their respective oxidation products, urobilin and stercobilin, being the most important compounds (Moscowitz, Weimer et al. 1971), that are excreted with the stool. A small amount of urobilinoids undergoes enterohepatic circulation, but they are easily excreted by the liver without conjugation. UCB reduction to urobilinoids by the intestinal microbial flora represents a natural detoxification mechanism. Despite the importance of these process only a few bacterial strains capable of UCB reduction have been described: *Bacteroides fragilis*, *Clostridium ramosum*, *C. difficile* and *C. perfringens* (Vitek, Kotal et al. 2000). The production of urobilinoids is highly efficient in adults when compared with that of present in infants during the first month of life. Low urobilinoid production in neonates is due to undeveloped intestinal microflora capable of reducing UCB. Detailed intestinal metabolism of bilirubin has not been clarified so far, enzyme(s) responsible for bilirubin reduction are awaiting to be identified.

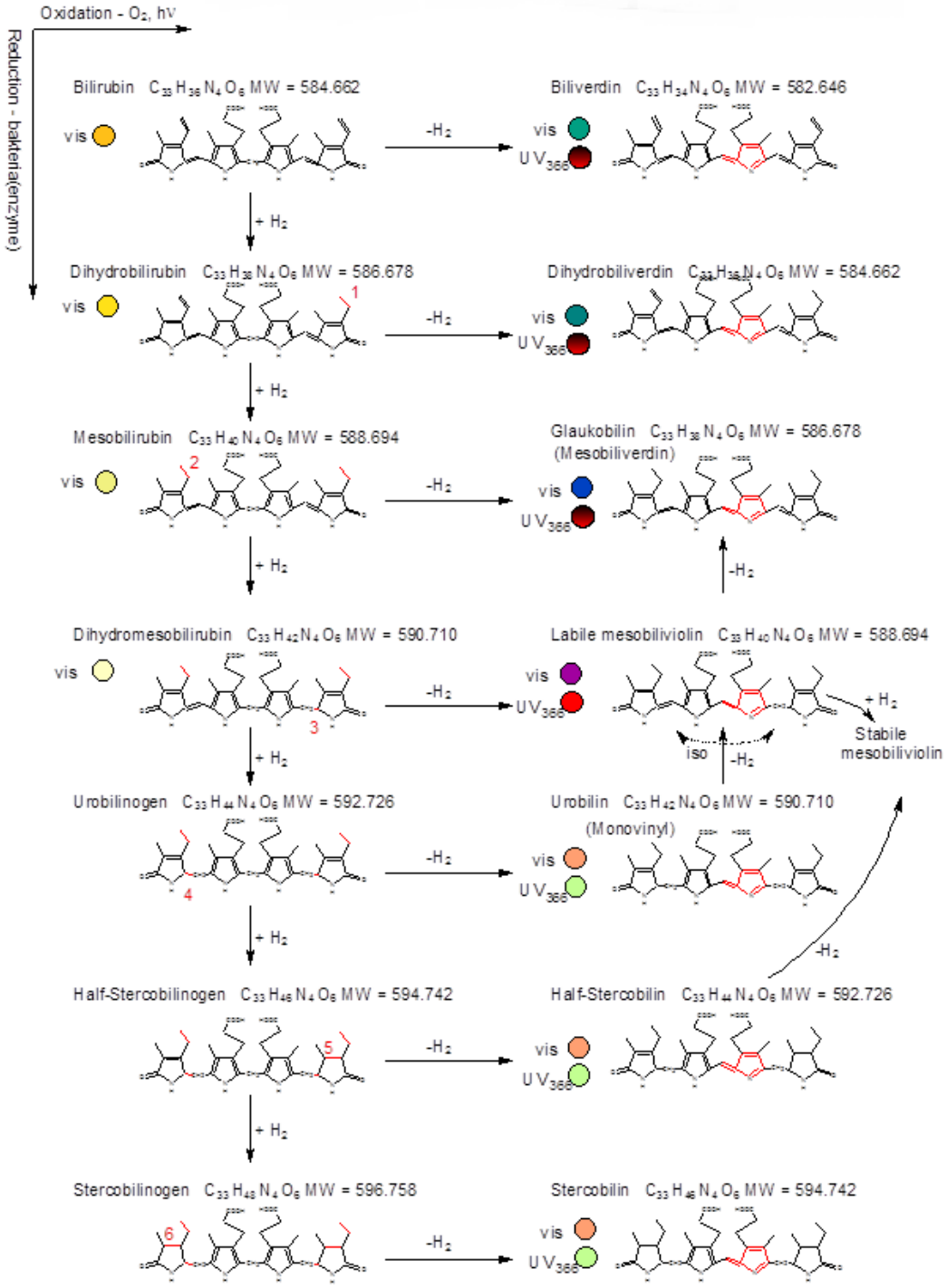

Fig.6. Formation of intestinal urobilinoids

The scheme shows the sequential reduction of bilirubin to urobilinogen or stercobilinogen with relevant oxidation products (Vitek, Majer et al. 2006).

1.2 Hyperbilirubinemias

Elevated serum bilirubin levels above the physiological range (2-17 µmol/L) are marked as hyperbilirubinemias. Hyperbilirubinemias are usually classified according to the type of elevated bilirubin as unconjugated (premicrosomal), conjugated (postmicrosomal) or mixed hyperbilirubinemia.

1.2.1 Premicrosomal hyperbilirubinemias

The causes of this type of hyperbilirubinemias include bilirubin overproduction, disordered bilirubin uptake by hepatocytes or its conjugation within the liver cell. The group of bilirubin overproduction conditions covers a wide range of diseases, including hemolytic anemias, ineffective erythropoiesis, or extravascular hemolytic conditions. Impaired conjugation of bilirubin within the liver cell is exemplified by mild unconjugated hyperbilirubinemia due to inherited deficiency of UGT1A1, known as benign hyperbilirubinemia or Gilbert syndrome (GS). GS occurs in about 3-10% of the population (Owens and Evans 1975, Sieg, Arab et al. 1987, Radu and Atsmon 2001) and is associated with decreased risk of oxidative stress-mediated diseases, including cancer (Vitek and Schwertner 2007).

On contrary, in Crigler-Najjar (CN) syndrome patients characterized by complete (CN syndrome type I) or less severe deficiency (CN syndrome type II) of UGT1A1, severe jaundice appears within the first days of life and persists thereafter. CN syndrome type I is caused by missense mutations of coding *UGT1A1* gene regions disrupting production of functional protein (Sampietro and Iolascon 1999). Serum bilirubin can reach extremely high concentrations (340-770 µmol/L), which may result in development of severe neurologic complications such as hearing problems, mental retardation, or even apparent kernicterus (Jansen 1999, Mohammadi Asl, Tabatabaiefar et al. 2013). CN syndrome type I is treated by lifelong phototherapy resulting in an elimination of water-soluble photoisomers of UCB *via* bile. The efficacy of the phototherapy may decrease gradually with age and patients are at higher risk of sudden brain damage (Sticova and Jirsa 2013). Liver transplantation is considered as efficient treatment for CN syndrome type I. CN syndrome type II is characterized by reduced UGT1A1 enzyme activity, the UCB level do not exceed 350 µmol/L and CN syndrome type II is rarely complicated by kernicterus.

1.2.2 Postmicrosomal hyperbilirubinemias

Postmicrosomal hyperbilirubinemias are the most common in the hospitalized patients, obstruction of bile duct system (such as from gallstones, cancer, or autoimmune diseases of the bile ducts) being the most frequent cause. It occurs very often also due to MRP2 inhibition by various drugs or Gramm–negative sepsis. This type of hyperbilirubinemias also include rare inherited defects in secretion of conjugated bilirubin, such as Dubin-Johnson or Rotor syndrome.

1.2.3 Neonatal jaundice

During the neonatal period, hyperbilirubinemia occurs in majority of infants. Indeed, serum UCB levels above 220 μmol/L occurs in approximately 8-20% full-term newborns (Maisels 1988). Physiological neonatal jaundice (defined in general as the elevation of serum bilirubin up to 340 μmol/L, where the kernicterus seldom occurs (Meyer 1956)) is believed to be a part of natural defense against increased oxidative stress (Ostrow, Pascolo et al. 2003, Pandey, Gupta et al. 2013) and has multifactorial etiopathogenesis (Watchko and Maisels 2003). The major factors involved include enhanced degradation of fetal hemoglobin, immature liver conjugation system or slow colonization of neonatal gastrointestinal tract with bilirubin-reducing bacteria (Vitek, Kotal et al. 2000). Extremely high UCB levels in the systemic circulation of newborns may be due to multiple causes, including neonatal prematurity, hemolysis (such as from Rh incompatibility), glucose-6-phosphate dehydrogenase deficiency, sepsis, or a rare CN syndrome. Severe hyperbilirubinemia may lead to development of acute bilirubin encephalopathy. The acute stage is manifested with somnolence, hypotonia, poor sucking reflex (Van Praagh 1961) and if unrecognized and untreated, it can be followed by an irreversible bilirubin neurologic damage (Bhutani and Johnson 2009) known as kernicterus (Bhutani, Zipursky et al. 2013). Classical kernicterus (chronic encephalopathy) affects the basal ganglia, specifically globus pallidus, subthalamic nucleus, with brainstem nuclei (especially the auditory), oculomotor, vestibular nuclei, cerebellum or colliculi. Severe damage of the brain can result in cerebral palsy, mental retardation and/or problems with vision and hearing or even death (Bhutani and Wong 2013). Less severe hyperbilirubinemia can result in subtle encephalopathy called bilirubin-induced neurologic dysfunction (BIND) consisting of neurological, cognitive, learning and perhaps movement disorders, isolated hearing loss and auditory dysfunction. The classical

kernicterus does not need to be present. Kernicterus as a complex syndrome is ranging from isolated conditions like auditory neuropathy, BIND to classical kernicterus, as described above (Shapiro 2005).

Jaundice in preterm infants is even more common and more severe. Prematurely born infants are at much higher risk for developing kernicterus than full-term newborns. It was described that kernicterus developed in premature infants even at serum UCB levels ranging 170-306 µmol/L (Watchko and Maisels 2003). This led to the discovery of the importance of Bf for the pathogenesis of the neurotoxic effects associated with neonatal jaundice. Among other factors, concentration of Bf is dependent also on serum albumin levels and this indicates that the serum UCB concentration need not always to be the correct indicator for real neurologic damage.

The golden standard in the treatment of severe neonatal jaundice is phototherapy. Phototherapy decreases serum UCB levels by photoisomeration, more polar photoisomers can be excreted into bile without conjugation. It has been described that phototherapy combined with administration of activated charcoal (Ulstrom and Eisenklam 1964), cholestyramin or formula supplemented with agar leads to interruption of the enterohepatic circulation by trapping bilirubin in intestinal lumen and results in decrease of UCB levels in neonatal hyperbilirubinemia (Poland and Odell 1971) . Phototherapy is generally considered to be a safe treatment modality. However, associated ultraviolet radiation represents certain risk for neonates (Gies and Roy 1990). Other side effects include interference with infant-maternal interaction, circadian rhythm disorder (Xiong, Tang et al. 2012), bronze baby syndrome, overheating with dehydration (Kjartansson, Hammarlund et al. 1992), disturbances in cytokine production (Sirota, Straussberg et al. 1999) or impairment of growth factor receptors (Jahanshahifard, Ahmadpour-Kacho et al. 2012). In long-term use, phototherapy may be associated with melanocytic nevi, skin cancer, allergic diseases, patent ductus arteriosus and retinal damage (Xiong, Tang et al. 2012). Other possible treatment for extreme neonatal hyperbilirubinemia is the exchange transfusion, by which is UCB rapidly eliminated from the circulation. Exchange transfusion, although currently only exceptionally used, brings more severe side effects than phototherapy treatment, such as cardiovascular collapse during the transfusion, subsequent complications of necrotizing enterocolitis,

bacterial sepsis, and/or pulmonary hemorrhage (Keenan, Novak et al. 1985, Jackson 1997). Thus, improvements in the management of severe neonatal jaundice are needed.

1.3 Beneficial effects of bile pigments

Apart from well-known, potentially deleterious effects of bilirubin, bile pigments can also have substantial beneficial effects. In fact, bilirubin and biliverdin are substances with potential antitumor (Ollinger, Kogler et al. 2007, Zheng, Nagda et al. 2014), anti-inflammatory (Wegiel and Otterbein 2012, Lenicek, Duricova et al. 2014) and antioxidant effects (Baranano, Rao et al. 2002, Jansen and Daiber 2012) with deep impact on ROS production. They can even serve as modulators of immune functions (Nakagami, Toyomura et al. 1993), cell signaling (Maines 2003), activators of a AhR (Sinal and Bend 1997, Phelan, Winter et al. 1998), inhibitors of protein phosphorylation (Hansen, Mathiesen et al. 1996) or NADPH oxidase activity (Lanone, Bloc et al. 2005). Even more, current studies are focused on artificial mild elevation of serum UCB concentrations to produce “iatrogenic Gilbert syndrome” with the aim to enhance antioxidant defense. Such approach is based either on induction of HMOX, inhibition of UCB conjugation (several drugs possessing this activity, such as atazanavir or probenecide have been described), inhibition of the UCB hepatocyte uptake (for example by rifampicin), or by less invasive way, such as by direct administration of bilirubin, biliverdin or bilirubin-like tetrapyrroles (McCarty 2007, Dekker, Dorresteijn et al. 2011). Interestingly, artificial bezoar (pulverized bovine gallstones) has been used for centuries as the natural source of bile pigments in traditional Chinese medicine for its beneficial impacts on human health. Other possibility to increase bile pigment intake may include ingestion of algal biliverdin metabolites-phycobilins, which may undergo further metabolizing by biliverdin reductase (Terry, Maines et al. 1993), and may have antioxidant properties comparable to UCB. Moreover, tetrapyrrole-rich algae, such as *Spirulina platensis* or *Chlorella* belong to popular dietary supplements.

Current research is focused on investigation of diverse biological effects of bile pigments that can finally lead to better understanding and novel treatment strategies of civilization diseases.

1.4 Tetrapyrroles in Nature

Bilirubin and biliverdin are only two members of a superfamily of tetrapyrrolic compounds. In fact, tetrapyrroles cover large group of organic compounds that are evolutionary very old and common in Nature. The evolutionary conservation is connected with the common and tightly regulated biosynthesis (in violet, see Fig. 7)**.** This is the reason, why tetrapyrroles can be found everywhere, like in fossils of the mollusk shells (Kennedy 1975), in plants, many bacteria and also in the animal realm. Plants are green because of chlorophylls, meat is red because of the heme presence, blue eggshells pigmentation is due to biliverdin (Kennedy and Vevers 1976), even feathers of some birds are colored with tetrapyrroles like red copper uroporphyrin III or green turacoverdin in *Turacos (*Nicholas and Rimington 1951).

Fig.7. Biosynthetic pathway of tetrapyrroles among living species showing the main common intermediates and different end products. Enzymes written in italics.

Tetrapyrroles, as the name says, contain four molecules of colorless pyrrole (Fig. 8).

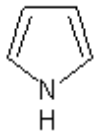

Fig. 8. A pyrrole unit built by 5-membered ring with one nitrogen

Four pyrroles are usually connected by unsaturated methine groups and build conjugated system of double bonds that strongly absorbs light. Tetrapyrroles are either linear like bilins, such as biliverdin, or phycocyanobilin (PCB); or cyclic as in the hemes, chlorophylls, corrins, such as vitamin B12 (Warren and Scott 1990). The name of open chain tetrapyrroles, bilins, is derived from „bile pigments“, because the first characterized bilin, bilirubin, was isolated from the bile. In cyclic tetrapyrroles, nitrogens from pyrrolic rings are oriented towards each other and form a space, where can be captured metal ion. In the living organisms, a number of various metals associated with tetrapyrroles including Mg, Fe, Mn, Co, Zn, Ni and V have been detected (Buchler 1975).

Roles of tetrapyrroles are closely associated with their structure properties. The main function of tetrapyrroles in Nature is the light harvesting during photosynthesis, where the light absorption results in electron excitation, energy (ATP) generation, reduction equivalents and final carbohydrate production, and as well they play an important role in carbohydrates oxidation. The other functions include transport and homeostasis of oxygen; protection against ROS (e.g. via tetrapyrrolic antioxidants like bilirubin), but on the other hand also production of ROS (e.g. via oxidative phosphorylation in mitochondria), they are also implicated in the cell signaling processes (Nose 2000, Valko, Leibfritz et al. 2007).

1.4.1 Resemblance of plant or cyanobacterial linear tetrapyrroles to bile pigments

The strong color in cyanobacteria or some lower organisms, such as algae, are due to chlorophylls and phycobiliproteins, a group of brilliantly colored fluorescent proteins that function as photosynthetic pigments. Phycobiliproteins are formed by protein binding made

by covalent thioether bond to cysteinyl residue with attached open-chain tetrapyrrolic chromophore, phycobilin, representing the light harvesting moiety. There are several members belonging to the group of phycobilins, such as phycoerythrobilin (red), phycourobilin (orange), phycoviolobilin (purple) and PCB (blue) (O'Carra, Murphy et al. 1980). Higher plants use phytochrome for light detection, a protein moiety with covalently bound chromophor (phytochromobilin) resembling PCB from Cyanobacteria or red algae. The bile pigment biliverdin is believed to be the common precursor in the biosynthetic pathway of different phycobilins (Beale and Cornejo 1983) and phytochromobilin. The structure similarities are obvious (Fig. 9) especially in the structure of PCB and phytochromobilin, where the conjugated system among pyrrolic nuclei is preserved. Even more, PCB, phycoerythrobilin and phytochromobilin can be enzymatically converted to rubinoid products by biliverdin reductase (Terry, Maines et al. 1993). This ubiquitous enzyme catalyzes the reduction of biliverdin to bilirubin in the heme catabolism as described above.

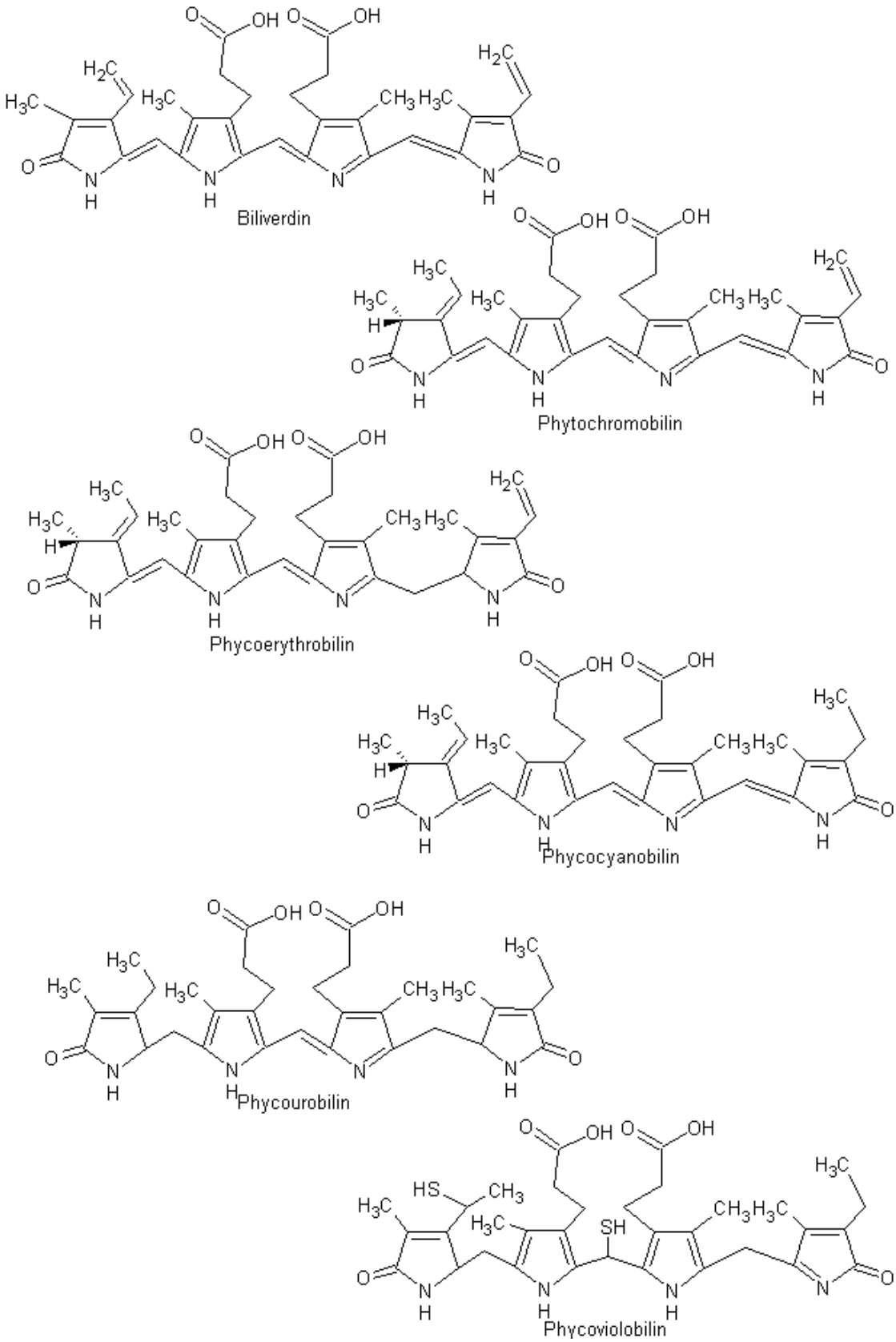

Fig. 9. Chemical structure of biliverdin, phytochromobilin and phycobilins

1.4.2 Chlorophylls and chlorophyllin

Chlorophylls are extremely important light-harvesting biomolecules that are present in all green plants, algae and cyanobacteria. Chlorophylls belong to cyclic tetrapyrroles having magnesium ion in the center. Various molecules of chlorophylls (a, b, c1, c2, d, f) differ in their side chain modification of tetrapyrrolic ring, they usually have attached isoprenoid chain, through which the chlorophyll molecule can be anchored in the biological membrane (Kodíček 2004). Chlorophylls are lipophilic and light sensitive compounds. Due to these reasons, chlorophyllin, a stable and water soluble man made derivate of chlorophyll is commonly used in biological experiments (as well as in food industry). Chlorophyll and its derivatives are effective in binding carcinogens such as polycyclic aromatic hydrocarbons, heterocyclic amines, aflatoxin, and other hydrophobic toxins. The chlorophyll-carcinogen complex lowers the bioavailability of carcinogen, that is then more difficult to absorb and can be excreted with the feces (Sarkar, Sharma et al. 1994, Donaldson 2004). Anti-cancer and chemopreventive effects of chlorophylls have been described in experimental as well as human studies (Dashwood, Negishi et al. 1998, Jubert, Mata et al. 2009, McQuistan, Simonich et al. 2012), but surprisingly, the published data on biological effects of chlorophylls are scarce.

2 Aims of the work

Objectives of this work were at the beginning focused on elucidation of some unknown aspects of the metabolism of bilirubin in the intestine, as well as in the brain. The bilirubin molecule was in the center of our further investigation and was intensively studied for its neurotoxic effects. These studies were performed to shed more light on potential anti-cancer effects of bilirubin, since the mechanisms of bilirubin neurotoxicity are practically identical with those related anticancer action. The other product of the heme catabolic pathway, CO, was studied for its antiproliferative effects in our further work. Finally, based on recently published studies focused on health protective impact of bile pigments and their resemblance with algal tetrapyrroles, we examined potential anti-cancer effects of blue-green alga *S. platensis* and its bilirubin-like tetrapyrrolic compounds.

UCB reduction by intestinal microflora to urobilinoids belongs to a natural way of UCB disposal from the body. Despite the importance of these processes, only a few bacterial strains capable of UCB reduction have been described. Moreover, bilirubin potently affects carcinogenesis of the intestine and its metabolism within the intestinal lumen seems to be crucial for this activity. The aim of our first presented work entitled **„Reduction of bilirubin ditaurate by the intestinal bacterium *Clostridium perfringens*“** was to examine the broad enzymatic equipment of *C. perfringens,* to assess whether bilirubin ditaurate (BDT), a pigment that naturally occurs in bile of lower vertebrates (Sakai, Watanabe et al. 1987), can be reduced by *C. perfringens* isolated from human neonatal feces, and also to characterize the formed reduction products.

Also the second work was related to unknown aspects of bilirubin metabolism, in this case in the brain during neonatal period. Risk of neurotoxic damage is related to the increased level of Bf. Only scarce data exist on the bilirubin distribution during neonatal period, when the bilirubin-induced neurological damage may occur. The main reason of this as well as the other following study was the fact that mechanisms of neurotoxic effects of bilirubin are predominantly identical with those, by which bilirubin inhibits cancer cells growth. The objective of the study entitled „**Bilirubin accumulation and *Cyp* mRNA expression in selected brain regions of jaundiced Gunn rat pups“** was to yield information on bilirubin

distribution in selected brain regions, as well as on regional brain expression of cytochrome P450 monooxygenases, which play role in protecting neuronal cells from bilirubin toxicity.

The aim of our next experimental study entitled „**Beyond plasma bilirubin: The effects of phototherapy and albumin on brain bilirubin levels in Gunn rats“** was focused on improvement of current therapy of neonatal jaundice. Specifically, the potential role of albumin supplementation in the treatment of severe unconjugated hyperbilirubinemias was assessed on hyperbilirubinemic Gunn rats.

In further work entitled **„Antiproliferative effects of carbon monoxide on pancreatic cancer“** potential anticancer effects of CO were investigated on experimental model of human pancreatic cancer. Additionally, we were as well interested in CO distribution within organs and tissue of experimental animals after CO exposure.

In our last paper entitled „**Anti-cancer effects of blue-green alga *Spirulina platensis*, a natural source of bilirubin-like tetrapyrrolic compounds”** we aimed to examine potential anticancer effects of the *S. platensis* alga and its bilirubin resembling tetrapyrrolic compounds.

3 Methods

Complete methods are in detail described in published papers. Below is the list of the method that I personally worked with.

3.1 Cultivation of *C. perfringens*

The used non-pathogenic strain of *C. perfringens* was isolated from neonatal stool (Vitek, Kotal et al. 2000). *C. perfringens* was cultured at 37°C under anaerobic condition (Anaerostat, Oxoid, GB) in 2% yeast extract (Oxoid, GB), that was dissolved in 100 mM phosphate buffer, pH=8. The growth was monitored according to the optical density of the culture (spectrophotometry at 600 nm). BDT or UCB were added in concentration 50 µmol/L to the late exponential phase culture. Based on their polarity, UCB was dissolved in dimethylsulfoxide (Sigma, St. Louis, MO, USA) and BDT in the broth. After 24 hours incubation in Anaerostat and centrifugation 15000 x g, the medium was sampled for urobilinoids analysis.

3.2 Purification of commercially available bilirubin and biliverdin

Purification of bile pigments were performed under the dim light, in the hood and if possible in aluminum wrapped tubes.

3.2.1 Purification of bilirubin

Purification of commercial UCB (Frontier Scientific) was modification of the method by McDonagh and Assisi (McDonagh and Assisi 1972). One hundred mg of UCB was dissolved in 180 ml of chloroform. The UCB-chloroform solution with boiling stones was heated in the water bath to approximately 61°C (chloroform boiling temperature) and boiled for another 5 minutes. After mild chilling, the solution was filtered through chloroform wetted filtration paper. Filtrate was washed once with approximately 1 volume of distilled water, twice with 1 volume of solution of 0.1 M $NaHCO_3$, once with 1 volume of solution of 10% NaCl, and finally four times with 1 volume of distilled water. During every wash, the filtrate was properly shaken approximately fifty times. And after every wash, a two-phase system appeared with UCB being in the lower chloroform phase (yellow). The upper phase and eventually phospholipids present on the interphase were aspirated. After all the washing steps, the chloroform phase was transferred into the clean and dry flask and a little bit of Na_2SO_4 was

added until a few single crystals was seen. The suspension was shaken fifty times and centrifuged. The yellow chloroform solution was filtrated through the chloroform wetted filtration paper. Filtrate was boiled with new boiling stones on the water bath until UCB was seen on the flask´s wall - UCB saturated chloroform solution was made. During stirring, 1 ml of methanol was slowly added to the saturated UCB solution. Strong orange turbidity appeared. The heating was stopped and another 30 ml of methanol was added. After cooling, the solution was centrifuged and the upper phase discarded. The orange sediment containing UCB was washed twice with 15 ml of methanol and finally lyophilized in the glass tube. Purified UCB was stored in the dark at 4°C in the exsiccator.

3.2.2 Purification of biliverdin

One hundred and fifteen mg of biliverdin (BV) was properly dissolved in about 10 ml of solution of chloroform:methanol 1:1 v/v. BV solution was loaded on the prepared silicagel column. About 75 ml of dry silicagel (KIESEL/gel 60 (0.063-0.100 mm), Merck) was mixed with 250 ml of de-aerated mixture of chloroform:methanol, 9:1 v/v. The empty glass column, that had 22 mm in diameter and a flow rate valve, was carefully filled with silicagel. The final height of sorbent in the column was about 23 cm. Sorbent was washed with mixture of chloroform:methanol, 9:1 v/v. The flow rate was adjusted to 1 ml/30 s. Loaded BV was washed with 200 ml of chloroform:methanol, 9:1 v/v. Elution was done with mixture of chloroform:methanol:acetic acid, 9:1:0,1 v/v/v. Green eluate with yellow touch was collected into clean glass flask (the first 25 ml were excluded). For the next elution step the mixture of chloroform:methanol:acetic acid, 9:2:0,1 v/v/v was used. The eluate was let to get dark green and at this moment the collection of BV was stopped. Collected fraction of BV solution was evaporated on the rotation vacuum evaporator, 55°C, 60 rpm, until only a few milliliters of liquid was left. BV was dissolved in 5-10 ml of 1 M NaOH and filtrated. The filtration paper was pre-washed with 1 M NaOH. BV precipitated in the filtrate after a few drops of acetic acid were added. The BV precipitates were centrifuged. The upper light green phase was aspirated and the BV precipitates were properly washed 4-times with distilled water. BV precipitates were freeze-dried in the glass vial and stored in the dark at 4°C in the exsiccator in the glass vial under argon atmosphere.

3.3 Isolation of tetrapyrroles

3.3.1 Isolation of urobilinoids from bacterial medium

Urobilinoids, bacterial reduction products of UCB and BDT, were isolated from the metabolized medium after 24 hours incubation of *C. perfringens* culture (see below) with UCB or BDT. The pigments were extracted from the culture medium using SPE column (Strata C8 500 mg/6 ml, Phenomenex, Torrance, CA, USA). The columns were prewashed with 1 volume of methanol and distilled water. The spun culture medium (15000 x g, 20 min, 4°C) was carefully aspirated and loaded on the prewashed columns under dim light. The urobilinoids were eluted with a minimal volume of methanol:H_2O mixture (1:1, by vol.). The elution mixture was evaporated in nitrogen flow at 70°C in the dark. The extracted pigments were dissolved in methanol and separated by TLC.

3.3.2 Isolation of bilirubin from tissues

UCB was isolated from samples of tissue according to Zelenka et al. (Zelenka, Lenicek et al. 2008). Because of photosensitivity of bilirubin, the whole isolation procedure was done under dim light. Piece of tissue (20 - 200 mg) was placed in tubes containing 1 mg of antioxidant substance BHT (2,6-di-tert-butyl-4-methylphenol), glass dust, 500 µl of deionized water and 50 µl of freshly thawed internal standard (mesobilirubin, 15 µmol/L, dissolved in DMSO). Tissue was disintegrated to a fine suspension by vigorous grinding with a glass rod for 5 minutes. The mixture was subsequently diluted with 6 ml of extraction solvent (methanol/chloroform/n-hexane 63:31:6 (v/v/v)) and whirled for 30 seconds. Then, 4.5 ml of extraction buffer (50 mmol/L phosphate buffer, pH 6.2, 150 mmol/L NaCl, 5 mmol/L EDTA) was added, the tube was vortexed for further 30 seconds and centrifuged at 1000 x g for 5 minutes. The whole lower organic phase (2 ml) containing UCB was transferred with a glass pipette into a new tube and mixed with 1.5 ml of n-hexane and 50 µl of loading buffer (100 mmol/L carbonate buffer, pH 10, 5 mmol/L EDTA). Suspension was vortexed for 30 seconds and then centrifuged at 1000 x g for 2 minutes. An aqueous droplet on the surface of organic phase was aspirated by a 100 µl Hamilton syringe (Hamilton, Bonaduz, Switzerland) and 50 µl immediately loaded onto the HPLC column.

3.3.3 Isolation of phycocyanobilin from *S. platensis*

PCB was isolated from lyophilized *S. platensis* according to Terry (Terry 2002). Whole isolation steps were performed under dim light in aluminum wrapped tubes. *S. platensis* powder was mixed with distilled water (1 g/30 ml), sonicated and incubated at room temperature for 10 minutes. Suspension was centrifuged at 8000 x g for 30 minutes and the blue supernatant was transferred into a new vial. Trichloracetic acid (TCA) was added to the supernatant to get the concentration of about 1% and the mixture was incubated for 30 minutes at 4°C. Sample was centrifuged at 8000 x g for 30 minutes, supernatant discarded and the protein pellet washed repeatedly with methanol and acetone until green color (chlorophyll) disappeared. Pellet was re-suspended in 10 ml of methanol containing 10 mg $HgCl_2$ and 50 mg of ascorbic acid and incubated at 60°C in dark for 24 hours to cleave PCB from protein. Suspension was centrifuged at 8000 x g for 10 minutes and supernatant was transferred into a new vial. Hg^{2+} ions were precipitated with 10 µl of 2-mercaptoethanol and suspension finally centrifuged at 8000 x g for 30 minutes. All solvents used in next steps were fortified with 0.1% ascorbic acid. Supernatant was ten times diluted with distilled water and loaded on the preconditioned SPE column (C18, Sep-Pak, Waters). SPE column was pre-washed with 1 volume of acetonitrile, 1 volume of distilled water and 1 volume of 0.1% TCA. After loading, the column was washed with 1 volume of 0.1% TCA and 1 volume of 20 % acetonitrile in 0.1% TCA. PCB (dark blue fraction) was eluted with minimal volume of 60% acetonitrile in 0.1% TCA. The eluate was mixed with 2 volumes of distilled water and 2 volumes of chloroform. The chloroform phase was washed twice with distilled water. Finally, chloroform was evaporated in nitrogen stream. Dried PCB was stored at -20°C in dark glass tube. Obtained PCB was confirmed by mass spectrometry (Esquire 3000, Bruker) and HPLC analysis, details are given below in the section „Analysis of tetrapyrroles“. Shortly before use, PCB was dissolved in the culture medium and its concentration was determined spectrofotometrically.

3.4 Analysis of tetrapyrroles

3.4.1 Thin layer chromatography (TLC)

TLC was used for separation of BDT and UCB reduction products, urobilinogen ditaurate and urobilinogen, respectively. Isolated urobilinoids were dissolved in methanol and loaded on

HPTLC aluminum plates coated with silica gel (RP-18 W/UV254, Macherey-Nagel, Germany). Entire manipulation was done under dim light. The solvent system was H_2O:MeOH:CH_3COOH (250:250:1, by vol.). After TLC was performed, the plate was left for about 40 minutes on the light and air to oxidize the separated tetrapyrroles. Reduction products were examined under both visible and UV light (CAMAG TLC Scanner II, CAMAG, Muttenz, Switzerland). Urobilin (Frontier Scientific, Inc., Logan, UT, USA) and urobilinogen ditaurate were used as standards. Urobilinogen ditaurate was prepared by amalgam reduction of BDT, as previously described (Watson 1953) with its structure confirmation by mass spectrometry (Esquire 3000, Bruker Daltonics, Bremen, Germany). The reduction of BDT and mass spectrometry analysis were kindly performed by Doc. RNDr. Ladislav Lešetický, CSc and RNDr. Martin Štícha from laboratory of NMR spectroscopy at the Faculty of Natural Sciences, Charles University in Prague.

3.4.2 Spectroscopic determination

Spectrophotometry (UV/Vis Spectrophotometer Lambda 20, Perkin-Elmer, USA) was used for determination of concentration of various tetrapyrroles. Concentrations were calculated based on data given in Table 2 (Terry, Maines et al. 1993) and Beer-Lambert law (A=clε).

Table 2. Spectrophotometric properties of used tetrapyrrols

Tetrapyrrole	Solvent	Absorbance A (nm)	Molar Extinction Coefficient ε(L/mol/cm)
UCB	Chloroform	450	55000
BV	2% HCl/methanol	377	66200
PCB	2% HCl/methanol	374	47900

Concentrations of the UCB and BDT reduction products were determined spectrophotometrically as the oxidation products of zinc complexes of urobilinoids (Kotal

and Fevery 1991), that have characteristic green fluorescence. Two hundred µl of metabolized bacterial medium was mixed with 1.2 ml of Zn-acetate solution (1% Zn-acetate dissolved in DMSO). Urobilinogen or urobilinogen ditaurate were oxidized by addition of 100 µl of iodine solution (25 mM I_2 dissolved in 120 mM KI solution in water). After vigorous vortexing the residue of iodine was reduced by addition of 50 µl of 82 mM cysteine in water. Sample was centrifuged at 3000 x g, for 5 min at room temperature and absorption spectrum (400 – 680 nm) was measured in supernatant. Quantification of urobilins was performed by comparing of absorption maximum of Zn-complex of urobilin (508.5 nm) with a calibration curve of Zn-complex of standard urobilin-i. The bile pigment conversion rate was calculated as a proportion of urobilinoid production to the initial bile pigment concentration.

3.4.3 High performance liquid chromatography (HPLC)

HPLC analyses of PCB and UCB were performed on Agilent 1200 HPLC instrument with diode array detector (Agilent, Santa Clara, CA, USA) based on a method described previously (Zelenka, Lenicek et al. 2008). The octyl reverse phase column with safety precolumn (Luna C8, size 4.6x150 mm, particles 3m/100A, Phenomenex, Torrance, CA, USA) and isocratic mobile phase (methanol/water/tetrabutyl amonium hydroxide, 59:40:1 (w/w/w), pH adjusted to 9.0 by phosphoric acid) were used. Flow rate was 0.5ml/min and the column temperature was kept at 40°C. In case of PCB analysis, the absorbance at 368 nm and the spectrum between 300-700 nm were monitored. During UCB analysis absorbance at 440 nm with reference wealth length 550 nm was collected.

3.5 Preparation of water extract from *S. platensis*

To each gram of lyophilized *S. platensis* powder, 30 ml of distilled water was added. The suspension was sonicated for 15 minutes, incubated for 10 minutes at room temperature, centrifuged 8000 x g, 30 minutes, 10°C, and finally lyophilized over-night. The extract was stored at 4°C in exsiccator in the dark. Shortly before use was dissolved in the culture medium, sterile-filtered and added to cancer cells.

3.6 Tissue culture

3.6.1 Cell culturing

Cancer cell lines were cultured at 37°C in the atmosphere of 5% CO_2 and 95% air. Human pancreatic adenocarcinoma cell lines - PATU-8902 (DSMZ, Germany), MiaPaCa-2 and BxPC-3 (ATCC, USA) were employed. PATU-8902 and MiaPaCa-2 were grown in Dulbecco's modified Eagle medium (DMEM; Sigma-Aldrich) with 10% bovine serum (BS; PAA), 100 units/ml of penicillin (Sigma-Aldrich), 0.01 mg/ml of streptomycin (Sigma-Aldrich). BxPC-3 cell line was cultured in RPMI (Sigma-Aldrich) with 10% bovine serum (BS; PAA), 100 units/ml of penicillin (Sigma-Aldrich), 0.01 mg/ml of streptomycin (Sigma-Aldrich). All cell lines were authenticated (STR analysis made by Generi Biotech) and regularly tested for Mycoplasma contamination (MycoAlert Detection Kit, Lonza). The cell line PATU-8902 was used in majority of our experiments due to its highest sensitivity to the tested tetrapyrroles.

3.6.2 MTT assay

Viability of cancer cell lines was examined by MTT assay (Mosmann 1983). Briefly, cancer cells were cultured in 96 well plate and incubated with or without the addition of UCB, BV, PCB or water extract from *S. platensis*. After 24 hours the medium was gently aspirated and new medium with 1 mg/ml of 3-(4,5-dimethylthiazol-2-yl)-2,5-diphenol tetrazolium bromide (MTT, Sigma-Aldrich) was added into each well. After 2 hours incubation the medium was carefully aspirated and the formazan reduction product of MTT that corresponds to the relative viable cell number, was dissolved in dimethyl sulphoxide (Sigma-Aldrich). Absorbance was measured at 545 nm with ELISA reader (Sunrise Absorbance Reader, Tecan).

3.6.3 Crystalline violet staining

Counting of cells cultured in 96 well plate was performed trough crystalline violet staining. Cells were incubated for 24 hours with or without addition of UCB, BV, PCB or water extract from *S. platensis.* Then the cells were fixed with addition of 10 µl of 11% glutaraldehyde into each well, into 100 µl of medium. Plates were shaken for ten minutes 500 cycles per minute and washed three times with water. After the 96 well plate became dry 100 µl of staining solution 0.1% crystalline violet was added to each well and the plate was shaken for 20 minutes. The crystalline violet dye penetrates into the nucleus and stains DNA. Plates were

three times washed with distilled water and air-dried. Dye was solubilized by adding 100 µl of 10% acetic acid. After final 10 minutes shaking the absorbance at 590 nm was measured.

3.7 Gene expression analysis

3.7.1 RNA isolation and transcription

PATU-8902 cells were grown in six well plate to 80% confluence and incubated 24 hours before experiment in medium without FBS. UCB (10 µM), PCB (30 µM) and extract from *S. platensis* (0.3 g/L) were added and after 1-24 hours RNA was isolated (PerfectPure RNA Cultured Cell Kit, 5PRIME). For cDNA synthesis were used 4 µl of isolated RNA and 4 µl of Random Hexamer Primer (25 pmol/µl). After 5 minutes incubation at 70°C and cooling down to 4°C, the reverse transcription reaction was carried out in 20 µl and contained 4 µl of isolated RNA, 4 µl of Random Hexamer Primer (25 pmol/µl, Biogen), 1.2 µl of Moloney Murine Leukemia Virus reverse transcriptase (M-MLV, 10 000 units, EastPort), 0.5 µl of RNase Inhibitor (RNasin Plus RNase Inhibitor, 10 000 units, EastPort), 1 µl of dNTPs (10 mM), 4 µl of M-MLV Reverse Transcriptase Buffer (5x, EastPort), 5.3 µl deionized water. Reverse transcription reaction was performed at 37°C for 60 minutes.

3.7.2 Real time polymerase chain reaction (RT-PCR)

RT-PCR was performed on ViiA 7 instrument (Applied Biosystems) in 20-µL reaction volumes, containing 4 µL of 10-fold diluted cDNA template from a completed reverse transcription reaction, 1x SYBR Green Master Mix (Applied Biosystems, Foster City, CA, USA), and 200-1000 nM of forward and reverse primers. Data were normalized to hypoxanthine phosphoribosyl transferase level and expressed in percentage to control. Primers used for RT-PCR analyses are given Table 3.

Table 3. Primer sequences for target and internal control genes

	Forward primer	Reverse primer	PCR product (bp)
VEGFA	ACTGAGGAGTCCAACATCACC	CTGCATTCACATTTGTTGTGC	104
NOX2	GATTCTCTTGCCAGTCTGTCG	ATTCCTGTCCAGTTGTCTTCG	94
P22	CTTCACCCAGTGGTACTTTGG	GGCGGTCATGTACTTCTGTCC	130
HPRT	CACTGGCAAAACAATGCAGAC	GGGTCCTTTTCACCAGCAAG	92

VEGFA, vascular endothelial growth factor A; *NOX2*, NADPH oxidase; *p22*, p22phox NADPH oxidase; *HPRT*, hypoxanthine phosphoribosyl transferase.

4 Publications

4.1 Reduction of bilirubin ditaurate by the intestinal bacterium *Clostridium perfringens*

Acta Biochim Pol 2012;59:289-92.

4.2 Bilirubin accumulation and *Cyp* mRNA expression in selected brain regions of jaundiced Gunn rat pups

Pediatr Res 2012;71:653-60.

4.3 Beyond plasma bilirubin: The effects of phototherapy and albumin on brain bilirubin levels in Gunn rats

J Hepatol 2013;58:134-40.

4.4 Antiproliferative effects of carbon monoxide on pancreatic cancer

Dig Liver Dis 2014;46:369-75.

4.5 Anti-cancer effects of blue-green alga *Spirulina platensis*, a natural source of bilirubin-like tetrapyrrolic compounds

Ann Hepatol 2014;13:273-83.

ACTA ABP BIOCHIMICA POLONICA

Vol. 59, No 2/2012
289–291
on-line at: www.actabp.pl

Regular paper

Reduction of bilirubin ditaurate by the intestinal bacterium *Clostridium perfringens*

Renata Koníčková[1*], Alena Jirásková[1,*], Jaroslav Zelenka[1,#], Ladislav Lešetický[2], Martin Štícha[2] and Libor Vítek[1,3]✉

[1]Institute of Medical Biochemistry and Laboratory Diagnostics, 1st Faculty of Medicine, Charles University in Prague, Prague, Czech Republic; [2]Department of Organic and Nuclear Chemistry, Faculty of Science, Charles University in Prague, Prague, Czech Republic; [3]4th Department of Internal Medicine, 1st Faculty of Medicine, Charles University in Prague, Prague, Czech Republic

Bilirubin is degraded in the human gut by microflora into urobilinoids. In our study we investigated whether the bilirubin-reducing strain of *Clostridium perfringens* can reduce bilirubin ditaurate (BDT), a bile pigment of some lower vertebrates, without hydrolysis of the taurine moiety. *C. perfringes* was incubated under anaerobic conditions with BDT; reduction products were quantified by spectrophotometry and separated by TLC. Based on Rf values of BDT reduction products and synthetic urobilinogen ditaurate, three novel taurine-conjugated urobilinoids were identified. It is likely that bilirubin-reducing enzyme(s) serve for the effective disposal of electrons produced by fermentolytic processes in these anaerobic bacteria.

Key words: *Clostridium perfringens*, bile pigments, bilirubin ditaurate, intestinal metabolism, urobilinoids

Received: 19 November, 2011; revised: 17 January, 2012; accepted: 26 April, 2012; available on-line: 27 April, 2012

INTRODUCTION

Unconjugated bilirubin (UCB), a yellow, poorly water-soluble pigment, is the main heme catabolic product in the intravascular compartment. The predominant source of UCB is the breakdown of heme, originating from senescent or hemolyzed red blood cells. After its biotransformation in the liver, secretion into the bile, and then in the intestinal lumen, bilirubin is rapidly reduced to urobilinoids by the intestinal microflora (Vítek & Ostrow, 2009). The term urobilinoids covers the group of reduction products of bilirubin, including urobilinogen and stercobilinogen, along with their oxidized derivatives urobilins and stercobilins (Moscowitz *et al*., 1970). In the absence of bilirubin-reducing microflora, such as in the early newborn period (Vítek *et al*., 2000), or in patients treated with systemic antibiotics (Vítek *et al*., 2005), UCB may undergo substantial enterohepatic and enterosystemic circulation. Severe unconjugated hyperbilirubinaemia in neonates is of concern because of the potential danger to their central nervous system.

UCB is reduced by multiple sequential reactions into a series of urobilinogens; in turn, these colorless chromogens may be oxidized to urobilins, their respective yellowish oxidation products. These substances are believed to be nontoxic due to their increased polarity. Despite the importance of this catabolic pathway, only a few bacterial strains involved in bilirubin reduction have so far been isolated: *Clostridium ramosum* (Gustafsson & Lanke, 1960), *C. perfringens*, *C. difficile* (Vítek *et al*., 2000), and *Bacteroides fragilis* (Fahmy *et al*., 1972). In our recent study (Vítek *et al*., 2006), we undertook a detailed analysis of the products of the bacterial reduction of bilirubin and its derivatives formed by a novel strain of *C. perfringens* isolated from neonatal feces (Vítek *et al*., 2000). The *C. perfringens* strain reduced a wide variety of bile pigments that differed substantially in both their polarity and structure. The end-catabolic bilirubin products resulting from bacterial reduction were identified as urobilinogen species. The reduction process catalyzed by the bacterial strain studied did not proceed to the production of stercobilinogen (Vítek *et al*., 2006).

The aim of the present study was to assess whether bilirubin ditaurate, a pigment that occurs naturally in the bile of certain lower vertebrates (such as the marine fish *Seriola quinqueradiata*) (Sakai *et al*., 1987), can be reduced by the aforementioned strain of *C. perfringens* isolated from human neonatal feces, and secondly, to characterize the reduction products formed.

MATERIAL AND METHODS

***C. perfringens* cultivation.** The strain of *C. perfringens* used in our studies was isolated from stool of a healthy neonate (Vítek *et al*., 2000). The strain was classified in the National Reference Laboratory for Anaerobic Bacteria (Ostrava, Czech Republic) as non-pathogenic, based on the absence of any toxin production. The strain was incubated with BDT and UCB (both from Frontier Scientific, Inc., Logan, UT, USA) in broth (2% Yeast Extract, Oxoid, GB; prepared in 100 mM phosphate buffer, pH=8). Based on their polarity, UCB was dissolved in dimethylsulfoxide (Sigma, St. Louis, MO, USA) and bilirubin ditaurate (BDT) in the broth; both pigments were added to the late exponential phase *C. perfringens* culture, at the final concentration of 50 μmol/L (final concentration of DMSO was <3%, this concentration was found in separate experiments not to influence the growth of *C. perfringens*). The growth phase was monitored according to the optical density of the culture (spectrophotometry at 600 nm). The conversion rates of both bile pigments were analyzed under exactly the same conditions, and calculated from five independent measurements. Af-

✉e-mail: vitek@cesnet.cz
*These authors contributed equally
#Current address: Institute of Physiology, Academy of Sciences of the Czech Republic, Prague, Czech Republic
Abbreviations: BDT, bilirubin ditaurate; UCB, unconjugated bilirubin

ter incubation for 24 h at 37°C in Anaerostat (Oxoid, GB), the medium was sampled for urobilinoid analyses.

Determination and isolation of urobilinoids. The rate of bile pigment conversion was calculated as the proportion of the urobilinoids produced to the initial bile pigment concentration. Concentrations of the UCB and BDT reduction products were determined spectrophotometrically (UV/Vis Spectrophotometer Lambda 20, Perkin-Elmer, USA) as the oxidation products of zinc complexes of urobilinoids, as previously described (Kotal & Fevery 1991).

The pigments were extracted from the culture medium using an SPE column (Strata C8 500 mg/6 ml, Phenomenex, Torrance, CA, USA). The columns were washed with 1 volume of methanol and distilled water. The urobilinoids were eluted with a minimal volume of MeOH:H_2O (1:1, by vol.). The elution mixture was evaporated; the extracted pigments were dissolved in methanol and separated by TLC.

To check whether the BDT-reducing enzyme(s) were secreted into the medium, BDT was incubated with a cell-free supernatant and a protein extract after a French press disintegration of bacterial cells. A *C. perfringens* culture grown overnight (500 ml) was centrifuged (15 000 × *g*, 10 min, 4°C) and the medium was filter-sterilized (Milipore Millex HV, PVDF 0.45 μm). The cells were re-suspended in a phosphate buffer (0.025 M, pH=8) containing 5 mM $MgCl_2$, 2 mM EDTA and 10% glycerol, and then disintegrated using a French press (6 cycles, 1500 psi, SLM-Aminco, USA). The cell debris was removed by centrifugation (15 000 × *g*, 10 min, 4°C) and the supernatant containing the protein extract was filter-sterilized as above. The cell-free supernatant and the protein extract were incubated separately with BDT, as described above; the production of urobilinoids was again determined.

Thin layer chromatography. Isolated BDT and UCB reduction products were separated by TLC, using HPTLC aluminum plates coated with silica gel (RP-18 W/UV_{254}, Macherey-Nagel, Germany) (solvent system: H_2O:MeOH:CH_3COOH (250:250:1, by vol.)) and examined under both visible and UV light (CAMAG TLC Scanner II, CAMAG, Muttenz, Switzerland). Urobilin (Frontier Scientific, Inc., Logan, UT, USA) and urobilinogen ditaurate were used as standards. Urobilinogen ditaurate was prepared by amalgam reduction of bilirubin ditaurate, as previously described (Watson, 1953); with its structure confirmed by mass spectrometry (Esquire 3000, Bruker Daltonics, Bremen, Germany).

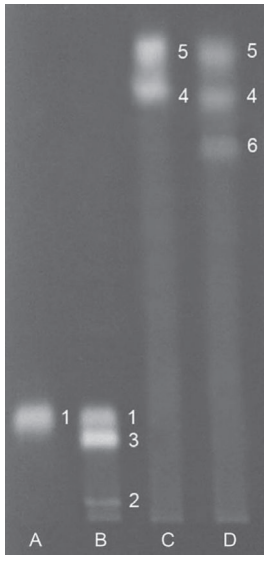

Figure 1. Products of UCB and BDT reduction by *C. perfringens*. The initial pigment concentration in the broth was 50 μmol/L. TLC system specification: HPTLC silica gel plate (RP-18 W/UV_{254}, Macherey-Nagel), solvent system: H_2O:MeOH:CH_3COOH (250:250:1, by vol.). **(Track A)** Urobilin (standard); **(Track B)** Reduction products of UCB; **(Track C)** Urobilinogen ditaurate (standard); **(Track D)** Reduction products of BDT. **(1)** Urobilin; **(2)** Mesobiliviolin; **(3)** Urobilinogen; **(4)** Urobilinogen ditaurate; **(5)** Urobilin ditaurate; **(6)** Mesobiliviolin ditaurate.

RESULTS AND DISCUSSION

The bilirubin-reducing strain of *C. perfringens* isolated from neonatal feces was able to reduce BDT efficiently. The conversion rates were 9±3 and 30±5% in 24 h for BDT and UCB, respectively; this is consistent with our previous findings (Vítek *et al.*, 2006). No reduction of BDT could be detected in cell-free post-culture medium; in contrast, a French press disintegration of the bacterial cells resulted in the release of enzyme(s) capable of reducing BDT, indicating that the BDT reductase is not secreted by the bacteria to the medium.

BDT was reduced by *C. perfringens* into several species of taurine-bound urobilinoids, demonstrating that taurine hydrolysis did not precede the enzymatic reduction (Fig. 1). After TLC separation, no unconjugated urobilinoids derived from BDT could be detected. Based on comparison of the bilirubin reduction products with synthetic urobilinogen ditaurate, three reduction products of BDT were identified: urobilinogen ditaurate, urobilin ditaurate, and (most likely) mesobiliviolin ditaurate (Fig. 1). A more polar taurine-bound urobilin derivative detected in both metabolized BDT and synthetic urobilinogen ditaurate tracks was most likely formed spontaneous oxidation of the urobilinogen ditaurate.

Another bilirubin conjugate, bisglucuronosyl bilirubin, was reduced by the same *C. perfringens* strain into unconjugated urobilinoids; the glucuronoside bond was hydrolyzed prior to the reduction of the tetrapyrroles (Vítek *et al.*, 2006). The amide bond of BDT is presumably resistant to hydrolysis by the enzymes of the intestinal microflora; surprisingly, however, BDT can still be reduced into taurine-bound urobilinoids. These results demonstrate a very broad substrate specificity of the enzyme(s) reducing bilirubin in the human gastrointestinal tract and may help to understand the function of bilirubin reductase. Such a broad substrate specificity of the bilirubin-reducing enzyme(s) presumably serve for the effective disposal of electrons produced by fermentolytic processes in these anaerobic bacteria in a manner similar to that described for microbial bile acid dehydroxylation (Ridlon *et al.*, 2006).

It is interesting to note that despite their ubiquitous occurrence in the human intestinal tract, as well as their high therapeutic potential, the bacterial enzymes responsible for bilirubin reduction have, to date, not been identified.

Acknowledgement

This work was supported by grant CZ:GA CR:P206/11/0836 from the Research Granting Agency of the Czech Republic.

REFERENCES

Fahmy K, Gray CH, Nicholson DC (1972) The reduction of bile pigments by faecal and intestinal bacteria. *Bioch Bioph Acta* **264**: 85–97.

Gustafsson BE, Lanke L (1960) Bilirubin and urobilins in germfree, exgermfree, and conventional rats. *J Exp Med* **112**: 975–981.

Kotal P, Fevery J (1991) Quantitation of urobilinogen in feces, urine, bile and serum by direct spectrophotometry of zinc complex. *Clin Chim Acta* **202**: 1–9.

Moscowitz A, Weimer M, Lightner A, Petryka ZJ, Davis E, Watson CJ (1970) The in vitro conversion of bile pigments to the urobilinoids by a rat clostridia species as compared with the human fecal flora; III. Natural d-Urobilin, synthetic i-urobilin, and synthetic i-urobilinogen. *Biochem Med* **4**: 149–164.

Ridlon JM, Kang DJ, Hylemon PB (2006) Bile salt biotransformations by human intestinal bacteria. *J Lip Res* **47**: 241–259.

Sakai T, Watanabe K, Kawatsu H (1987) Occurrence of ditaurobilirubin, bilirubin conjugated with two moles of taurine, in the gallbladder bile of yellowtail, Seriola quinqueradiata. *J Biochem* **102**: 793–796.

Vítek L, Ostrow JD (2009) Bilirubin chemistry and metabolism; harmful and protective aspects. *Curr Pharm Des* **15**: 2869–2883.

Vítek L, Kotal P, Jirsa M, Malina J, Černá M, Chmelař D, *et al.* (2000). Intestinal colonization leading to fecal urobilinoid excretion may play a role in the pathogenesis of neonatal jaundice. *J Ped Gastroenterol Nutr* **30**: 294–298.

Vítek L, Zelenka J, Zadinová M, Malina J (2005). The impact of intestinal microflora on serum bilirubin levels. *J Hepatol* **42**: 238–243.

Vítek L, Majer F, Muchová L, Zelenka J, Jirásková A, Branny P, *et al.* (2006). Identification of bilirubin reduction products formed by Clostridium perfringens isolated from human neonatal fecal flora. *J Chromat B* **833**: 149–157.

Watson CJ (1953). The direct preparation of crystalline urobilin from bilirubin. *J Biol Chem* **200**: 691–696.

Bilirubin accumulation and *Cyp* mRNA expression in selected brain regions of jaundiced Gunn rat pups

Silvia Gazzin[1], Jaroslav Zelenka[2], Lucie Zdrahalova[2], Renata Konickova[2], Carlos Coda Zabetta[1], Pablo J. Giraudi[1], Andrea L. Berengeno[1], Alan Raseni[3], Maria C. Robert[1], Libor Vitek[4], and Claudio Tiribelli[5]

INTRODUCTION: Few data exist on regional brain bilirubin content in the neonatal period when acute bilirubin-induced neurologic damage (BIND) may occur, and no information is available on regional brain expression of cytochrome P450 monooxygenases (Cyps) that oxidize bilirubin.

METHODS: Bilirubin content was analyzed by high-performance liquid chromatography and *Cyp1a1, 1a2,* and *2a3* mRNA expression was analyzed by quantitative PCR (qPCR) in cortex (Cx), cerebellum (Cll), superior colliculi (SC), and inferior colliculi (IC) of 17-d-old hyperbilirubinemic (jj) Gunn rat pups before and after administration of sulphadimethoxine to acutely displace bilirubin from plasma albumin.

RESULTS: There was no difference in bilirubin content among brain regions in untreated rats. After intraperitoneal sulphadimethoxine, bilirubin content peaked at fourfold in Cx and SC at 1 h; but at 11- to 13-fold in Cll and IC at 24 h; returning to control levels at 72 h. The *Cyp* mRNA peaked at 30–70 times control at 1 h in Cx and SC, but at 3–9 times control at 24 h in Cll and IC.

DISCUSSION: The close relationship in distinct brain regions between the extent of bilirubin accumulation and induction of mRNA of *Cyps* suggests Cyps may have a role in protecting selected brain areas from bilirubin neurotoxicity.

Although physiological neonatal jaundice is believed to protect newborns against oxidative stress (1), severe unconjugated hyperbilirubinemia may cause irreversible bilirubin-induced neurologic damage (BIND) (2). Recent findings emphasize that diffusion of unconjugated bilirubin (UCB) into cells, causing neurotoxicity, is related to the unbound, free fraction of plasma UCB (Bf), rather than the total plasma UCB level (3–5).

Visible staining with UCB in the basal ganglia of both newborn babies who died from extreme hyperbilirubinemia and of jaundiced Gunn rats (the classic animal model of neonatal hyperbilirubinemia and Crigler-Najjar type I syndrome) after a bilirubin load (6–8) is called "kernicterus." However, there are very few reports in humans that strictly describe such selective bilirubin accumulation in specific brain regions (9). Similarly, kernicterus in experimental animals seems to occur only under extreme conditions, e.g., when agents acutely displacing UCB from albumin engender a sudden entry of UCB into the central nervous system. Moreover, previous studies utilized poor analytical methods to document the increases in brain UCB content, so that they were limited to these experimental conditions (6,7).

The first aim of this work was to apply a sensitive, specific high-performance liquid chromatography method (10) to assess tissue UCB levels spontaneously present in Gunn (jj) rats with jaundice due to a homozygous mutation, leading to loss of function of bilirubin-UDP glucuronosyl transferase (UGT1A1), and their heterozygous (Jj) and wild-type (JJ) littermates. The second aim was to study serial changes in regional brain UCB levels when jj Gunn rats were treated with sulphadimethoxine to acutely displace UCB from albumin, mimicking the effects of acute increases in unconjugated hyperbilirubinemia that can occur in jaundiced newborns and patients with Crigler-Najjar type I.

Hyperbilirubinemic Gunn rats partially compensate for their inability to conjugate UCB by its oxidation catalyzed by hepatic cytochrome P450 monooxygenases (Cyps) 1a1, 1a2 (11–13), and 2a3 (Cyp2a5 in humans) (14). Export of UCB by two ATP-binding cassette transporters (ABCc1 and ABCb1) has a role in protecting cultured central nervous system cells from UCB toxicity (15–19). Therefore, the mRNA expression of the three Cyps and two ABC transporters was assessed in selected brain regions by quantitative PCR (qPCR).

RESULTS

Total Bilirubin and Albumin in Plasma

As expected (**Table 1**), the jj rats had much higher plasma bilirubin concentrations at all postnatal ages as compared with both JJ and Jj animals ($P < 0.001$). In jj animals, the bilirubin concentration peaked at day 9 (d9; around 250 μmol/l), remained comparable until d17, and then decreased to about 80 μmol/l at d60 (d60 jj vs. d2, d9, and d17 jj: $P < 0.01$). In heterozygous Jj Gunn rats, plasma bilirubin concentrations at d2 and d9 were 9- and 13-fold higher, respectively, than in

The first two authors contributed equally to this work.
[1]Fondazione Italiana Fegato (Italian Liver Foundation), Trieste, Italy; [2]Institute of Clinical Biochemistry and Laboratory Diagnostics, 1st Faculty of Medicine, Charles University, Prague, Czech Republic; [3]S.C. Laboratorio Analisi Cliniche, IRCCS Burlo Garofolo, Trieste, Italy; [4]Department of Internal Medicine, 1st Faculty of Medicine, Charles University, Prague, Czech Republic; [5]Department of Medical Sciences, 1st Faculty of Medicine, Charles University, Prague, Czech Republic. Correspondence: Silvia Gazzin (silvia.gazzin@csf.units.it)

Received 06 July 2011; accepted 25 January 2012; advance online publication 21 March 2012. doi:10.1038/pr.2012.23

Table 1. Postnatal changes in plasma bilirubin and albumin in Gunn rats

	TBil (μmol/l)			Albumin (μmol/l)			B/A ratio		
	JJ	Jj	jj	JJ	Jj	jj	JJ	Jj	jj
d2	7.3 ± 1.5	66.6 ± 23.4	234.5 ± 33	178 ± 84.2	182.4 ± 69	178.6 ± 66	0.04	0.36	1.31
d9	6.3 ± 1.0	82.3 ± 21.0	247.8 ± 26	238.6 ± 77.6	245.1 ± 77.8	230 ± 85.1	0.03	0.33	1.08
d17	5.7 ± 1.5	6.9 ± 3.8	231.2 ± 57	432.5 ± 83.9	456.7 ± 40.2	420.8 ± 75.6	0.01	0.015	0.55
d60	3.2 ± 0.9	3.1 ± 1.0	82.1 ± 8.7	591.3 ± 20.35	607.5 ± 32.5	581.1 ± 38.3	0.005	0.005	0.14

B/A ratio, plasma bilirubin/albumin molar ratio; d, postnatal day; JJ, wild-type; Jj, heterozygous; jj, homozygous recessive; TBil, total bilirubin in plasma.

age-matched JJ animals ($P < 0.001$), but decreased to levels comparable with JJ animals at d17. In JJ animals, plasma bilirubin levels remained low and constant from d2 to adulthood.

Plasma albumin levels increased significantly from d2 to adulthood ($P < 0.01$, Table 1), without differences among genotypes.

In both JJ and Jj animals, during the whole postnatal period, the plasma bilirubin/albumin molar ratio (B/A) was below 0.6, the cutoff value for increased risk of bilirubin neurotoxicity (20). In contrast, in hyperbilirubinemic jj rats, the ratio was clearly >1 at d2 and at d9, declining to 0.55 at d17. At d60, the B/A ratio in jj rats was within a safe range (Table 1).

Organ UCB Levels in Untreated Gunn Rat Pups at d9 and d17

In jj Gunn rats, at both ages, UCB content in the liver was almost 10 times that of the brain, with intermediate levels in spleen and kidneys, and was significantly greater than in the same organs of Jj and JJ rats (Figure 1).

During development, the organ bilirubin content significantly decreased (by 37–66%) in liver, kidney, and brain of JJ and Jj rats, whereas no statistically significant changes were detected in the same organs of jj animals. Splenic bilirubin content increased significantly with age in jj Gunn rats but did not change in normobilirubinemic animals (Figure 1).

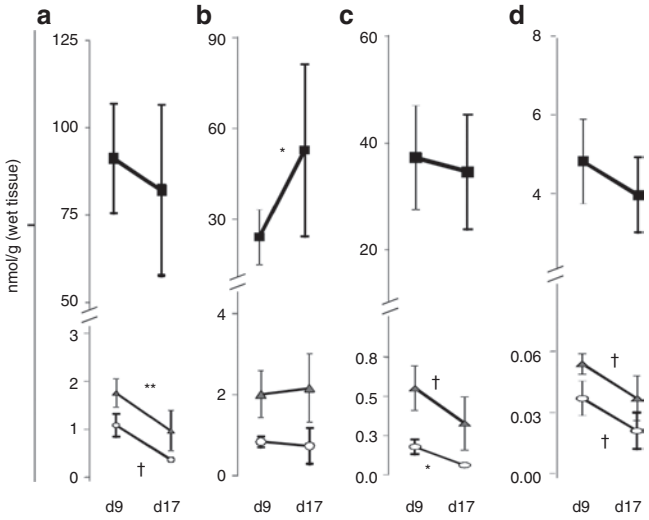

Figure 1. Tissue UCB content in abdominal organs and brain of Gunn rats. d: postnatal age (in days). Filled squares, hyperbilirubinemic jj; filled triangles, heterozygous Jj; and open circles, wild-type JJ Gunn rats. (**a**) Liver; (**b**) spleen; (**c**) kidney; and (**d**) brain. *$P \le 0.05$; **$P \le 0.01$; †$P \le 0.005$. Not statistically significant if not indicated. UCB, unconjugated bilirubin.

Tissue Bilirubin in Selected Brain Regions of Gunn Pups and Effect of Sulphadimethoxine

No differences were detected in UCB content among the four brain regions in the jj rat strain (Figure 2a); this was true also in Jj and JJ pups (data not shown). Despite the similar tissue UCB contents in cortex (Cx) and cerebellum (Cll) of jj animals, a relevant cerebellar hypotrophy was detected in jj animals starting from d9 ($P < 0.01$) and becoming even more drastic at d17 ($P < 0.01$) (Figure 2b); Cx growth was unaffected.

As shown in Figure 3a, the plasma bilirubin level plummeted 90% by 60 min after sulphadimethoxine administration and rose to almost 70% of the original value after 6 h, but took more than 48 h to return to pretreatment levels. This was associated with accumulation of bilirubin in the brain, but the timing and the extent of UCB deposition greatly varied in the different regions explored (Figure 3b–e). In the (b) Cx and (c) superior colliculi (SC), a fourfold increase was observed at 60 min, which then slowly and progressively decreased to or below pretreatment values at 72 h. Bilirubin deposition in the (d) Cll differed markedly, with an 11-fold increase at 6 h that lasted to 24 h and then declined

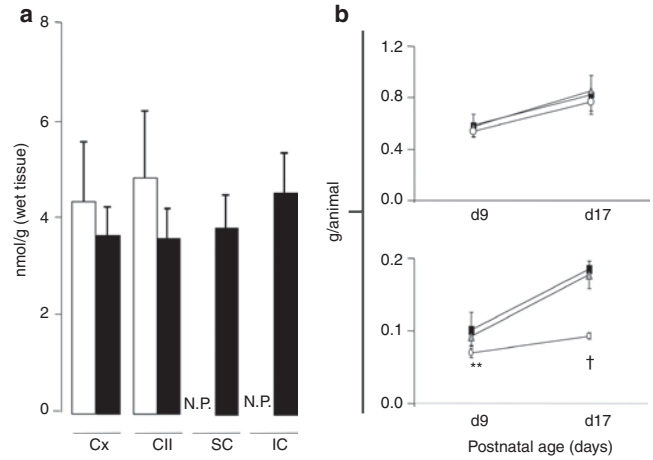

Figure 2. Data on brain regions of untreated, jaundiced jj Gunn rats. (**a**) Tissue UCB content in selected brain regions. White bars: day 9 (d9); black bars: d17. (**b**) Wet weight of cortex (above) and Cll (below). Filled squares, hyperbilirubinemic jj; filled triangles, heterozygous Jj; and open circles, wild-type JJ Gunn rats. **$P \le 0.01$; †$P \le 0.005$. Other differences not statistically significant. Cll, cerebellum; Cx, cerebral cortex; IC, inferior collicula; N.P., not performed; SC, superior collicula; UCB, unconjugated bilirubin.

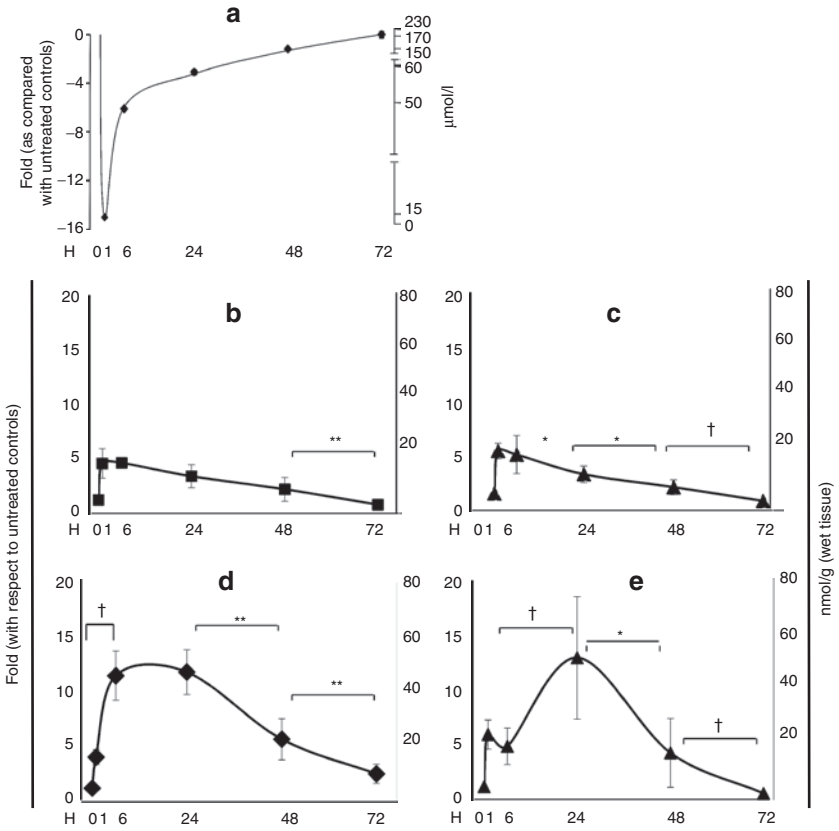

Figure 3. UCB levels in (**a**) plasma and (**b**–**e**) selected brain regions of day 17 jj Gunn rats after sulphadimethoxine exposure. (**b**) Cerebral cortex, (**c**) superior colliculi, (**d**) cerebellum, and (**e**) inferior colliculi. *$P \leq 0.05$; **$P \leq 0.01$; †$P \leq 0.005$. Other differences not statistically significant. The UCB content of each cerebral region of sulphadimethoxine-exposed jj rat is expressed as the ratio to the UCB content in the same region of vehicle-treated jj littermate (control). H, hours after sulphadimethoxine exposure; UCB, unconjugated bilirubin.

slowly to twofold baseline levels at 72 h. In the (e) inferior colliculi (IC), the peak of bilirubin content (13-fold of baseline) was reached at 24 h and returned to pretreatment values at 72 h.

Effects of Sulphadimethoxine on Expression of Cyps in Brain Regions of d17 jj Rats

Similar patterns of mRNA expression of *Cyp1a1, Cyp1a2,* and *Cyp2a3* isoforms were detected in brains of sulphadimethoxine-exposed rats (Figure 4). In the Cx, a strong increase (25- to 70-fold as compared with unexposed, control jj littermates) was observed at 1 and 6 h, decreasing from 24 to 72 h to levels similar to those of unexposed littermates. A similar kinetics was also observed in the SC, where *Cyp* mRNAs were upregulated 20- to 45-fold after 1 h, dropping thereafter to or below pretreatment levels.

In sharp contrast, the Cll and IC exhibited a delayed and less pronounced response to sulpha. *Cyp* mRNAs were unchanged at 1 and 6 h, but at 24 h peaked at 3–5 times controls in the Cll and 5–9 times controls in the IC; levels in both regions declined gradually to normal levels at 72 h.

Effects of Sulphadimethoxine on Expression of ABCs in Brain Regions of d17 jj Rats

Only slight modulation of *ABCc1* and *ABCb1* occurred after sulphadimethoxine treatment (Figure 5). In Cx, *ABCc1* mRNA was unchanged, whereas *ABCb1* expression increased threefold at 1 and 6 h, slowly decreasing to control levels by 72 h. In SC, expression of both *ABCc1* and *ABCb1* displayed similar three- to fourfold upregulation at 1 and 6 h, then gradually declined to or below control levels at 72 h. In Cll, *ABCc1* mRNA gradually increased from 1 to 48 h, then declined to control levels at 72 h; by contrast, *ABCb1* peaked with similar intensity at 24 h. In IC, both transporter mRNAs attained maximal expression after 1 h, then returned to control levels from 6 h on.

Sulphadimethoxine itself did not affect the expression of any Cyp isoenzymes or ABC transporters in the nonjaundiced JJ rats (Figure 6).

DISCUSSION

Only the unbound fraction of UCB (Bf) can enter tissues. This process becomes clinically relevant when the load of bilirubin is excessive or when agents competitively displace UCB from binding sites on albumin (3,5). Because of multiple factors affecting UCB binding and Bf, it has not been possible to define a bilirubin/albumin molar ratio (B/A) considered to be safe in protecting against BIND. In humans, at B/A ≥ 0.7 in blood, irreversible neurological damage often occurs, whereas at B/A ≥ 0.6, it is usually reversible (20). *In vitro* studies suggest that cultured central nervous system cells may suffer UCB toxicity

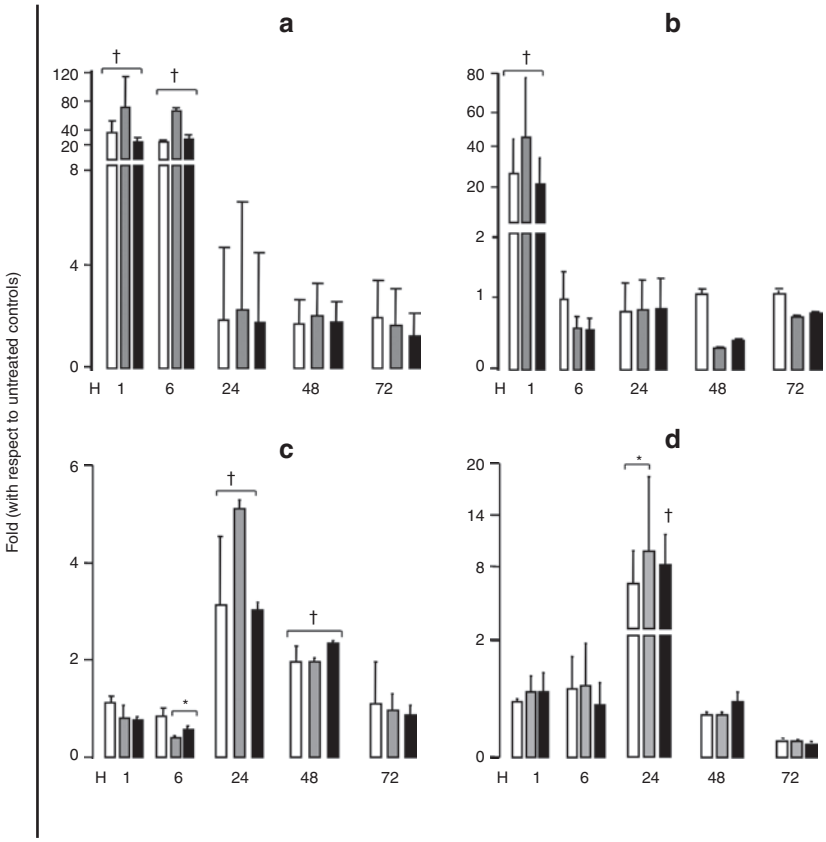

Figure 4. *Cyp* mRNA expression in selected brain regions of day 17 jj Gunn rats after sulphadimethoxine exposure. (**a**) Cerebral cortex, (**b**) superior colliculi, (**c**) cerebellum, and (**d**) inferior colliculi. *$P \leq 0.05$; †$P \leq 0.005$. Other differences not statistically significant. White bars, *Cyp1a1*; gray bars, *Cyp1a2*; and black bars, *Cyp2a3* mRNA expression. *Cyp*, cytochrome P450 monooxygenase; H, hours after sulphadimethoxine exposure.

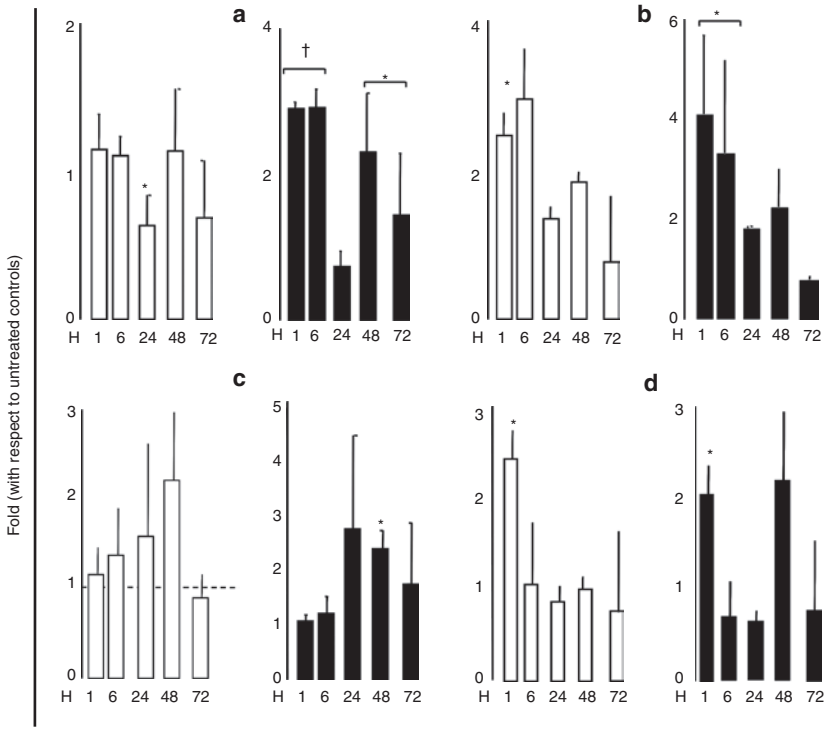

Figure 5. *ABC* mRNA expression in selected brain regions of day 17 jj Gunn rats after sulphadimethoxine exposure. (**a**) Cerebral cortex, (**b**) superior colliculi, (**c**) cerebellum, and (**d**) inferior colliculi. *$P \leq 0.05$; †$P \leq 0.005$. Other differences not statistically significant. White bars, *ABCc1*; black bars, *ABCb1* mRNA expression. H, hours after sulphadimethoxine exposure.

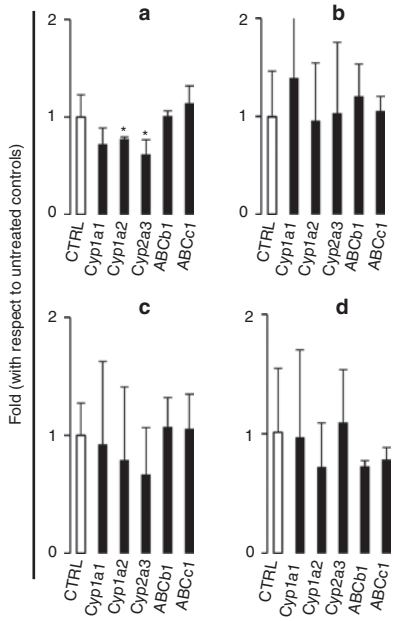

Figure 6. *Cyp* and *ABC* mRNA modulation by sulphadimethoxine in selected brain regions of day 17 JJ Gunn rats. (**a**) Cerebral cortex, (**b**) superior collicula, (**c**) cerebellum, and (**d**) inferior collicula. *$P \leq 0.05$. Other differences not statistically significant. White bars, controls (vehicle-injected animals) and black bars, sulpha-treated rats. *Cyp*, cytochrome P450 monooxygenase.

at even lower ratios (<0.5) (3,21,22), but caution is advised in extrapolation of the *in vitro* data to the much more complicated situation *in vivo*.

Hyperbilirubinemia in jj Gunn rats results from a deficiency of hepatic UGT1A1, similar to that seen in human patients with Crigler-Najjar type I and analogous to the decreased conjugating activity seen in human neonates during the first days of life (23). As in severely jaundiced newborns, the high levels of UCB in plasma of jj Gunn rat pups, with B/A ratios exceeding 1.0 at d2 and d9, resulted in accumulation of UCB in the tissues in the early neonatal period; in jj Gunn pups, this causes marked cerebellar hypotrophy from d9 onward (24,25). In heterozygous (Jj) Gunn rats, the milder, early, temporary hyperbilirubinemia did not impair cerebellar growth, suggesting that the 0.36 B/A ratio found at d2 may be safe. It is interesting that d2 jj rats showed no signs of bilirubin toxicity (4,25), suggesting that it takes time for UCB to accumulate in the central nervous system and/or for neurotoxicity to develop.

In jj Gunn rats, we found UCB content to be higher in liver than in spleen and kidneys, and much lower in whole brain (Figure 1). As reported in humans (20), visceral bilirubin concentrations decreased less rapidly than plasma bilirubin levels from d9 to d17, whereas brain UCB content declined more rapidly (24%) than plasma bilirubin levels (6.5%) during the same period. The decline of UCB content in all organs is likely in part related to the large increase in plasma albumin from d9 to d17, enhancing the decrease in plasma B/A ratio and Bf concentration as total plasma UCB levels decline. This is consistent with previous reports of lower bilirubin concentrations in liver, spleen, kidney, and whole brain of adult Gunn rats than in pups (26).

The differences in UCB content and rates of decline among the organs (Figure 1) indicate, however, that tissue UCB levels must also be controlled by other mechanisms. The production rates of UCB in the organ and the permeability to UCB of the blood–organ barriers (10) determine the supply of UCB. Because Gunn (jj) rats cannot conjugate bilirubin, the cellular export of UCB (15,16,18,19) and UCB oxidation (12,14,26–28) might play a role in UCB removal from the brain of these animals.

Our study in jj rats after sulphadimethoxine administration provides important new data on the time dependency of the consequent sudden, massive accumulation and gradual clearance of UCB in different brain regions (Figure 3b–e). Notable are the much greater and longer-lasting accumulations of UCB in the Cll and IC, whose functions (motor coordination and auditory, respectively) are impaired in bilirubin encephalopathy of sudden onset after sulphadimethoxine administration (29), and the more gradual onset in jaundiced neonates and jj Gunn rats. By contrast, UCB accumulation after sulphadimethoxine was limited and brief in the Cx and IC, whose functions (cognition and vision, respectively) are unimpaired in BIND. The spatial nearness of the SC and IC suggest further that their markedly different kinetics and severity of UCB accumulation after sulphadimethoxine are unlikely to be due to differences blood supply or blood–brain barriers, but most probably are linked to cellular mechanisms for removal of UCB.

This conclusion is further supported by the relationships between expression of Cyps known to oxidize UCB and the dynamics of tissue UCB in the selected brain regions. Figures 4 and 5 show an immediate and massive upregulation of the *Cyp* mRNAs and much smaller immediate upregulation of the ABC transporters in the unaffected brain regions (Cx and SC), in striking contrast to the delayed and relatively puny upregulation of Cyps and ABC transporters in the affected brain regions (Cll and IC). The timing seems to fit with the decline in tissue UCB levels after 1 h in the unaffected regions but only after 6 h in the affected regions (Figure 4). This suggests that these Cyps (and, presumably, UCB oxidation) provide major protection against acute accumulation of UCB in the unaffected regions, with the ABC transporters playing a minor role. Because only mRNA expression was assessed, confirmation of this hypothesis will require further studies of upregulation of enzyme and transporter protein levels and activities. It needs to be determined also if similar, differential, short-term upregulation of Cyps is stimulated by the relatively rapid, albeit less massive and precipitous, spontaneous increases in brain UCB content during the week after birth in untreated jj Gunn pups

The similarity of increments in tissue UCB levels 1 h after sulpha administration suggests that there are similar rates of passive diffusion of UCB in all four brain regions during this early accumulation of UCB. Selective upregulation of Cyps, enhancing UCB oxidation, more likely accounts for the subsequent decline in tissue UCB levels. Based on this reasoning, we speculate that limited passive diffusion

across the blood–brain and blood–cerebrospinal fluid barriers, rather than oxidation or export of UCB, is also the dominant factor determining the similarity of UCB content observed among the four brain regions of untreated jj Gunn rats at d17 (Figure 2). The reasons why the upregulation differs among different portions of the brain need to be further investigated.

Our data suggest that the historical concept of kernicterus, based on selective damage due to regional bilirubin accumulation in the brain, should be reassessed. Our study shows that regional modulation of Cyps may account for the differences among brain regions in severity and duration of bilirubin accumulation during sudden increases in Bf. It remains to be determined whether BIND in jaundiced Gunn rat pups and neonates is similarly influenced by modulation of intracellular defensive mechanisms, such as oxidation of UCB.

METHODS

Animals

Hyperbilirubinemic Gunn rats (jj) (30) with congenital deficiency of UGT1A1 (23) and their heterozygous (Jj) and normobilirubinemic wild-type (JJ) littermates (31) were bred in the animal facility of the CSPA, University of Trieste. Parturitions were synchronized to obtain a sufficient number of littermate pups of each genotype and postnatal age (d ± 1).

Animal care and procedures were conducted according to the guidelines approved by Italian Law (decree 116-92) and by European Community directive 86-609-EEC. The study was approved by the animal care and use committee of the University of Trieste.

Experimental Plan

Scheme A: Tissue bilirubin contents in untreated jj, Jj, and JJ Gunn rat pups (Figure 7a). Based on previous reports (6,24,25,32), six pups were studied at each of two postnatal ages: d9, when cerebellar growth arrests, and d17, when plasma UCB levels begin to decline. Tissue bilirubin was analyzed in organs involved in heme catabolism or affected by bilirubin toxicity.

Scheme B: Regional brain UCB content in d17 jj Gunn rat pups given sulphadimethoxine (Figure 7b). As described by others (6,8), sulphadimethoxine (200 mg/kg, 3 mg/ml in phosphate-buffered saline) was injected intraperitoneally to displace UCB from plasma albumin and acutely shift UCB (as Bf) from blood to brain. After isofluorane anesthesia, and the first blood sample collection, the animals were administered sulphadimethoxine solution (sulpha) or an equal volume of phosphate-buffered saline (controls), and all pups returned to the wet-nurse. Six (jj) pups each were killed at 1, 6, 24, 48, and 72 h after sulpha administration, and blood and four selected brain regions were analyzed for UCB content.

Animal Sacrifice and Sample Collection

Under deep urethane anesthesia (1.0–1.2 g/kg intraperitoneally.), a heparinized blood sample was collected by jugular puncture. To minimize contamination of tissues with UCB in blood, the animals were immediately perfused (10) through the incanulated heart left

a

T1: few seconds	Blood sample collection		
T2: few seconds	Animal perfusion		
T3: 5–10 min	Sample dissection		
	JJ	Jj	jj
P9 (*n*)	3	6	6
P17 (*n*)	6	6	6

b

T1: few seconds	Blood collection				
T2: few seconds	Sulphadimethoxine (200 mg/kg) injection (IP)				
$T2_1$: 1 h later $T2_6$: 6 h later $T2_{24}$: 24 h later $T2_{48}$: 48 h later $T2_{72}$: 72 h later	Animals returned to mothers				
T3: few seconds	2_{nd} blood collection				
T4: few seconds	Animal anesthesia				
T4: few seconds	Animal perfusion				
T5: 5–10 min	Sample collection				
H	1	6	24	48	72
Control (*n*)	6	6	6	6	6
Treated (*n*)	6	6	6	6	6

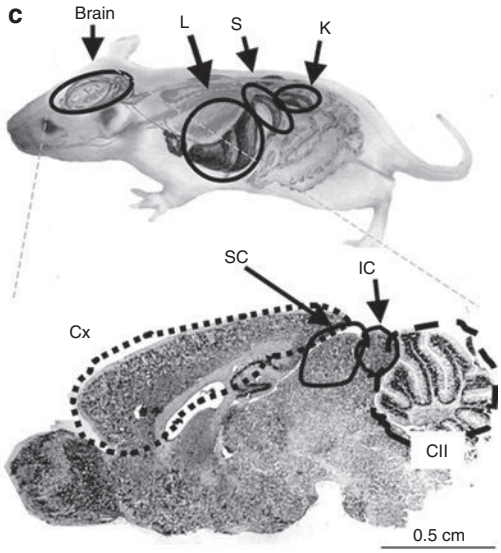

Figure 7. Experimental scheme. (**a**) Tissue bilirubin in untreated Gunn rat pups. JJ: wild-type, Jj: heterozygous, and jj: homozygous recessive, hyperbilirubinemic Gunn rats. (**b**) Tissue bilirubin in Gunn rat pups after exposure to sulphadimethoxine. (**c**) Drawing of dissected organs/tissues. CII, cerebellum; Cx, cortex; d, postnatal age in days; H, hours after sulphadimethoxine exposure; IC, inferior colliculi; IP, intraperitoneal; K, kidney; L, liver; *n*, number of animals used; S, spleen; SC, superior colliculi. Cerebral microsection provided by courtesy of G. Meroni and F. Petrera.

Table 2. qPCR primer specifications

Gene	Accession number	Sense	Antisense	Amplicon length (bp)	Efficiency (%)
Cyp1a1	NM_01254.2	CAGGCGAGAAGGTGGATATGAC	GGTCTGTGTTTCTGACTGAAGTTG	181	91.5
Cyp1a2	NM_012541.3	GTGGTGGAATCGGTGGCTAATGTC	GGGCTGGGTTGGGCAGGTAG	175	116.9
Cyp2a3	NM_007812	ACACAGGCACCCCAGGACATC	CCAGGCTCAACGGGACAAGAAAC	99	109.2
ABCc1	NM_022281	ATGGTGTCAGTGGTTTAGG	TGTGGGAAGAAGAGTTGC	111	99.2
ABCb1	NM_133401	GAGGGCGAGGTCAGTATC	AATCATAGGCATTGGCTTCC	193	92.9
Actin	NM_031144.2	GGTGTGATGGTGGGTATG	CAATGCCGTGTTCAATGG	103	95.5
Gapdh	NM_017008	CTCTCTGCTCCTCCCTGTTC	CACCGACCTTCACCATCTTG	87	106
Hprt1	NM_12583.2	AGACTGAAGAGCTACTGTAATGAC	GGCTGTACTGCTTGACCAAG	163	94.9

bp, base pairs.

ventricle using a peristaltic pump, until the effluent was visibly free of red cells.

After decapitation, the Cx, Cll, SC, and IC were dissected and cleaned of meninges and choroid plexuses as described previously for Cx (33). In scheme A, the abdominal organs mainly involved in metabolism of bilirubin (liver, spleen, kidney) were also collected (**Figure 7c**). Each tissue/organ sample was divided into two parts, one for tissue bilirubin quantification and the second one for mRNA extraction followed by qPCR analysis. Samples were immediately stored at −80 °C until analysis. All sampling and subsequent analyses were performed under dim light, using foil-wrapped tubes, to minimize bilirubin photooxidation.

Tissue Bilirubin Quantification

UCB content was determined on rapidly thawed samples using high-performance liquid chromatography with diode array detector (Agilent, Santa Clara, CA) as described (10). Briefly, 300 pmol of mesobilirubin in dimethylsulfoxide (internal standard) was added, and samples were homogenized on ice. Bile pigments were then extracted into chloroform/hexane (5:1 vol/vol) at pH 6.0, and contaminants removed by extraction of the pigments in a minimum volume of methanol/sodium carbonate (pH 10). The resulting polar droplet was loaded onto a C-8 reverse-phase column (Phenomenex, Torrance, CA), and separated pigments were detected at 440 nm. The concentration of UCB, determined from the area under the curve of the UCB peak in reference to the internal standard of mesobilirubin, was calculated as nmol/g of wet tissue weight.

Total Bilirubin and Albumin Determination in Plasma

After centrifugation (2,500 rpm, 20 min at room temperature), plasma was collected and immediately frozen at −20 °C until assayed. Plasma total bilirubin and albumin were quantified, respectively, by the diazo-reaction (Boehringer-Mannheim Kit 1552414, Monza, Italy) and by the ALB-Plus BCG (Roche Diagnostic, Milan, Italy) kits on an automated Roche–Hitachi analyzer (Roche Diagnostic, Milan, Italy). Samples with hemolysis were discarded.

qPCR Analysis of *Cyp* and *ABC* Transcripts

Total RNA from each region dissected from d17 jj animals exposed to sulpha or vehicle alone was isolated in TriReagent (Sigma-Aldrich, St Louis, MO) and retro-transcribed (1 μg) using the iScript cDNA Synthesis kit (Bio-Rad Laboratories, Hercules, CA) according to the manufacturer's instructions. Three d17 JJ animals were also injected with sulpha or vehicle to assess a possible direct effect of sulphadimethoxine *per se* (1 h) in animals who generate little Bf because of very low serum UCB levels.

Tissue mRNA levels were determined for *Cyp1a1, Cyp1a2, Cyp2a3, ABCc1,* and *ABCb1,* and the housekeeping genes (*actin*; hypoxanthine-guanine phosphoribosyltranferase, *Hprt1;* and glyceraldehydes 3-phosphate dehydrogenase, *Gapdh*) (for details see **Table 2**). The qPCR was performed on 25 ng cDNA with gene-specific sense and antisense primers (250 nmol/l, all genes) with iQ SYBR Green Supermix in an i-Cycler IQ thermocycler (both from Bio-Rad Laboratories). The thermal cycler conditions consisted of 3 min at 95 °C and 40 cycles each at 95 °C for 20 s, 60 °C for 20 s, and 72 °C for 30 s. Specificity of the amplification was verified by a melting-curve analysis: nonspecific products of PCR were not found in any case.

The relative quantification was made using Genex software (Bio-Rad Laboratories) based on the ΔΔCt method, taking into account the efficiencies of individual genes and normalizing the results to the three housekeeping genes. The levels of mRNA were expressed relative to a selected sample.

Statistical Analysis

All data are given as means ± SD. Statistical differences between age-matched animals with the same genotype were analyzed using the unpaired, nonparametric, two-tail, Mann–Whitney test. Comparison of different postnatal ages within the same genotype was performed by ANOVA, followed by Tukey–Kramer multiple comparisons test. Differences were considered statistically significant at a P value < 0.05.

ACKNOWLEDGMENTS

The authors thank P. Zarattini and A. Lorenzon (CSPA, University of Trieste) for help in the experimental procedure concerning the sulphadimethoxine treatments, J. Donald Ostrow for helpful discussions and critical reading of the manuscript, and G. Meroni and F. Petrera for the cerebral microsection in **Figure 7**.

STATEMENT OF FINANCIAL SUPPORT

This work was supported by the Regione Friuli Venezia Giulia (Fondo Regionale FVG LR26/2005), the Telethon grant (GGP10051), the Italian Ministry of Foreign Affairs, Rome, Italy (PhD fellowships to A.L.B., M.C.R., and C.C.Z.) and by the Czech Ministry of Education (2B06155) and the Research Granting Agency of the Czech Republic (CZ:GA CR:P206/11/0836).

REFERENCES

1. Benaron DA, Bowen FW. Variation of initial serum bilirubin rise in newborn infants with type of illness. Lancet 1991;338:78–81.
2. Bhutani VK, Johnson L. 2005 Kernicterus: a preventable neonatal brain injury. J Arab Neonatal Forum 2005;2:12–24.
3. Calligaris SD, Bellarosa C, Giraudi P, Wennberg RP, Ostrow JD, Tiribelli C. Cytotoxicity is predicted by unbound and not total bilirubin concentration. Pediatr Res 2007;62:576–80.
4. Takahashi M, Sugiyama K, Shumiya S, Nagase S. Penetration of bilirubin into the brain in albumin-deficient and jaundiced rats (AJR) and Nagase analbuminemic rats (NAR). J Biochem 1984;96:1705–12.
5. Ahlfors CE, Wennberg RP. Bilirubin-albumin binding and neonatal jaundice. Semin Perinatol 2004;28:334–9.
6. Cannon C, Daood MJ, O'Day TL, Watchko JF. Sex-specific regional brain bilirubin content in hyperbilirubinemic Gunn rat pups. Biol Neonate 2006;90:40–5.
7. Aono S, Semba R, Sato H, Kashiwamata S. Mode of bilirubin deposition in the cerebellum of developing jaundiced Gunn rats. Biol Neonate 1989;55:119–23.
8. Daood MJ, Watchko JF. Calculated *in vivo* free bilirubin levels in the central nervous system of Gunn rat pups. Pediatr Res 2006;60:44–9.
9. Hansen TW. Pioneers in the scientific study of neonatal jaundice and kernicterus. Pediatrics 2000;106:E15.
10. Zelenka J, Lenícek M, Muchová L,*et al*. Highly sensitive method for quantitative determination of bilirubin in biological fluids and tissues. J Chromatogr B Analyt Technol Biomed Life Sci 2008;867:37–42.
11. Kapitulnik J, Gonzalez FJ. Marked endogenous activation of the CYP1A1 and CYP1A2 genes in the congenitally jaundiced Gunn rat. Mol Pharmacol 1993;43:722–5.
12. De Matteis F, Lord GA, Kee Lim C, Pons N. Bilirubin degradation by uncoupled cytochrome P450. Comparison with a chemical oxidation system and characterization of the products by high-performance liquid chromatography/electrospray ionization mass spectrometry. Rapid Commun Mass Spectrom 2006;20:1209–17.
13. Pons N, Pipino S, De Matteis F. Interaction of polyhalogenated compounds of appropriate configuration with mammalian or bacterial CYP enzymes. Increased bilirubin and uroporphyrinogen oxidation in vitro. Biochem Pharmacol 2003;66:405–14.
14. Abu-Bakar A, Moore MR, Lang MA. Evidence for induced microsomal bilirubin degradation by cytochrome P450 2A5. Biochem Pharmacol 2005;70:1527–35.
15. Hankø E, Tommarello S, Watchko JF, Hansen TW. Administration of drugs known to inhibit P-glycoprotein increases brain bilirubin and alters the regional distribution of bilirubin in rat brain. Pediatr Res 2003;54:441–5.
16. Watchko JF, Daood MJ, Mahmood B, Vats K, Hart C, Ahdab-Barmada M. P-glycoprotein and bilirubin disposition. J Perinatol 2001;21:Suppl 1:S43–7; discussion S59–62.
17. Corich L, Aranda A, Carrassa L, Bellarosa C, Ostrow JD, Tiribelli C. The cytotoxic effect of unconjugated bilirubin in human neuroblastoma SH-SY5Y cells is modulated by the expression level of MRP1 but not MDR1. Biochem J 2009;417:305–12.
18. Calligaris S, Cekic D, Roca-Burgos L,*et al*. Multidrug resistance associated protein 1 protects against bilirubin-induced cytotoxicity. FEBS Lett 2006;580:1355–9.
19. Falcão AS, Bellarosa C, Fernandes A,*et al*. Role of multidrug resistance-associated protein 1 expression in the *in vitro* susceptibility of rat nerve cell to unconjugated bilirubin. Neuroscience 2007;144:878–88.
20. Strauss KA, Robinson DL, Vreman HJ, Puffenberger EG, Hart G, Morton DH. Management of hyperbilirubinemia and prevention of kernicterus in 20 patients with Crigler-Najjar disease. Eur J Pediatr 2006;165:306–19.
21. Ostrow JD, Pascolo L, Shapiro SM, Tiribelli C. New concepts in bilirubin encephalopathy. Eur J Clin Invest 2003;33:988–97.
22. Watchko JF. Kernicterus and the molecular mechanisms of bilirubin-induced CNS injury in newborns. Neuromolecular Med 2006;8:513–29.
23. Chowdhury JR, Kondapalli R, Chowdhury NR. Gunn rat: a model for inherited deficiency of bilirubin glucuronidation. Adv Vet Sci Comp Med 1993;37:149–73.
24. Conlee JW, Shapiro SM. Development of cerebellar hypoplasia in jaundiced Gunn rats: a quantitative light microscopic analysis. Acta Neuropathol 1997;93:450–60.
25. Keino H, Sato H, Semba R, Aono S, Aoki E, Kashiwamata S. Mode of prevention by phototherapy of cerebellar hypoplasia in a new Sprague-Dawley strain of jaundiced Gunn rats. Pediatr Neurosci 1985;12:145–50.
26. Schmid R, Hammaker L. Metabolism and disposition of c14-bilirubin in congenital nonhemolytic jaundice. J Clin Invest 1963;42:1720–34.
27. Kapitulnik J, Ostrow JD. Stimulation of bilirubin catabolism in jaundiced Gunn rats by an induced of microsomal mixed-function monooxygenases. Proc Natl Acad Sci USA 1978;75:682–5.
28. Zaccaro C, Sweitzer S, Pipino S,*et al*. Role of cytochrome P450 1A2 in bilirubin degradation Studies in Cyp1a2 (-/-) mutant mice. Biochem Pharmacol 2001;61:843–9.
29. Ahlfors CE, Shapiro SM. Auditory brainstem response and unbound bilirubin in jaundiced (jj) Gunn rat pups. Biol Neonate 2001;80:158–62.
30. Gunn CH. Hereditary acholuric jaundice in a new mutant strain of rats. J Hered 1938;29:137–9.
31. Zarattini P, Gazzin S, Stebel M. Improvement of a historical animal model for Crigler Najjar Type I syndrome: development of the normobilirubinemic JJ genotype as a true control for the Gunn jaundiced rat, 2011. Experimental Models: 110-114. (http://www.felasa.eu/media/uploads/Proceedings_FELASA-ScandLAS-2010_small_SEC.pdf).
32. Gazzin S, Berengeno AL, Strazielle N,*et al*. Modulation of Mrp1 (ABCc1) and Pgp (ABCb1) by bilirubin at the blood-CSF and blood-brain barriers in the Gunn rat. PLoS ONE 2011;6:e16165.
33. Gazzin S, Strazielle N, Schmitt C,*et al*. Differential expression of the multidrug resistance-related proteins ABCb1 and ABCc1 between blood-brain interfaces. J Comp Neurol 2008;510:497–507.

Research Article

EASL EUROPEAN ASSOCIATION FOR THE STUDY OF THE LIVER | JOURNAL OF HEPATOLOGY

Beyond plasma bilirubin: The effects of phototherapy and albumin on brain bilirubin levels in Gunn rats

Frans J.C. Cuperus[1,†], Andrea B. Schreuder[1,†], Deirdre E. van Imhoff[2], Libor Vitek[3,4], Jana Vanikova[3], Renata Konickova[3], Charles E. Ahlfors[5], Christian V. Hulzebos[2], Henkjan J. Verkade[1,*]

[1] *Pediatric Gastroenterology and Hepatology, Department of Pediatrics, Center for Liver, Digestive, and Metabolic Diseases, Beatrix Children's Hospital – University Medical Center Groningen, University of Groningen, Hanzeplein 1, 9713 GZ Groningen, The Netherlands;* [2]*Neonatology, Department of Pediatrics, Beatrix Children's Hospital – University Medical Center Groningen, Hanzeplein 1, 9713 GZ Groningen, The Netherlands;* [3]*Institute of Clinical Biochemistry and Laboratory Diagnostics, 1st Faculty of Medicine, Charles University, U Nemocnice 2, 12808 Prague 2, Czech Republic;* [4]*4th Department of Internal Medicine, 1st Faculty of Medicine, Charles University, U Nemocnice 2, 12808 Prague 2, Czech Republic*
[5]*Stanford University, School of Medicine, 750 Welch Road, Suite 212, Palo Alto, CA 94304, USA*

Background & Aims: Severe unconjugated hyperbilirubinemia, as occurs in Crigler–Najjar disease and neonatal jaundice, carries the risk of neurotoxicity. This neurotoxicity is related to the increased passage of free bilirubin (UCB_{free}), the fraction of bilirubin that is not bound to plasma proteins, into the brain. We hypothesized that albumin treatment would lower the UCB_{free} fraction, and thus decrease bilirubin accumulation in the brain.
Methods: We treated chronic (e.g., as a model for Crigler–Najjar disease) and acute hemolytic (e.g., as a model for neonatal jaundice) moderate hyperbilirubinemic Gunn rats with phototherapy, human serum albumin (HSA) or phototherapy + HSA.
Results: In the chronic model, adjunct HSA increased the efficacy of phototherapy; it decreased plasma UCB_{free} and brain bilirubin by 88% and 67%, respectively (p <0.001). In the acute model, adjunct HSA also increased the efficacy of phototherapy; it decreased plasma UCB_{free} by 76% (p <0.001) and completely prevented the hemolysis-induced deposition of bilirubin in the brain. Phototherapy alone failed to prevent the deposition of bilirubin in the brain during acute hemolytic jaundice.
Conclusions: We showed that adjunct HSA treatment decreases brain bilirubin levels in phototherapy-treated Gunn rats. We hypothesize that HSA decreases these levels by lowering UCB_{free} in the plasma. Our results support the feasibility of adjunct albumin treatment in patients with Crigler–Najjar disease or neonatal jaundice.

Keywords: Unconjugated hyperbilirubinemia; Phototherapy; Albumin; Brain; Gunn rat.
Received 20 February 2012; received in revised form 9 August 2012; accepted 13 August 2012; available online 21 August 2012
* Corresponding author. Tel.: +31 50 36 15513; fax: +31 50 36 11671.
E-mail address: h.j.verkade@umcg.nl (H.J. Verkade).
† These authors contributed equally to this work.

Introduction

Crigler–Najjar patients and hemolytic neonates suffer from unconjugated hyperbilirubinemia [1]. Severe unconjugated hyperbilirubinemia can lead to brain damage. This damage is mediated by the ability of "free" bilirubin (UCB_{free}), the small (<1%) fraction of unconjugated bilirubin (UCB) not bound to plasma proteins, to cross the blood–brain barrier (BBB) [2–6]. Within the brain, UCB disrupts several vital cell functions and induces apoptosis and necrosis. Bilirubin-induced neurotoxicity may eventually lead to kernicterus and even death [3,7,8].

Severe unconjugated hyperbilirubinemia is conventionally treated by phototherapy, which converts UCB into photoisomers that can readily be excreted in the bile [9]. Phototherapy, however, has some disadvantages. Crigler–Najjar patients, who suffer from a permanent unconjugated hyperbilirubinemia due to a genetically absent (type I) or decreased (type II) capacity to conjugate bilirubin in the liver, may need up to 16 h of phototherapy treatment per day. In spite of this intensive regimen, up to 25% of these patients will eventually develop brain damage [10,11]. Phototherapy is more effective during neonatal hemolytic jaundice, but may still require additional, potentially dangerous, exchange transfusions [12]. The efficacy of phototherapy is often estimated by its hypobilirubinemic effect. Plasma bilirubin levels, however, correlate poorly with the occurrence of brain damage in individual patients [6]. The reason for this poor correlation lies in the inability of protein-bound bilirubin (>99% of total plasma bilirubin) to leave the circulation [2,3,5,6]. Only UCB_{free}, is able to translocate across the blood–brain barrier (BBB), and thus plays a key role in the pathogenesis of bilirubin-induced brain damage. UCB_{free} concentrations, however, are not routinely evaluated in phototherapy-treated patients. The main reason for this lies in the inaccuracy of the commercial UCB_{free} test, most notably caused by a 42-fold sample dilution that alters bilirubin–albumin binding [13].

We reasoned that decreasing UCB_{free} in the plasma could prevent bilirubin deposition in the brain. Human serum albumin (HSA) infusion could, theoretically, achieve this goal by providing

additional binding sites for UCB_{free} in the plasma. Interestingly, HSA treatment has been used in severely jaundiced neonates [14–18]. Its efficacy, however, has been difficult to establish. This difficulty is due to the obvious inability to measure bilirubin brain levels in humans, but also to the aforementioned inaccuracy of the commercially available UCB_{free} test. Recently, Zelenka *et al.* developed a highly sensitive method for tissue bilirubin determinations, while Ahlfors *et al.* developed an automated UCB_{free} test with minimal sample dilution [13,18]. We now use these techniques to evaluate the effect of HSA treatment on plasma UCB_{free} and brain bilirubin levels in two well-established animal models. As a moderate chronic model, resembling patients with Crigler–Najjar disease, we treated adult Gunn rats with long-term phototherapy, HSA or phototherapy + HSA [19]. As an acute model, resembling severe hemolytic jaundice, we induced hemolysis by 1-acetyl-2-phenyl-hydrazine (APHZ) in adult Gunn rats, and then treated these animals for 48 h with phototherapy, HSA, or phototherapy + HSA [20]. We demonstrate that HSA treatment decreases plasma UCB_{free} and brain bilirubin levels in phototherapy-treated Gunn rats, during both chronic and acute jaundice. We speculate that HSA and phototherapy work in tandem: HSA binds to UCB_{free} within the plasma, and phototherapy then promotes its excretion via the bile. Our results underline the need to evaluate the use of HSA as adjunct to phototherapy in randomized clinical trials.

Materials and methods

Animals

Homozygous male Gunn rats, the animal model for Crigler–Najjar disease type I (RHA/jj; 225–340 g, aged 10–12 weeks), were obtained from our breeding colony, kept in an environmentally controlled facility, and fed *ad libitum* with free access to water. Food intake, fluid intake, and body weight were determined regularly. The Animal Ethics Committee of the University of Groningen (Groningen, The Netherlands) approved all experimental protocols.

Materials

Hope Farms B.V. (Woerden, The Netherlands) produced the semi-synthetic control diet (code 4063.02), containing 13 energy% fat and 5.2 wt% long-chain fatty acids. In previous studies, we noticed that diet and diet-composition influence plasma bilirubin levels. We used the same semi-synthetic control diet and animal model (identical strain and breeding colony) as in previous studies to enhance reproducibility and to allow comparison between studies (please refer to references [21–23] for a further characterization). Gunn rats were fed this diet during a 5-week run-in period, to ensure steady-state conditions, and during the experiments. HSA (Albuman®; 200 g/L, fatty acid free) was purchased from Sanquin (Amsterdam, The Netherlands). APHZ, horseradish peroxidase type 1, D-glucose, glucose oxidase, hydrogen peroxide and UCB were purchased from Sigma Chemical Co. (St. Louis, MO). Commercial UCB was further purified according to the method of Ostrow *et al.* [24]. Phototherapy was administered continuously to Gunn rats (shaven on flank and back) via two blue phototherapy lamps (Philips, TL-20W/03T) suspended in a reflective canopy 20 cm above the cage. The phototherapy dose (17 $\mu W/cm^2/nm$; 380–480 nm) was measured by an Elvos-LM-1010 Lux meter at 20-cm distance [23].

Methods

Permanent unconjugated hyperbilirubinemia

Adult Gunn rats were randomized to receive either no treatment (n = 13) or phototherapy (17 $\mu W/cm^2/nm$; n = 14) for 16 days. After 14 days of phototherapy treatment, to ensure steady-state conditions [21–23], we randomized the animals to receive either no treatment (n = 7), phototherapy (17 $\mu W/cm^2/nm$) + NaCl 0.9% (w/v; n = 7), HSA (2.5 g/kg, n = 6), or phototherapy + HSA (n = 7), for another 48 h. NaCl 0.9% (control/sham) and HSA were administered as a single i.p. injection at t = 14 days. We determined plasma bilirubin concentrations from tail vein blood at t = 0, 14, and 16 days, and determined plasma UCB_{free} at t = 16 days under isoflurane anesthesia. After 16 days, all animals were exsanguinated via the descending aorta and flushed via the same port with 100–150 ml NaCl 0.9% under isoflurane anesthesia. Brain, liver, and aliquots of visceral fat were subsequently harvested for the determination of tissue bilirubin levels. These samples were rinsed 2 times in phosphate buffered saline, snap frozen in liquid nitrogen, and immediately stored (wrapped in aluminum foil) at −80 °C until analysis [25].

Acute unconjugated hyperbilirubinemia

Adult Gunn rats received a single APHZ injection i.p. (15 mg/kg BW; t = −24 h) to induce hemolysis. We then randomized these animals after 24 h (t = 0 h) to receive either no treatment (n = 6), phototherapy + NaCl 0.9% (17 $\mu W/cm^2/nm$; n = 6), HSA (2.5 g/kg; n = 6), or phototherapy + HSA (n = 6) for another 48 h. NaCl 0.9% (control/sham) and HSA were administered as a single i.p. injection at t = 0 h. We determined plasma bilirubin, UCB_{free} and albumin concentrations from tail vein blood at t = −24, −12, 0, 12, 24, 36, and 48 h under isoflurane anesthesia. Hemoglobin (Hb), reticulocyte count and hematocrit (Ht) were determined at t = −24 h and t = 48 h. After 48 h, all animals were exsanguinated and brain, liver, and visceral fat samples were subsequently harvested for the determination of tissue bilirubin levels, as described above [25].

Plasma analysis

Blood samples were protected from light, stored at −20 °C under argon, directly after collection, and processed within 2 weeks. UCB concentrations were determined by routine spectrophotometry on a P800 unit of a modular analytics serum work area from Roche Diagnostics Ltd. (Basel, Switzerland). Hb, Ht, and reticulocytes were determined on a Sysmex XE-2100 hematology analyzer (Goffin Meyvis, Etten-Leur, The Netherlands). We previously found in Gunn rats that the total bilirubin concentration, measured by spectrophotometry, equaled the total UCB concentration, measured by high-liquid performance chromatography (HPLC) after chloroform extraction (coefficient of variation: ~5%) [21,22]. UCB_{free} was determined using a Zone Fluidics system (Global Flopro, Global Fia Inc, WA), as previously described by Ahlfors *et al.* [13].

Tissue bilirubin analysis

Tissue bilirubin content was determined using HPLC with diode array detector (Agilent, Santa Clara, CA, USA) as described earlier [25]. Briefly, 300 pmol of mesobilirubin in DMSO (used as an internal standard) was added and samples were homogenized on ice. Bile pigments were then extracted into chloroform/hexane (5:1) solution at pH 6.0, and subsequently extracted in a minimum volume of methanol/carbonate buffer (pH 10) to remove contaminants. The resulting polar droplet (extract) was loaded onto C-8 reverse phase column (Phenomenex, Torrance, CA, USA) and separated pigments were detected at 440 nm. The concentration of bilirubin was calculated as nmol/g of wet tissue weight. All steps were performed under dim light in aluminum-wrapped tubes. We did not specifically measure bilirubin deposition in the brain nuclei, but relied on total tissue bilirubin measurements.

Statistical analysis

Normally distributed data that displayed homogeneity of variance (by calculation of Levene's statistic) were expressed as means ± SD, and analyzed with parametric statistical tests. Analysis of variance (ANOVA) with *post hoc* Tukey correction was performed for comparisons between groups, and the Student's-*t* test for comparison of paired data within groups. The level of significance was set at $p < 0.05$. Analyses were performed using PASW Statistics 17.0 for Mac (SPSS Inc., Chicago, IL).

Results

Chronic unconjugated hyperbilirubinemia

Adjunct HSA treatment decreases plasma UCB_{free} concentrations

We first treated permanently jaundiced Gunn rats, as a model for Crigler–Najjar disease, with routine phototherapy, HSA, or phototherapy + HSA for 16 days. Fig. 1A shows that phototherapy and phototherapy + HSA decreased plasma UCB concentrations to a similar extent (46% and 54% at t = 16 days, respectively), compared with untreated controls ($p < 0.001$). HSA alone increased plasma UCB concentrations by 65% compared with

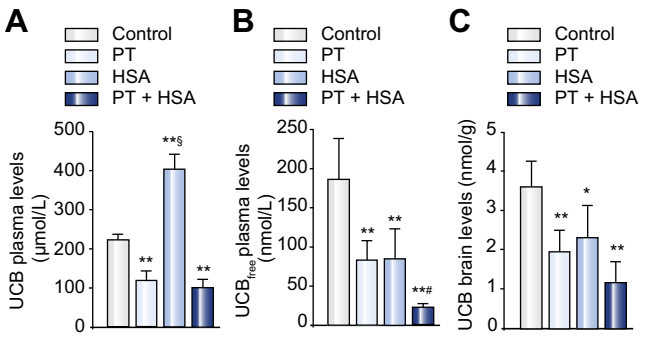

Fig. 1. Plasma and brain results of chronic unconjugated hyperbilirubinemia experiments. Effects of no treatment (controls), routine phototherapy (PT), human serum albumin (HSA), or PT + HSA on (A) plasma UCB, (B) plasma UCB_{free}, and (C) brain bilirubin levels in Gunn rats at t = 16 days. Adult Gunn rats were randomized to receive either no treatment or phototherapy (17 μW/cm^2/nm) for 16 days. After t = 14 days, we randomized animals to receive no treatment, PT (17 μW/cm^2/nm), HSA (2.5 g/kg), or PT + HSA for another 48 h. $^{*}p$ <0.01, $^{**}p$ <0.001 compared with controls. $^{\#}p$ <0.05, $^{\S}p$ <0.001 compared with phototherapy alone.

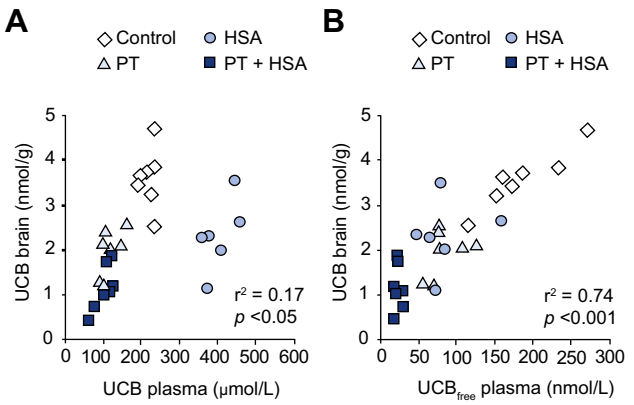

Fig. 2. Correlations of the chronic unconjugated hyperbilirubinemia experiments. (A) Correlation between plasma UCB and brain bilirubin levels, and (B) between plasma UCB_{free} and brain bilirubin levels in Gunn rats at t = 16 days. Adult Gunn rats were randomized to receive either no treatment or PT (17 μW/cm^2/nm) for 16 days. After t = 14 days, we randomized the animals to receive no treatment, PT (17 μW/cm^2/nm), human serum albumin (HSA: 2.5 g/kg), or PT + HSA for another 48 h.

controls (p <0.001). Fig. 1B shows that phototherapy, HSA and phototherapy + HSA decreased plasma UCB_{free} concentrations by 55%, 54%, and 88%, respectively (p <0.001). HSA alone decreased the unbound fraction of UCB from 0.08% to 0.02% (−71%; p <0.001), compared with controls. HSA, as expected, also decreased this fraction during phototherapy treatment. As a result, adjunct HSA lowered plasma UCB_{free} levels by 33%, compared with phototherapy alone (p <0.01). Mean growth rates did not differ significantly between experimental and control groups during the experiment (data not shown).

Adjunct HSA treatment decreases brain bilirubin levels

Fig. 1C shows that phototherapy, HSA alone, and phototherapy + HSA decreased brain bilirubin levels by 45%, 35%, and 67%, respectively (p <0.01), compared with untreated controls. Adjunct HSA thus lowered brain bilirubin levels by an additional 22% (n.s.), compared with phototherapy alone. Adjunct HSA significantly decreased hepatic bilirubin levels by an additional 33% (p <0.01), compared with phototherapy alone (Supplementary Fig. 1A), but failed to induce a significant additive decrease in visceral fat bilirubin levels (Supplementary Fig. 1B).

The correlation between UCB_{free} and brain bilirubin levels

Fig. 2A illustrates the poor correlation between plasma UCB concentrations and brain bilirubin levels ($y = 0.0037x + 1.52$; $r^2 = 0.17$; p <0.05). The HSA group, with bilirubin levels above 300 μmol/L, seemed mainly responsible for this poor correlation. Fig. 2B shows that plasma UCB_{free} concentrations correlated well with brain bilirubin levels ($y = 0.013x + 1.00$; $r^2 = 0.74$; p <0.001).

Acute unconjugated hyperbilirubinemia

APHZ induces comparable hemolysis in all treatment groups

As a model for acute unconjugated hyperbilirubinemia, we then used APHZ to induce hemolytic jaundice in Gunn rats. APHZ administration induced a comparable hemolysis in all groups, as indicated by the similar changes in Hb, Ht, and reticulocyte levels (Supplementary Fig. 2A–C). Supplementary Fig. 2D shows that a single i.p. HSA injection increased plasma albumin within 12 h (+34% and +40% in HSA and phototherapy + HSA-treated animals, respectively), compared with untreated controls. Mean growth rates did not differ significantly between experimental and control groups during the experiment (data not shown).

Adjunct HSA treatment decreases plasma UCB concentrations

We treated the hemolytic Gunn rats with routine phototherapy, HSA, or phototherapy + HSA for 48 h. Fig. 3A shows that phototherapy and phototherapy + HSA both decreased the severity of hemolytic unconjugated hyperbilirubinemia, compared with untreated hemolytic controls. Phototherapy decreased plasma UCB concentrations by 14% at t = 36 h (p <0.01), while phototherapy + HSA decreased these concentrations by at least 29% from t = 36 h onwards (p <0.001). Adjunct HSA thereby lowered plasma bilirubin levels by an additional 14–16%, compared with phototherapy alone (p <0.05). HSA alone failed to decrease plasma UCB concentrations.

Adjunct HSA treatment decreases plasma UCB_{free} concentrations

Fig. 3B shows that phototherapy decreased plasma UCB_{free} concentrations by 31% at t = 48 h (p <0.05), compared with controls, while phototherapy + HSA decreased these concentrations by at least 41% from t = 12 h onwards (p <0.001). Adjunct HSA thereby lowered plasma UCB_{free} concentrations by an additional 25–47%, respectively, compared with phototherapy alone (p <0.05). HSA alone failed to decrease plasma UCB_{free} concentrations, in spite of a transient drop in UCB_{free} concentrations during the first 24 h of treatment.

Adjunct HSA treatment decreases brain bilirubin levels

Fig. 3C shows that phototherapy alone and HSA alone both failed to decrease brain bilirubin levels. Combining phototherapy with HSA, however, resulted in a 50%-decrease in brain bilirubin levels, compared with untreated hemolytic controls (p <0.001). Adjunct HSA thereby decreased brain bilirubin levels to 2.9 ± 1.2 nmol/g, which was comparable with the brain bilirubin content of non-hemolytic control animals (3.6 ± 0.7 nmol/g; Fig. 1C).

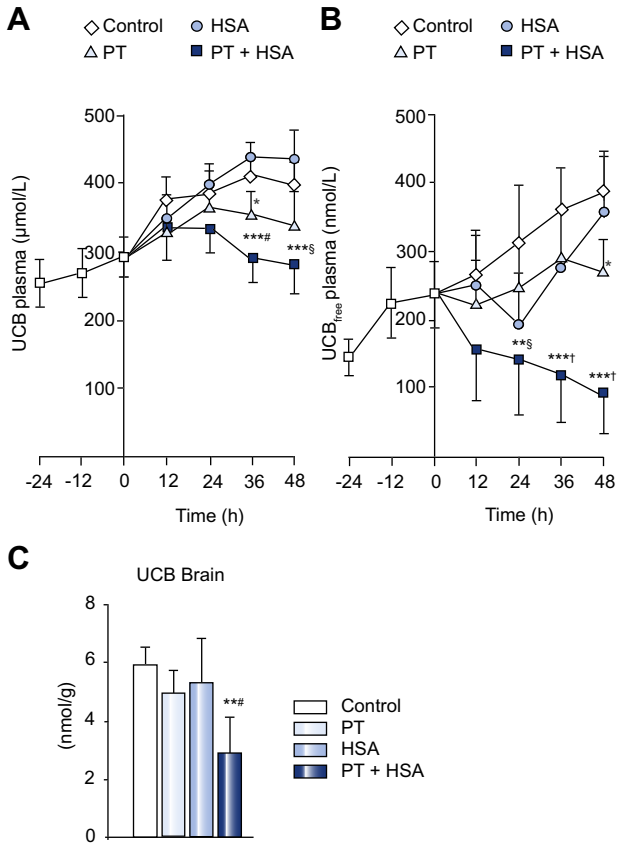

Fig. 3. Plasma and brain results of acute unconjugated hyperbilirubinemia experiments. Effects of no treatment (controls), routine phototherapy (PT), human serum albumin (HSA), or PT + HSA on (A) plasma UCB, (B) plasma UCB_{free}, and (C) brain bilirubin levels at t = 48 h in hemolytic Gunn rats. Adult Gunn rats received APHZ i.p. to induce hemolysis, and were randomized after 24 h to receive no treatment, phototherapy (17 µW/cm^2/nm), HSA (2.5 g/kg), or PT + HSA for 48 h. Plasma bilirubin concentrations were similar in all groups during the 24-h run-in period after APHZ injection. $^{*}p$ <0.05; $^{**}p$ <0.01; $^{***}p$ <0.001, compared with controls. $^{\#}p$ <0.05; $^{\S}p$ <0.01; $^{\dagger}p$ <0.001, compared with single PT.

Adjunct HSA thus completely prevented the deposition of bilirubin in the brain during hemolytic jaundice.

Adjunct HSA also decreased hepatic bilirubin levels by an additional 36% (p <0.01), compared with routine phototherapy (Supplementary Fig. 1C), and phototherapy + HSA was the only treatment that decreased bilirubin levels in visceral fat, compared with controls (−41%, p <0.05; Supplementary Fig. 1D).

The correlation between plasma UCB_{free} and brain bilirubin levels

Fig. 4A shows the correlation between plasma bilirubin and brain bilirubin levels during acute jaundice. Fig. 4B shows that plasma UCB_{free} correlates reasonably well with brain bilirubin levels in hemolytic Gunn rats (y = 0.0078x + 2.63; r^2 = 0.48; p <0.001).

Discussion

In this study, we demonstrate that HSA effectively decreases brain bilirubin levels in phototherapy-treated Gunn rats. The decrease was apparent during both chronic and acute hemolytic jaundice. Our results support the feasibility of HSA treatment as

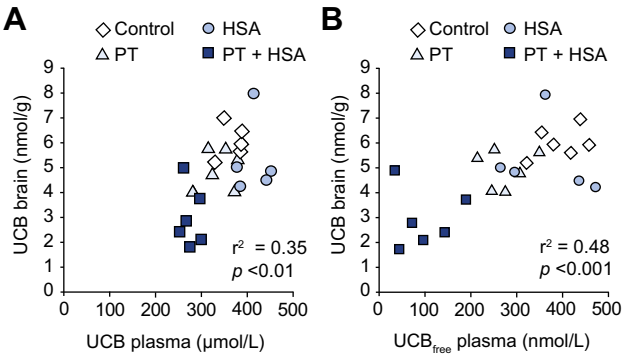

Fig. 4. Correlations of acute unconjugated hyperbilirubinemia experiments. (A) Correlation between plasma UCB and brain bilirubin levels, and (B) between plasma UCB_{free} and brain bilirubin levels in Gunn rats at t = 48 h. Adult Gunn rats received APHZ i.p. to induce hemolysis, and were randomized after 24 h to receive no treatment, PT (17 µW/cm^2/nm), human serum albumin (HSA: 2.5 g/kg), or PT + HSA for 48 h.

adjunct to phototherapy in Crigler–Najjar disease and neonatal jaundice.

The rationale behind HSA treatment is based on the premises that UCB_{free} translocates into the brain and, secondly, that i.v. albumin prevents this translocation by binding to UCB_{free} within the plasma. The role of UCB_{free} translocation became apparent in the 1950s, when sulfisoxazole-treated neonates developed kernicterus in the presence of unusually low plasma bilirubin concentrations [26,27]. It was soon discovered that sulfisoxazole displaced UCB from albumin, which first suggested the importance of the non-albumin bound UCB fraction [28]. Since then, many studies have supported the critical role of UCB_{free} in the pathogenesis of bilirubin-induced brain damage [2,3,5,6]. These studies also demonstrated that plasma UCB_{free} levels increased proportionally as the plasma albumin binding affinity or capacity decreased, or during inflammation. Ahlfors *et al.* have recently underlined the importance of UCB_{free} by showing that auditory brainstem response screening, a quantifiable method to evaluate bilirubin-induced neurotoxicity, correlates with UCB_{free} rather than with total bilirubin concentrations [4]. The protective role of HSA administration has also been investigated in neonates. Its efficacy, however, has never been established in randomized controlled trials. Two retrospective studies have shown reduced UCB_{free} concentrations in jaundiced neonates after HSA administration [16,18]. One additional small cohort study has shown some protective effect of HSA administration on the development of brain damage, as measured by auditory brainstem response screening [17]. Other studies, however, failed to demonstrate beneficial effects of HSA treatment [15]. Importantly, most human studies did not assess plasma UCB_{free}, or used methods that seriously underestimate UCB_{free} levels due to a 42-sample dilution [15–18,29]. The absence of reliable data on UCB_{free} concentrations obviously impeded the interpretability of these studies. In addition, human studies are intrinsically limited by the impossibility of measuring brain bilirubin levels. Recently, Ahlfors *et al.* automated and improved the available UCB_{free} test, while Zelenka *et al.* developed a sensitive method for tissue bilirubin determinations [13,25]. These newly developed methods allowed us to reliably measure UCB_{free} and brain bilirubin levels in two well-established animal models [19,20].

We first investigated the efficacy of adjunct HSA treatment in moderately chronic hyperbilirubinemic Gunn rats. Routine

phototherapy decreased unconjugated hyperbilirubinemia in these animals, while HSA alone increased plasma UCB levels. Routine phototherapy and HSA alone both decreased UCB_{free} and brain bilirubin levels. The decrease in brain bilirubin in the HSA-alone group was in concordance with previous animal studies by Diamond *et al.*, who described that bilirubin ^{14}C deposited in the brain could in part be mobilized and returned to the circulation by subsequent treatment with HSA [2]. Next, we investigated adjunct HSA treatment during phototherapy in Gunn rats. Rats treated with adjunct HSA treatment had lower UCB_{free} and, to a lesser extent, brain bilirubin levels, compared with phototherapy alone. These results, when taken together, support a model in which only UCB_{free} is able to move between the vascular and extravascular (tissue) compartment of the bilirubin pool (Supplementary Fig. 3A). This translocation of UCB_{free} occurs across both the vascular endothelial cells and the BBB. In this model, HSA administration could act in tandem with phototherapy. HSA first binds covalently to plasma $UCB_{free,}$ which decreases the free bilirubin concentration within the vascular compartment. This decrease promotes a bilirubin shift from the extravascular pool, as reflected by the increased plasma UCB concentrations during HSA-treatment. The newly recruited intravascular bilirubin is then, after its exposure to photo-isomerization, rapidly transported to the liver, and excreted via the bile (Supplementary Fig. 3B) and urine [30].

Our results in acutely jaundiced Gunn rats showed that APHZ administration induced a comparable hemolysis in all groups. Routine phototherapy thus did not affect the severity of hemolysis, or did treatment with HSA alone, as indicated by similar decreases in Hb and Ht (Supplementary Fig. 2). APHZ increased plasma UCB and UCB_{free} concentrations by 30–60% within 2 days after administration. Phototherapy mitigated this increase, but to a relatively small extent. HSA alone treatment again tended to increase, rather than decrease, plasma UCB concentrations. The most striking finding, however, was the synergistic effect of combined phototherapy and HSA treatment. Adjunct HSA not only decreased UCB_{free} concentrations in the plasma, but it also completely prevented the hemolysis-induced deposition of bilirubin in the brain, in contrast to phototherapy and single HSA treatment. The failure of single HSA treatment demonstrates the importance of phototherapy in our model. When HSA induces a bilirubin shift from the extravascular to the vascular compartment, phototherapy is needed to convert this newly recruited intravascular bilirubin into photoisomers that can be readily excreted via the bile. Without phototherapy, bilirubin will move back from blood into tissues as the plasma albumin levels return to baseline (i.e., within 48 h; Supplementary Fig. 2D). The observed lack of effect of single phototherapy on brain bilirubin levels may be time-related: phototherapy decreased plasma UCB within 36 h, but did not decrease UCB_{free} levels until after 48 h of treatment. Indeed, long-term phototherapy apparently circumvented this delayed decrease in UCB_{free} levels, and decreased both UCB_{free} and brain bilirubin in permanently jaundiced Gunn rats. We cannot exclude the possibility that non-protein bound bilirubin is less readily converted into photoisomers than the protein-bound fraction. Taken together, our results not only demonstrate the benefits of adjunct HSA, but also question the efficacy of phototherapy during acute hemolytic jaundice.

The correlation between plasma and brain bilirubin levels was virtually absent in our chronic and acute experiments. These data are consistent with clinical evidence that shows a poor predictive value of plasma bilirubin, especially above 300 μmol/L, for neurotoxicity [6]. Together, these observations illustrate that UCB is, at best, a poor predictor for bilirubin deposition within the brain. UCB_{free} concentrations correlated reasonably well with individual brain bilirubin levels in our experiments. Yet, the r^2-value in our acute experiment indicated that the variation in brain bilirubin is clearly not solely related to plasma UCB_{free} concentrations. Also, it is interesting to note that the HSA-induced decrease in brain bilirubin concentrations is less pronounced than the HSA-induced decrease in plasma UCB_{free} concentrations. These observations confirm that, apart from UCB_{free}, other factors (e.g., changes in blood pH, BBB integrity, active transport of bilirubin across the BBB, hemolysis, inflammation) are also highly important in the pathogenesis of bilirubin-induced neurological damage [31,32]. It would be interesting to investigate these factors, as well as the accumulation of bilirubin in *specific* brain regions (since bilirubin predominantly accumulates in the deep nuclei of the brain) during HSA treatment in future animal experiments. Also, studies with different HSA dosages would be required to determine dose dependency relationships between HSA and its bilirubin effects, since it seems reasonable to assume that another dosage of HSA would result in quantitatively different outcomes. Taken together, these issues demonstrate the need for a further evaluation of HSA administration in future experiments.

It is worth noticing the differences between chronic and acute hyperbilirubinemia models. The acute model, in contrast to the chronic model, does not reflect a steady state condition. In the chronic model, the UCB production rate is stable, whereas the UCB production rate is increased in the acute model. This results in different kinetics that might influence the (re)distribution of bilirubin from the blood into the tissue compartment, and *vice versa*. To exclude the possibility that the differences between our models were induced by APHZ, rather than by hemolysis, we performed additional experiments. In these experiments we induced hyperbilirubinemia in Gunn rats via a different strategy, namely transfusion with 1-week old donor rat erythrocytes (data not shown). Rats were then treated with or without phototherapy. Compared with the APHZ results, the effects on total plasma UCB, UCB_{free} and brain bilirubin and their interrelationships were similar. These results strongly indicated that the differences between our models were induced by hemolysis, and not directly by the APHZ compound.

For the interpretation and extrapolation of the results, we underline that species differences in bilirubin kinetics do apply between humans and rats, even when both are completely deficient in UDPGT1A1 activity (Crigler–Najjar type I patients and Gunn rats, respectively). For example, the hyperbilirubinemia in Gunn rats is less severe than that in Crigler–Najjar type I patients, and the natural course of the disease is milder. Furthermore, in Gunn rats the accumulation of bilirubin does not usually produce neonatal morbidity or a kernicterus pattern. Also, we studied adult Gunn rats because it was not feasible to reliably administer and assess the effects of phototherapy for 16 days in Gunn rat pups. The central nervous system is less vulnerable in adult rats. We are consequently aware that bilirubin distribution and affinities could be different in the neonatal or adult central nervous system [33–35]. Although the adult Gunn rat model has been proven valuable in studying bilirubin (patho)physiology, these observations justify some caution in extrapolating our results to Gunn rat pups or hyperbilirubinemic patients.

In our study we have used a commercially available HSA solution and found clear proof that it enhanced the therapeutic efficacy of routine phototherapy. We used human serum albumin (HSA) rather than rat serum albumin (RSA), to mimic the clinical situation as closely as possible and to use a treatment that is presently already available for patients. The albumin solution used in our experiments is currently widely applied in neonates, which greatly increases its therapeutic potential and will facilitate the set up of future clinical trials [15–18,29]. These trials should ideally incorporate UCB_{free} measurements and auditory brainstem response screening to monitor the efficacy of treatment. UCB_{free} measurements should be performed according to the recently developed method of Ahlfors *et al.* that enables an automated and reliable measurement of UCB_{free} in a clinical setting. HSA administration has previously been used in jaundiced neonates, mainly before phototherapy became available. Although generally safe, HSA was associated with side effects, such as fluid overload. Theoretically, HSA administration could also induce infections or immunological reactions. The occurrence of these side effects, although uncommon, should be monitored in future clinical trials [18,29].

Taken together, our data show that HSA enhances the efficacy of routine phototherapy in phototherapy-treated Gunn rats, both during permanent and acute jaundice. Our study underlines the need to critically evaluate the use of HSA as adjunct to phototherapy in randomized controlled clinical trials. We expect that a focus on tissue, rather than on plasma bilirubin concentrations, could induce a paradigm shift that will allow the development of increasingly efficient treatment strategies. These strategies will, hopefully, further decrease the burden of bilirubin-induced brain damage in the near future.

Financial support

This work was partly supported by grant CZ:GA CR:P206/11/0836, from the Research Granting Agency of the Czech Republic.

Conflict of interest

The authors who have taken part in this study declared that they do not have anything to disclose regarding funding or conflict of interest with respect to this manuscript.

Supplementary data

Supplementary data associated with this article can be found, in the online version, at http://dx.doi.org/10.1016/j.jhep.2012.08.011.

References

[1] Crigler JF, Najjar VA. Congenital familial nonhemolytic jaundice with kernicterus. Pediatrics 1952;10:169–180.
[2] Diamond I, Schmid R. Experimental bilirubin encephalopathy. The mode of entry of bilirubin-^{14}C into the central nervous system. J Clin Invest 1966;45:678–689.
[3] Calligaris SD, Bellarosa C, Giraudi P, Wennberg RP, Ostrow JD, Tiribelli C. Cytotoxicity is predicted by unbound and not total bilirubin concentration. Pediatr Res 2007;62:576–580.
[4] Ahlfors CE, Amin SB, Parker AE. Unbound bilirubin predicts abnormal automated auditory brainstem response in a diverse newborn population. J Perinatol 2009;29:305–309.
[5] Zucker SD, Goessling W, Hoppin AG. Unconjugated bilirubin exhibits spontaneous diffusion through model lipid bilayers and native hepatocyte membranes. J Biol Chem 1999;274:10852–10862.
[6] Wennberg RP, Ahlfors CE, Bhutani VK, Johnson LH, Shapiro SM. Toward understanding kernicterus: a challenge to improve the management of jaundiced newborns. Pediatrics 2006;117:474–485.
[7] Ostrow JD, Pascolo L, Brites D, Tiribelli C. Molecular basis of bilirubin-induced neurotoxicity. Trends Mol Med 2004;10:65–70.
[8] Ahlfors CE, Wennberg RP, Ostrow JD, Tiribelli C. Unbound (free) bilirubin: improving the paradigm for evaluating neonatal jaundice. Clin Chem 2009;55:1288–1299.
[9] Ostrow JD. Photocatabolism of labeled bilirubin in the congenitally jaundiced (Gunn) rat. J Clin Invest 1971;50:707–718.
[10] Van der Veere CN, Sinaasappel M, McDonagh AF, Rosenthal P, Labrune P, Odievre M, et al. Current therapy for Crigler–Najjar syndrome type 1: report of a world registry. Hepatology 1996;24:311–315.
[11] Yohannan MD, Terry HJ, Littlewood JM. Long term phototherapy in Crigler–Najjar syndrome. Arch Dis Child 1983;58:460–462.
[12] Keenan WJ, Novak KK, Sutherland JM, Bryla DA, Fetterly KL. Morbidi ty and mortality associated with exchange transfusion. Pediatrics 1985;75:417–421.
[13] Ahlfors CE, Marshall GD, Wolcott DK, Olson DC, Van Overmeire B. Measurement of unbound bilirubin by the peroxidase test using zone fluidics. Clin Chim Acta 2006;365:78–85.
[14] Odell GB, Cohen SN, Gordes EH. Administration of albumin in the management of hyperbilirubinemia by exchange transfusions. Pediatrics 1962;30:613–621.
[15] Chan G, Schiff D. Variance in albumin loading in exchange transfusions. J Pediatr 1976;88:609–613.
[16] Hosono S, Ohno T, Kimoto H, Nagoshi R, Shimizu M, Nozawa M. Effects of albumin infusion therapy on total and unbound bilirubin values in term infants with intensive phototherapy. Pediatr Int 2001;43:8–11.
[17] Hosono S, Ohno T, Kimoto H, Nagoshi R, Shimizu M, Nozawa M, et al. Follow-up study of auditory brainstem responses in infants with high unbound bilirubin levels treated with albumin infusion therapy. Pediatr Int 2002;44:488–492.
[18] Caldera R, Maynier M, Sender A, Brossard Y, Tortrat D, Galiay JC, et al. The effect of human albumin in association with intensive phototherapy in the management of neonatal jaundice. Arch Fr Pediatr 1993;50:399–402.
[19] Labrune P, Myara A, Trivin F, Odievre M. Gunn rats: a reproducible experimental model to compare the different methods of measurements of bilirubin serum concentration and to evaluate the risk of bilirubin encephalopathy. Clin Chim Acta 1990;192:29–33.
[20] Rice AC, Shapiro SM. A new animal model of hemolytic hyperbilirubinemia-induced bilirubin encephalopathy (kernicterus). Pediatr Res 2008;64:265–269.
[21] Cuperus FJC, Hafkamp AM, Havinga R, Vitek L, Zelenka J, Tiribelli C, et al. Effective treatment of unconjugated hyperbilirubinemia with oral bile salts in Gunn rats. Gastroenterology 2009;136:e1.
[22] Cuperus FJC, Iemhoff AA, van der Wulp M, Havinga R, Verkade HJ. Acceleration of the gastrointestinal transit by polyethylene glycol effectively treats unconjugated hyperbilirubinaemia in Gunn rats. Gut 2010;59:373–380.
[23] Hafkamp AM, Havinga R, Ostrow JD, Tiribelli C, Pascolo L, Sinaasappel M, et al. Novel kinetic insights into treatment of unconjugated hyperbilirubinemia: phototherapy and orlistat treatment in Gunn rats. Pediatr Res 2006;59:506–512.
[24] Ostrow JD, Mukerjee P. Solvent partition of ^{14}C-unconjugated bilirubin to remove labeled polar contaminants. Transl Res 2007;149:37–45.
[25] Zelenka J, Lenicek M, Muchova L, Jirsa M, Kudla M, Balaz P, et al. Highly sensitive method for quantitative determination of bilirubin in biological fluids and tissues. J Chromatogr B Anal Technol Biomed Life Sci 2008;867:37–42.
[26] Harris RC, Lucey JF, Maclean JR. Kernicterus in premature infants associated with low concentrations of bilirubin in the plasma. Pediatrics 1958;21:875–884.
[27] Andersen DH, Blanc WA, Crozier DN, Silverman WA. A difference in mortality rate and incidence of kernicterus among premature infants allotted to two prophylactic antibacterial regimens. Pediatrics 1956;18:614–625.
[28] Odell GB. Studies in kernicterus. I. The protein binding of bilirubin. J Clin Invest 1959;38:823–833.

[29] Ebbesen F, Brodersen R. Comparison between two preparations of human serum albumin in treatment of neonatal hyperbilirubinaemia. Acta Paediatr Scand 1982;71:85–90.
[30] Agati G, Fusi F, Pratesi S, Galvan P, Donzelli GP. Bilirubin photoisomerization products in serum and urine from a Crigler–Najjar type I patient treated by phototherapy. J Photochem Photobiol B: Biol 1998;47:181–189.
[31] Ahlfors CE, Wennberg RP. Bilirubin–albumin binding and neonatal jaundice. Semin Perinatol 2004;28:334–339.
[32] Ahlfors CE. Bilirubin–albumin binding and free bilirubin. J Perinatol 2001;21:S40–S42, [discussion S59–S62].
[33] Conlee JW, Shapiro SM. Development of cerebellar hypoplasia in jaundiced Gunn rats: a quantitative light microscopic analysis. Acta Neuropathol 1997;93:450–460.
[34] Favrais G, van de Looij Y, Fleiss B, Ramanantsoa N, Bonnin P, Stoltenburg-Didinger G, et al. Systemic inflammation disrupts the developmental program of white matter. Ann Neurol 2011;70:550–565.
[35] Harry GJ, Kraft AD. Microglia in the developing brain: a potential target with lifetime effects. Neurotoxicology 2012;33:191–206.

Digestive and Liver Disease 46 (2014) 369–375

Contents lists available at ScienceDirect

Digestive and Liver Disease

journal homepage: www.elsevier.com/locate/dld

Oncology

Antiproliferative effects of carbon monoxide on pancreatic cancer

Libor Vítek[a,b,*], Helena Gbelcová[c,1], Lucie Muchová[a], Kateřina Váňová[a], Jaroslav Zelenka[a,2], Renata Koníčková[a], Jakub Šuk[a], Marie Zadinova[a], Zdeněk Knejzlík[c], Shakil Ahmad[d,e], Takeshi Fujisawa[d], Asif Ahmed[d,e], Tomáš Ruml[c,**]

[a] Institute of Medical Biochemistry and Laboratory Diagnostics, 1st Faculty of Medicine, Charles University in Prague, Prague 2, Czech Republic
[b] 4th Department of Internal Medicine, 1st Faculty of Medicine, Charles University in Prague, Prague 2, Czech Republic
[c] Department of Biochemistry and Microbiology, Institute of Chemical Technology, Prague 6, Czech Republic
[d] Queen's Medical Research Institute, University of Edinburgh, Edinburgh, UK
[e] School of Life & Health Sciences, Aston University, Birmingham, UK

ARTICLE INFO

Article history:
Received 14 June 2013
Accepted 4 December 2013
Available online 14 January 2014

Keywords:
Anticancer effects
Heme catabolic pathway
Heme oxygenase

ABSTRACT

Background: Carbon monoxide, the gaseous product of heme oxygenase, is a signalling molecule with a broad spectrum of biological activities. The aim of this study was to investigate the effects of carbon monoxide on proliferation of human pancreatic cancer.
Methods: In vitro studies were performed on human pancreatic cancer cells (CAPAN-2, BxPc3, and PaTu-8902) treated with a carbon monoxide-releasing molecule or its inactive counterpart, or exposed to carbon monoxide gas (500 ppm/24 h). For *in vivo* studies, pancreatic cancer cells (CAPAN-2/PaTu-8902) were xenotransplanted subcutaneously into athymic mice, subsequently treated with carbon monoxide-releasing molecule (35 mg/kg b.w. i.p./day), or exposed to safe doses of carbon monoxide (500 ppm 1 h/day; $n = 6$ in each group).
Results: Both carbon monoxide-releasing molecule and carbon monoxide exposure significantly inhibited proliferation of human pancreatic cancer cells ($p < 0.05$). A substantial decrease in Akt phosphorylation was observed in carbon monoxide-releasing molecule compared with inactive carbon monoxide-releasing molecule treated cancer cells (by 30–50%, $p < 0.05$). Simultaneously, carbon monoxide-releasing molecule and carbon monoxide exposure inhibited tumour proliferation and microvascular density of xenotransplanted tumours ($p < 0.01$), and doubled the survival rates ($p < 0.005$). Exposure of mice to carbon monoxide led to an almost 3-fold increase in carbon monoxide content in tumour tissues ($p = 0.006$).
Conclusion: These data suggest a new biological function for carbon monoxide in carcinogenesis, and point to the potential chemotherapeutic/chemoadjuvant use of carbon monoxide in pancreatic cancer.

1. Introduction

For decades, carbon monoxide (CO) exposure has been considered a potential threat to human health, and the endogenous production of this gaseous molecule was only thought to be a waste product, a biologically inactive by-product of heme catabolism. However, it is now widely accepted that CO formed endogenously by heme oxygenase (HMOX) confers cytoprotection against tissue and cellular injury [1,2]. CO acts as a smooth muscle relaxant as well as an inhibitor of platelet aggregation *via* guanylate cyclase and cGMP generation [2]. The functional properties of CO have often been compared with nitric oxide (NO), another endogenous gaseous molecule. Indeed, CO shares a number of biological functions analogous to NO [1]. The ability of both NO and CO to act as a vasodilator and to modulate endothelial cell permeability makes it plausible that they could also play essential roles in angiogenesis. It has previously been reported that NO has a dual effect on angiogenesis, and can either promote or inhibit angiogenesis in a dose-dependent manner [3]. Although certain studies have reported that CO is pro-angiogenic [4], the similarity of CO to NO could lead to the speculation that CO might also inhibit carcinogenesis, at least partially, *via* the suppression of angiogenesis. Under stress conditions, the production of CO is increased owing to the upregulation of the stress-responsive heme oxygenase isoenzyme,

* Corresponding author at: Institute of Medical Biochemistry and Laboratory Diagnostics, 1st Faculty of Medicine, Charles University in Prague, Na Bojišti 3, 12000 Praha 2, Czech Republic. Tel.: +420 224964203; fax: +420 224964203.
** Corresponding author at: Department of Biochemistry and Microbiology, Institute of Chemical Technology, Technická 5, 16628 Praha 6, Czech Republic. Tel.: +420 220443022; fax: +420 220445140.
E-mail addresses: vitek@cesnet.cz (L. Vítek), Tomas.Ruml@vscht.cz (T. Ruml).
[1] Current address: Institute of Medical Biology, Genetics and Clinical Genetics, Faculty of Medicine, Comenius University, Spitalska 24, Bratislava 81372, Slovakia.
[2] Address: Institute of Physiology, The Academy of Sciences of the Czech Republic, Prague, Czech Republic.

1590-8658/$36.00
http://dx.doi.org/10.1016/j.dld.2013.12.007

HMOX1 (OMIM*141250) [5]. The recent discovery of transition metal carbonyls that act as CO-releasing molecules (CORMs) has provided a new impetus for the investigation of CO as a cellular messenger, as well as a potential therapeutic agent [6,7]. Both CORMs and CO at doses free from toxic side-effects have been shown to exert important biological functions in numerous model *in vitro* and *in vivo* systems, including vasodilating, antiproliferative, anti-inflammatory effects, contributing to the amelioration of many pathological conditions such as ischaemia – reperfusion injury, inflammatory bowel disease, and organ rejection (for a comprehensive review of the biological effects of CO, see Motterlini and Otterbein [7]). A wide range of CORMs/CO dosages have been tested in these models, depending on CORM type, the means of delivery, and the model used [7]. Significantly, the CO delivered was demonstrated to be non-toxic for healthy tissues, when keeping the CO haemoglobin levels within safe levels [8]. Based on these data, a CO inhalation system for human use has been developed and used in the first clinical trials [7].

Pancreatic tumours, having high mortality and recurrence rates, are an example of a tumour type in which any type of medical therapy has, at best, been only modestly effective [9]. Thus, the effective therapy for pancreatic cancer depends on the search for alternative therapeutic modalities that have the potential to inhibit multiple signalling pathways. Although pancreatic carcinogenesis is a very complex issue, with numerous intracellular pathways involved, the phosphatidylinositol-3 kinase/Akt (protein kinase B) seems to play a key role [10]. Akt activation is frequent in pancreatic cancer and correlates well with prognosis [11]; its inhibition has been reported to sensitise cancer cells to the tumour-suppressive effects of chemotherapy [12,13].

All of these facts led us to investigate the potential antiproliferative effects of CO and/or CORM-2 (a ruthenium-based, lipid-soluble CORM) on human pancreatic cancer, using experimental *in vitro* and *in vivo* models, with a special focus on the possible CO-mediated effects on Akt phosphorylation.

2. Methods

2.1. Reagents

All cell culture reagents and chemicals, and tricarbonyldichlororuthenium(II) dimer ($[Ru(CO)_3Cl_2]_2$) (more commonly known as CORM-2), were obtained from Sigma Aldrich (Prague, Czech Republic). The CO (500 ppm) gas mixture (20% O_2, 0.03% CO_2, remainder nitrogen) for *in vitro* studies was obtained from Linde Gas (Prague, Czech Republic).

2.2. Cell cultures

The pancreatic cancer cell lines CAPAN-2, BxPc3 (ATCC, Manassas, VA, USA), and PaTu-8902 (DSMZ, Braunschweig, Germany) were used for the *in vitro* studies. The cell lines were cultured as described previously [14]. The cell suspensions ($2 \times 10^{5-6}$ cells/ml) were used for the inoculation of individual wells in the 6-well plate. Cells were treated with either a ruthenium-based CORM (CORM-2, 50 μmol/L; this relatively high concentration was used for all *in vitro* studies because of the very short half-life of CORM-2 [7]) or its inactive counterpart, iCORM-2 (a CO-free CORM-2). The use of iCORM-2 as a control is important, since the Ru-based carrier molecule may exert some biological properties itself. Either the CORM-2 or iCORM-2 was dissolved in a solution of DMSO in PBS (final concentration of DMSO did not exceed 1%, vol/vol), on a daily basis for a period of three days. The plates were incubated at 37 °C in a humidified atmosphere of 5% CO_2 in air. The iCORM-2 was prepared by leaving CORM-2 at room temperature for 2 days, and flushing with nitrogen to remove the residual CO [6]. Before initiating the experiments, the release of CO from freshly diluted CORM-2 was confirmed by gas chromatography (for methodology see below). Alternatively, pancreatic cancer cells, cultured in an analogous manner to that described above, were directly exposed to CO (500 ppm) for 24 h using specific air jars (Oxoid CZ, Thermo Fisher Scientific, Prague, Czech Republic). After treatment, the cells (experiments were performed in triplicate) were washed with PBS, harvested by 0.25% trypsin, and re-suspended. Both cell growth and viability were assessed by the direct counting of trypan blue dye (0.4%) excluding cells.

To study the distribution of CO within the cells exposed to CORM, CORM-2 was incubated with PaTu-8902 pancreatic cancer cells for 75 min at 37 °C in a humidified atmosphere of 5% CO_2 in air. The iCORM-2 and 1% DMSO in PBS were used as controls. The CO concentration in the cells and media were measured as described below.

2.3. Determination of Akt phosphorylation

Akt phosphorylation in cancer cell lysates was determined by ELISA (based on anti-phospho-Akt Ser473 antibody, SuperArray Bioscience Corporation, MD, USA), after treatment of CAPAN-2 pancreatic cancer cells with CORM-2/iCORM-2 (50 mol/L) for 75 min, according to the manufacturer's instructions. Cells exposed to 1% DMSO in PBS (solvent for CORM-2) were also compared with untreated cells. Experiments were performed in hexaplets.

Simultaneously, Western blot analyses of phosphorylated Akt protein were performed on the CAPAN-2 and PaTu-8902 pancreatic cancer cells, treated in an identical manner (CORM-2/iCORM-2, 50 mol/L, 75 min incubation). The cells were lysed in Cell Lysis Buffer (Cell Signaling Technology, MA, USA), according to the manufacturer's instructions. Protein concentration was determined using a BCA assay (Thermo Scientific, IL, USA). Thirty micrograms of protein lysate were separated by SDS-PAGE electrophoresis (10% gel). The proteins were transferred to a PVDF membrane and then immunoblotted with anti-phospho-Akt (Ser473), anti-Akt, and anti-β-actin (Cell Signaling Technology, MA, USA). Antibodies were detected using Goat Anti-Rabbit IgG H&L (HRP) antibody (Abcam, UK), and analysed by ECL (LumiGLO®, Cell Signaling Technology, MA, USA). A Fusion Fx7 device and Bio-1D software (Vilber Lourmat, France) were used to quantify the signals. Results were expressed as the percentage of the total Akt level that was phospho-Akt.

2.4. In vivo tumour models

Six- to eight-week-old athymic mice (strain CD-1, Charles River WIGA, Sulzfeld, Germany) were transplanted subcutaneously with either 10^7 human CAPAN-2 or PaTu-8902 pancreatic cancer cells mixed with matrigel. Seven to ten days after tumour cell implantation, the CAPAN-2-bearing mice received a daily intra-peritoneal treatment of either CORM-2 or iCORM-2 ($n = 6$ in each group) dissolved in 1% DMSO in PBS (35 mg/kg), whereas the PaTu-8902-bearing mice were exposed for 1 h daily to either 500 ppm CO in the synthetic air or ambient air *per se*. The primary outcome of this type of *in vivo* study was the survival time; tumour progression was assessed simultaneously as well (tumour size was monitored every three days in all groups, and the tumour volume determined as described previously [15]). In an additional *in vivo* study, the animals treated with CORM-2 or iCORM-2 ($n = 6$ in each group) were sacrificed at day 14 for the quantification of the capillary density of the tumour. Finally, other sets of animals ($n = 6$ for each group) were exposed to CO (500 ppm of CO in synthetic air for 1 h a day). These animals were either sacrificed immediately after the last CO exposure, for the determination of COHb and CO content in the tumour

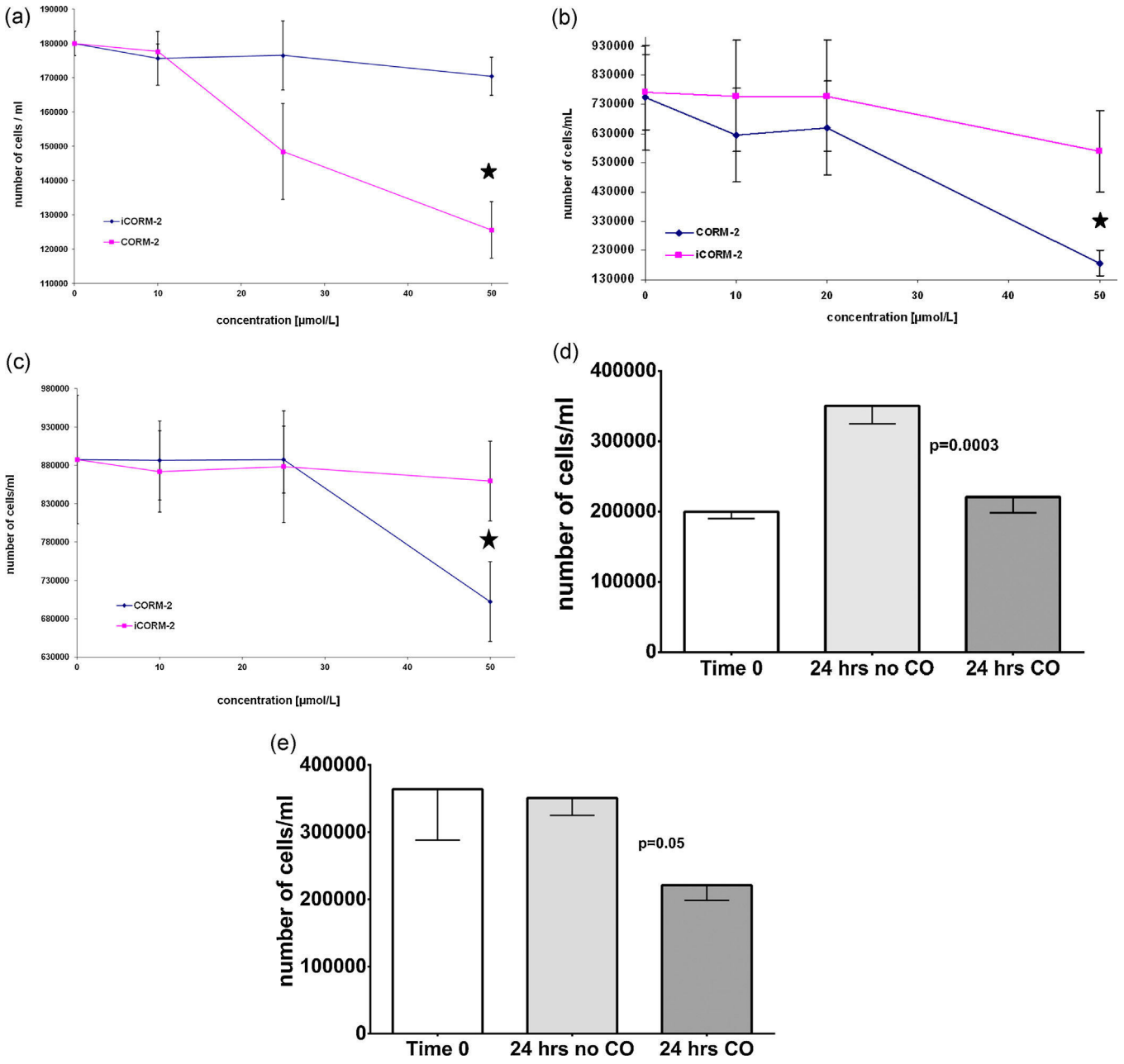

Fig. 1. CO inhibits pancreatic cancer cell proliferation *in vitro*. The effect of CORM-2 (48-h exposure) on pancreatic cancer cell lines: (a) PaTu-8902; (b) CAPAN-2; (c) BxPc3. $^{*}p < 0.05$ (CORM-2 treatment *vs.* iCORM-2, based on ANOVA on Ranks with Dunn's *post hoc* testing). ANOVA, analysis of variance; CORM, carbon monoxide-releasing molecule; iCORM, inactive CORM. The effect of 24-h CO exposure (500 ppm) on the proliferation of human pancreatic cancer cell lines: (d) PaTu-8902; (e) CAPAN-2; $n = 6$ for each group. CO, carbon monoxide.

tissue; or with an 8-h latency after the last exposure, to assess the long-term distribution of CO in various organs (liver, heart, spleen, kidneys, lung and brain).

The local animal research committee approved the protocols for all aspects of the animal studies in accordance with the Guide for the Care and Use of Laboratory Animals, as adopted and promulgated by the United States National Institutes of Health.

2.5. CO measurement

For the determination of CO in the tissues, samples (150–200 mg) were harvested, thoroughly washed in heparinized saline, diluted 1:4 (w/w) in ice-cold reaction buffer (0.1 M PBS, pH 7.4), diced, and sonicated with an ultrasonic tissue disruptor (model XL2000, Misonics, Framingdale, NY, USA). Forty microliters of tissue sonicate were added to CO-free, septum-sealed vials containing 5 μL of 30% (w/v) sulphosalicylic acid. After 30 min incubation on ice, the CO released into the vial headspace was quantified by gas chromatography with a reduction gas analyser (Trace Analytical, Menlo Park, CA, USA), as previously described [16]. This method has a detection limit of 1 pmol of CO, with a linear range of 1–500 pmol of CO. Tissue CO content was calculated as pmol of CO per mg of tissue. CO content in the cells (expressed as pmol of CO per mg of protein) and in the media from the *in vitro* experiments were measured in an analogous way.

To determine CO liberation from CORM-2, CORM-2 or its inactive counterpart (iCORM2) were dissolved in 1% DMSO in PBS and immediately mixed with the mouse blood in a CO-free vial. Next,

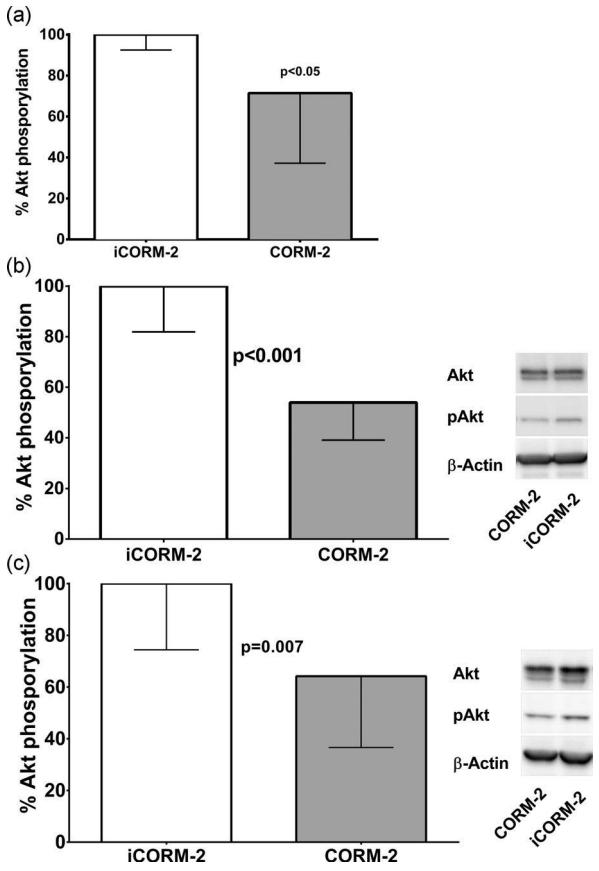

Fig. 2. CORM-2 inhibits Akt protein phosphorylation in pancreatic cancer cells. (a) Akt protein phosphorylation in CAPAN-2 cell lysates determined by ELISA. (b) Akt protein phosphorylation in CAPAN-2 cell lysates determined by Western blot. (c) Akt protein phosphorylation in PaTu-8902 cell lysates determined by Western blot. CAPAN-2 and PaTu-8902 pancreatic cancer cells were exposed to CORM-2 (50 μmol/L, 75 min exposure); data expressed as mean ± SD; $n = 6$ for each group. Two bands of Akt protein correspond to different Akt isoforms [36]. CORM, carbon monoxide-releasing molecule; iCORM, inactive CORM.

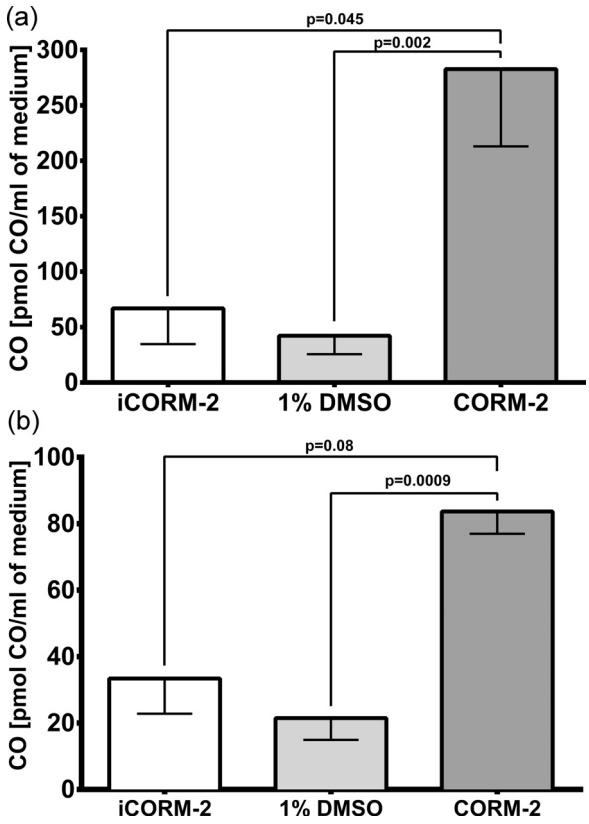

Fig. 3. CO distribution in the PaTu-8902 pancreatic cancer cells exposed to CORM-2. (a) CO content within PaTu-8902 pancreatic cancer cells exposed to CORM-2 (50 mol/L, 75-min exposure). (b) CO content in the culture media of PaTu-8902 pancreatic cancer cells exposed to CORM-2 (50 μmol/L, 75-min exposure); $n = 6$ for each group. CO, carbon monoxide; CORM, carbon monoxide-releasing molecule; iCORM, inactive CORM.

CO-haemoglobin formation was measured by gas chromatography as previously described [17]. The CO-haemoglobin method has a detection limit of 1 pmol of CO per vial.

2.6. Immunohistochemistry and quantification of capillary density

The immunohistochemistry was performed as previously described [18] on frozen or formalin-fixed, paraffin-embedded, randomly sampled, 3-μm sections of tumours with a 1:100 dilution of rat anti-mouse CD31 (BD Biosciences Oxford, UK), peroxidise-labelled rabbit anti-rat antibody (1:250). The mean density of CD31-positive vessels was determined in two areas per section per animal, with these images captured and analysed using Image Pro Plus image analysis software (Media Cybernetics Europe, Berkshire, UK).

2.7. Statistical analyses

All data are presented as the mean ± SD, or median and 25–75% range, when the data were non-normally distributed. Statistical comparisons of *in vitro* data were performed using ANOVA followed by the Student–Newman–Keuls test, or ANOVA on ranks with Dunn's *post hoc* testing, as appropriate. The statistical significance of differences between *in vivo* variables was evaluated by t-test or the Mann–Whitney rank sum test. Kaplan–Meier log rank survival analysis with Holm–Sidak *post hoc* testing was used to assess the effect of CORM-2 treatment on the survival of the animals. Group mean differences in tumour size were measured by repeated measures analysis of variance (RM ANOVA) with Holm–Sidak *post hoc* testing. When needed, log transform values of tumour size were used for comparisons to comply with equal variance requirements. Statistical significance was set at the value of $p < 0.05$.

3. Results

3.1. CO inhibits pancreatic cancer cell proliferation in vitro

Carbon monoxide, in the form of CORM-2, markedly inhibited proliferation of all tested human pancreatic cancer cell lines in a dose-dependent manner ($p < 0.05$, Fig. 1a–c).

To analyse whether CO in the form of CORM-2 might affect phosphorylation of the Akt protein (one of the key events in pancreatic carcinogenesis [10–13]), CAPAN-2 pancreatic cancer cells were treated with CORM-2 (50 μmol/L). Consistent with its antiproliferative effects, this concentration of CORM-2 was found to inhibit Akt phosphorylation in CAPAN-2 and PaTu-8902 pancreatic cancer cells by 30–50% compared with iCORM-2 (its inactive counterpart), as confirmed by both ELISA and Western blotting analyses ($p < 0.05$, Fig. 2a–c).

In order to assess whether the observed antiproliferative effects were only related to CO released from the CORM-2 molecule, PaTu-8902 and CAPAN-2 pancreatic cancer cells were directly exposed to CO in synthetic air (500 ppm) for 24 h. In these studies, CO clearly prevented proliferation of the PaTu-8902 cells ($p < 0.05$, Fig. 1d),

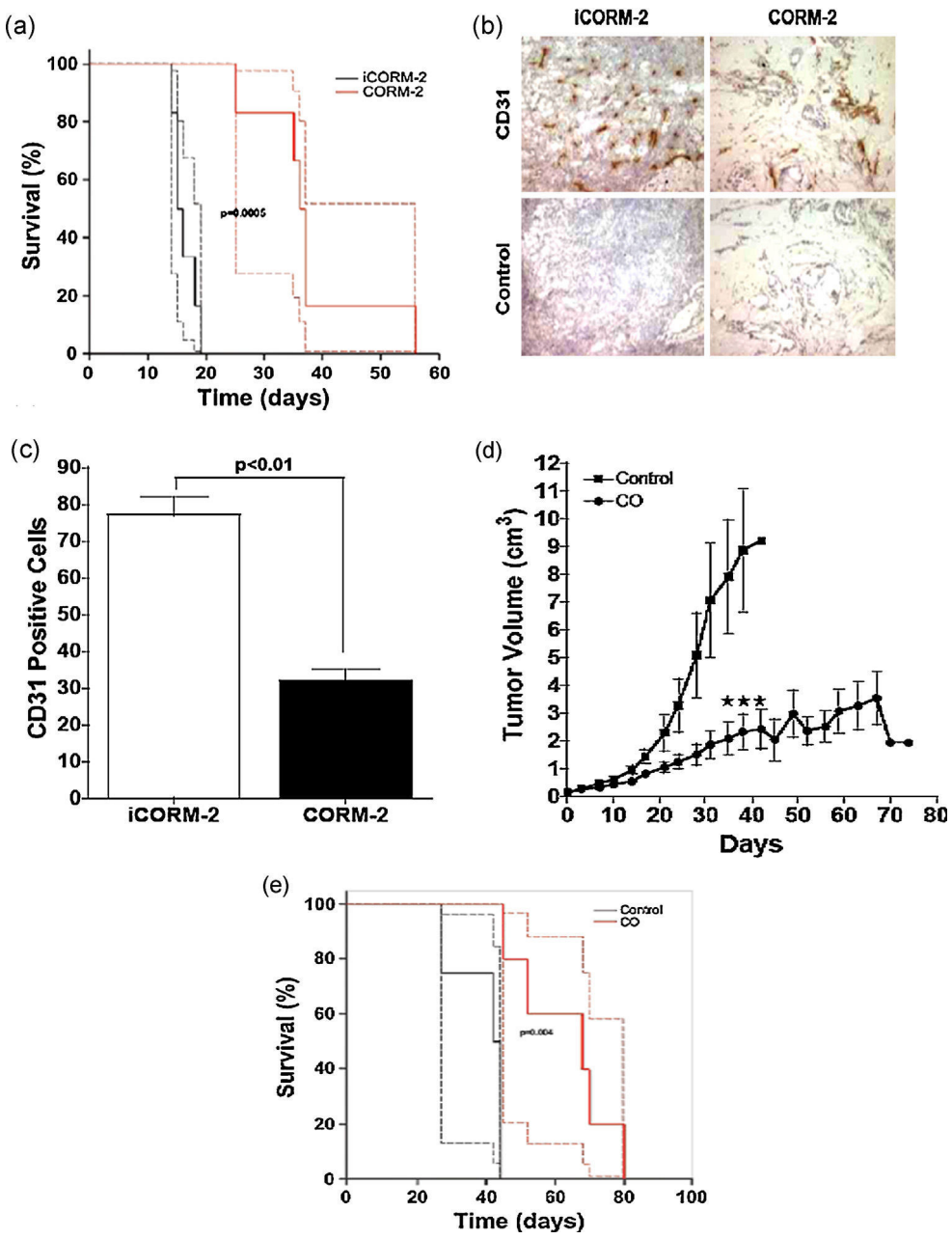

Fig. 4. CO inhibits pancreatic tumour progression *in vivo*. (a) Survival of athymic mice bearing CAPAN-2 human pancreatic cancer cells treated with CORM-2 (35 mg/kg/day, i.p. administration). Data expressed as mean ± SD, graphs represent survival times (continuous line) and respective upper and lower confidence intervals (dashed lines), $n = 6$ for each group. (b) Immunohistochemical localisation and (c) quantification of CD31-positive vessels in CAPAN-2 tumours from mice after 14 days of treatment with CORM-2. (d) Tumour size in athymic mice bearing PaTu-8902 human pancreatic cancer cells exposed to CO (500 ppm CO for 1 h/day). $^*p < 0.05$ (CO treatment *vs.* control, based on RM ANOVA with Holm–Sidak *post hoc* testing). (e) Survival curve of athymic mice bearing PaTu-8902 human pancreatic cancer cells exposed to CO (500 ppm CO for 1 h/day). Data expressed as mean ± SD, graphs represent survival times (continuous line) and respective upper and lower confidence intervals (dashed lines), $n = 6$ for each group. ANOVA, analysis of variance; CO, carbon monoxide; CORM, carbon monoxide-releasing molecule; iCORM, inactive CORM; SD, standard deviation; ppm, parts per million.

and was even able to induce apoptosis in the CAPAN-2 pancreatic cancer cell line ($p < 0.05$, Fig. 1e).

Analysis of CO in the PaTu-8902 pancreatic cancer cells, exposed to 50 μmol/L of CORM-2, revealed a substantial increase in CO concentration within the cells (Fig. 3a) as well as the culture media (Fig. 3b).

3.2. CO inhibits pancreatic tumour growth in vivo

To confirm our *in vitro* data, the anticancer effects of CO were validated in an experimental animal cancer model, represented by athymic mice xenografted subcutaneously with human pancreatic cancer cells (CAPAN-2/PaTu-8902).

In the first model, athymic mice carrying CAPAN-2 xenografts were administered a dose of 35 mg/kg CORM-2 intraperitoneally, on a daily basis. Treatment with CORM-2 induced a significant increase in the survival rate, compared with the iCORM-2 treated control animals (37.7 ± 10.1 *vs.* 17.2 ± 2.1 days, $p = 0.0005$, Fig. 4a). Analysis of the capillary density of the tumour revealed a decrease in the number of CD31-positive vessels in CORM-2-treated, CAPAN-2 xenografted animals, compared with mice receiving iCORM-2 ($p < 0.01$, Fig. 4b and c); indicating that CORM-2 was able to substantially affect *de novo* angiogenesis. This finding was consistent with

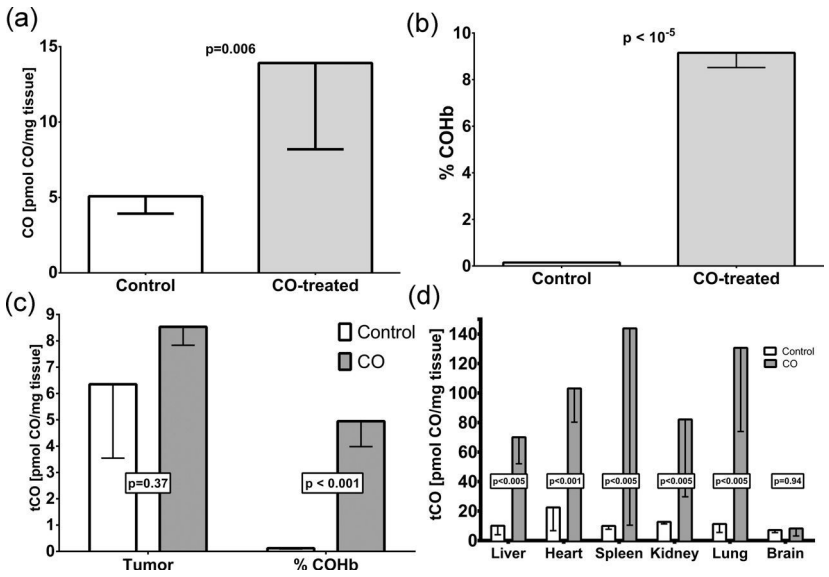

Fig. 5. The effect of CO exposure on its distribution in the body. (a) CO levels in tumour tissues, and (b) CO-haemoglobin levels in animals sacrificed immediately after the last exposure (day 14) to CO (500 ppm CO for 1 h/day). (c) CO levels in tumour tissue and CO-haemoglobin proportion, and (d) CO levels in various other organs of animals sacrificed 8 h after the last exposure (day 14) to CO (500 ppm CO for 1 h/day) control = tissues from animals unexposed to CO; $n = 6$ for each group. CO, carbon monoxide; SD, standard deviation; ppm, parts per million.

our *in vitro* data on CORM-2-induced suppression of Akt phosphorylation, since downstream signals from the Akt signalling pathway are known to contribute significantly to cancer neovascularisation [19].

Similarly, as in the *in vitro* studies, in order to verify whether CO released from the CORM-2 molecule was responsible for the observed antiproliferative/antiangiogenic effects of CORM-2, we also investigated the effect of CO *per se*. We assessed the tumour volume and survival in mice carrying subcutaneous human pancreatic ductal adenocarcinoma PaTu-8902 xenografts, which were treated with CO (500 ppm, 1-h exposure per day). CO-treated PaTu-8902 tumour-bearing mice showed a significant decrease in mean tumour volume ($p < 0.05$, Fig. 4d) and a two-fold increase in survival rate ($p = 0.004$, Fig. 4e), compared with the control mice exposed to air.

Analysis of CO levels in the tumour tissue, performed immediately after the last exposure to CO, demonstrated more than an 170% increase in CO concentrations at target tumours, compared with those of control mice ($p = 0.006$, Fig. 5a); this was paralleled by a marked increase in serum CO-haemoglobin levels ($p < 10^{-5}$, Fig. 5b). To assess the long-term distribution effects of CO exposure, we also assessed tissue levels of CO 8 h after the last exposure to the treatment gas. Consistent with its systemic effects on pancreatic cancer proliferation, CO concentrations in various organs, including subcutaneously xenografted pancreatic cancer, remained substantially high (Fig. 5c) even after this prolonged period of time, indicating the long-term systemic distribution of CO.

4. Discussion

For a long time, CO has been considered a toxic gas with potentially lethal consequences; however, it now appears to have multiple beneficial effects for human health. The importance of CO is underlined by the fact that substantial amounts of this gas is produced endogenously, as a result of the action of HMOX, which is among the most important stress enzymes in the human body [20].

Our *in vitro* and *in vivo* data show that exogenously administered CO, either in the form of CORM-2 or as direct CO exposure, acts as a potent inhibitor of pancreatic carcinogenesis. Indeed, in mice carrying human pancreatic xenografts, CO reduces tumour volume, limits tumour neovascularisation and profoundly prolongs survival. The doses of CO used in our *in vivo* study (500 ppm of CO for 1 h a day) are far below lethal doses for mice, which is equal to inhalation of 2400 ppm for 4 h [21]. This is also evidenced by the acceptable CO-haemoglobin levels of the CO-treated animals, which are even below the CO-haemoglobin concentrations achieved from clinically relevant CO dosages, using a FDA-approved CO inhalation device for human use [7]. Based on the very promising therapeutic potential of CO, the effects of CO inhalation at dosing regimens equivalent to those used in our work are currently being investigated in other clinical trials with patients suffering from pulmonary or intestinal diseases with safety and tolerability issues being investigated as well.[3]

Collectively, our data point to the antiproliferative nature of CO, which may genuinely have a chemotherapeutic/chemoadjuvant potential against certain cancers. CO along with NO and H_2S, belong to the potent bioactive gases having multiple, often shared, biological functions [22]. However, the observed antiproliferative action of CO appears to have the opposite effects to that of NO. NO generated following activation of endothelial nitric oxide synthase (NOS) promotes malignant progression [23] and VEGF-driven neovascularisation [24,25] through activation of the pro-survival Akt pathway [26], which is critical for ischemic and VEGF-mediated angiogenesis [19]. Positive inducible NOS expression correlates with increased microvessel density in human gastric cancer [27], although a dual role of NO in human carcinogenesis has been documented [28]. Based on our data, CO seems to inhibit Akt phosphorylation, which in turn is reflected by decreased neovascularization, as observed in our CORM-2 treated mice. This is in accord with the report by Becker et al. [29], which demonstrated a better prognosis for colon cancer patients overexpressing HMOX1 (responsible for endogenous CO production) in tumour tissues. Furthermore, Ferrando et al. demonstrated that HMOX1 overexpression in prostate cancer cells potently suppressed angiogenesis [30].

[3] www.clinicaltrials.gov [accessed 15.10.13].

Nevertheless, CO seems to contribute to the suppression of carcinogenesis by several additional mechanisms, as shown in the CO-induced inhibition of photocarcinogenesis [31] or migration of hepatoblastoma HepG2 cells [32]. CO derived from CORM-3 was also shown to interfere with the p38 MAPK signalling pathway in endothelial cells [33], which is consistent with our data on the CO-induced inhibition of Akt phosphorylation in pancreatic cancer cells. Furthermore, CO, a potent activator of guanylate cyclase [34], may also modulate cellular proliferation *via* increased cGMP production [35]. Additionally, for the first time we can report pharmacokinetic data of CO inhaled by experimental animals demonstrating a clinically important CO distribution within the various organs and tissues of the mouse body, including subcutaneously xenografted tumours, even after a prolonged period of time. Consistent with these data, we have also validated the efficient distribution of CO within pancreatic cancer cells exposed to the CORM-2 molecule. These kinetic data support the idea that CO might possibly be used in clinical settings.

In conclusion, we found that CO in relatively low (but clinically relevant and applicable) doses acts as a potent anticancer agent. These data suggest that CO could potentially be exploited as a novel chemotherapeutic/chemoadjuvant gas for inhibiting tumour growth.

Fundings

This work was supported by the Czech Ministry of Health (conceptual development of research organization RVO-VFN64165/2013), the Czech Ministry of Education (LH11030), and Charles University in Prague (PRVOUK-P25/LF1/2, SVV 266516/2013). None of the granting agencies had any influence upon the collection, analysis, interpretation of data, writing of the report, or on the decision to submit the paper for publication.

Conflict of interest statement

None to report.

Acknowledgements

We wish to thank Prof. Roberto Motterlini from INSERM, University Paris-Est, France for his critical reading of the manuscript; Prof. David K. Stevenson at Stanford University, Stanford, USA for loan of the Reduction Gas CO analyser; and Dr. Hendrik J. Vreman for making it functional in our Prague laboratory.

References

[1] Dulak J, Deshane J, Jozkowicz A, et al. Heme oxygenase-1 and carbon monoxide in vascular pathobiology: focus on angiogenesis. Circulation 2008;117:231–41.
[2] Wu L, Wang R. Carbon monoxide: endogenous production, physiological functions, and pharmacological applications. Pharmacological Reviews 2005;57:585–630.
[3] Jones MK, Tsugawa K, Tarnawski AS, et al. Dual actions of nitric oxide on angiogenesis: possible roles of PKC, ERK, and AP-1. Biochemical and Biophysical Research Communications 2004;318:520–8.
[4] Choi YK, Kim CK, Lee H, et al. Carbon monoxide promotes VEGF expression by increasing HIF-1alpha protein level via two distinct mechanisms, translational activation and stabilization of HIF-1alpha protein. Journal of Biological Chemistry 2010;285:32116–25.
[5] Abraham NG, Jiang H, Balazy M, et al. Methods for measurements of heme oxygenase (HO) isoforms-mediated synthesis of carbon monoxide and HO-1 and HO-2 proteins. Methods in Molecular Medicine 2003;86:399–411.
[6] Motterlini R, Clark JE, Foresti R, et al. Carbon monoxide-releasing molecules: characterization of biochemical and vascular activities. Circulation Research 2002;90:E17–24.
[7] Motterlini R, Otterbein LE. The therapeutic potential of carbon monoxide. Nature Reviews Drug Discovery 2010;9:728–43.
[8] Guo YR, Stein AB, Wu WJ, et al. Administration of a CO-releasing molecule at the time of reperfusion reduces infarct size in vivo. American Journal of Physiology Heart and Circulatory Physiology 2004;286:H1649–53.
[9] Ko AH, Dito E, Schillinger B, et al. A phase II study evaluating bevacizumab in combination with fixed-dose rate gemcitabine and low-dose cisplatin for metastatic pancreatic cancer: is an anti-VEGF strategy still applicable. Investigational New Drugs 2008;26:463–71.
[10] Parsons CM, Muilenburg D, Bowles TL, et al. The role of Akt activation in the response to chemotherapy in pancreatic cancer. Anticancer Research 2010;30:3279–89.
[11] Schlieman MG, Fahy BN, Ramsamooj R, et al. Incidence, mechanism and prognostic value of activated AKT in pancreas cancer. British Journal of Cancer 2003;89:2110–5.
[12] Fahy BN, Schlieman MG, Virudachalam S, et al. Inhibition of AKT abrogates chemotherapy-induced NF-kappaB survival mechanisms: implications for therapy in pancreatic cancer. Journal of the American College of Surgeons 2004;198:591–9.
[13] Fahy BN, Schlieman M, Virudachalam S, et al. AKT inhibition is associated with chemosensitisation in the pancreatic cancer cell line MIA-PaCa-2. British Journal of Cancer 2003;89:391–7.
[14] Gbelcova H, Lenicek M, Zelenka J, et al. Differences in antitumor effects of various statins on human pancreatic cancer. International Journal of Cancer 2008;122:1214–21.
[15] McKeage MJ, Kelland LR, Boxall FE, et al. Schedule dependency of orally administered bis-acetato-ammine-dichloro-cyclohexylamine-platinum(IV) (JM216) in vivo. Cancer Research 1994;54:4118–22.
[16] Vreman HJ, Wong RJ, Kadotani T, et al. Determination of carbon monoxide (CO) in rodent tissue: effect of heme administration and environmental CO exposure. Analytical Biochemistry 2005;341:280–9.
[17] Vreman HJ, Kwong LK, Stevenson DK. Carbon monoxide in blood; an improved microliter blood-sample collection system, with rapid analysis by gas chromatography. Clinical Chemistry 1984;30:1382–6.
[18] Bussolati B, Dunk C, Grohman M, et al. Vascular endothelial growth factor receptor-1 modulates vascular endothelial growth factor-mediated angiogenesis via nitric oxide. American Journal of Pathology 2001;159:993–1008.
[19] Ackah E, Yu J, Zoellner S, et al. Akt1/protein kinase Balpha is critical for ischemic and VEGF-mediated angiogenesis. Journal of Clinical Investigation 2005;115:2119–27.
[20] Ryter SW, Alam J, Choi AM. Heme oxygenase-1/carbon monoxide: from basic science to therapeutic applications. Physiological Reviews 2006;86:583–650.
[21] Rose CS, Jones RA, Jenkins Jr LJ, et al. The acute hyperbaric toxicity of carbon monoxide. Toxicology and Applied Pharmacology 1970;17:752–60.
[22] Olson KR, Donald JA, Dombkowski RA, et al. Evolutionary and comparative aspects of nitric oxide, carbon monoxide and hydrogen sulfide. Respiratory Physiology and Neurobiology 2012;184:117–29.
[23] Fukumura D, Kashiwagi S, Jain RK. The role of nitric oxide in tumour progression. Nature Reviews Cancer 2006;6:521–34.
[24] Ahmad S, Hewett PW, Wang P, et al. Direct evidence for endothelial vascular endothelial growth factor receptor-1 function in nitric oxide-mediated angiogenesis. Circulation Research 2006;99:715–22.
[25] Murohara T, Asahara T, Silver M, et al. Nitric oxide synthase modulates angiogenesis in response to tissue ischemia. Journal of Clinical Investigation 1998;101:2567–78.
[26] Dimmeler S, Assmus B, Hermann C, et al. Fluid shear stress stimulates phosphorylation of Akt in human endothelial cells: involvement in suppression of apoptosis. Circulation Research 1998;83:334–41.
[27] Chen CN, Hsieh FJ, Cheng YM, et al. Expression of inducible nitric oxide synthase and cyclooxygenase-2 in angiogenesis and clinical outcome of human gastric cancer. Journal of Surgical Oncology 2006;94:226–33.
[28] Ridnour LA, Thomas DD, Donzelli S, et al. The biphasic nature of nitric oxide responses in tumor biology. Antioxidants and Redox Signalling 2006;8:1329–37.
[29] Becker JC, Fukui H, Imai Y, et al. Colonic expression of heme oxygenase-1 is associated with a better long-term survival in patients with colorectal cancer. Scandinavian Journal of Gastroenterology 2007;42:852–8.
[30] Ferrando M, Gueron G, Elguero B, et al. Heme oxygenase 1 (HO-1) challenges the angiogenic switch in prostate cancer. Angiogenesis 2011;14:467–79.
[31] Allanson M, Reeve VE. Carbon monoxide signalling reduces photocarcinogenesis in the hairless mouse. Cancer Immunology and Immunotherapy 2007;56:1807–15.
[32] Zou C, Zhang H, Li Q, et al. Heme oxygenase-1: a molecular brake on hepatocellular carcinoma cell migration. Carcinogenesis 2011;32:1840–8.
[33] Bergstraesser C, Hoeger S, Song H, et al. Inhibition of VCAM-1 expression in endothelial cells by CORM-3: the role of the ubiquitin-proteasome system, p38, and mitochondrial respiration. Free Radical Biology and Medicine 2012;52:794–802.
[34] Brune B, Ullrich V. Inhibition of platelet aggregation by carbon monoxide is mediated by activation of guanylate cyclase. Molecular Pharmacology 1987;32:497–504.
[35] Pilz RB, Casteel DE. Regulation of gene expression by cyclic GMP. Circulation Research 2003;93:1034–46.
[36] Diez H, Garrido JJ, Wandosell F. Specific roles of Akt iso forms in apoptosis and axon growth regulation in neurons. PLoS One 2012;7:e32715.

ANNALS of Hepatology

ORIGINAL ARTICLE

March-April, Vol. 13 No. 2, 2014: 273-283

Anti-cancer effects of blue-green alga *Spirulina platensis*, a natural source of bilirubin-like tetrapyrrolic compounds

Renata Koníčková,* Kateřina Vaňková,* Jana Vaníková,* Kateřina Váňová,* Lucie Muchová,* Iva Subhanová,* Marie Zadinová,† Jaroslav Zelenka,‡ Aleš Dvořák,*,‡ Michal Kolář,§ Hynek Strnad,§ Silvie Rimpelová,|| Tomáš Ruml,|| Ronald J. Wong,¶ Libor Vítek*,**

* Institute of Medical Biochemistry and Laboratory Diagnostics, 1st Faculty of Medicine, Charles University, Prague, Czech Republic.
† Institute of Biophysics, 1st Faculty of Medicine, Charles University, Prague, Czech Republic.
‡ Institute of Physiology, Academy of Sciences of the Czech Republic, Prague, Czech Republic.
§ Institute of Molecular Genetics, Academy of Sciences of the Czech Republic, Prague, Czech Republic.
|| Department of Biochemistry and Microbiology, Institute of Chemical Technology, Prague, Czech Republic.
¶ Department of Pediatrics, Stanford University School of Medicine, Stanford, CA, USA.
** 4th Department of Internal Medicine, 1st Faculty of Medicine, Charles University, Prague, Czech Republic.

ABSTRACT

Spirulina platensis is a blue-green alga used as a dietary supplement because of its hypocholesterolemic properties. Among other bioactive substances, it is also rich in tetrapyrrolic compounds closely related to bilirubin molecule, a potent antioxidant and anti-proliferative agent. The aim of our study was to evaluate possible anticancer effects of *S. platensis* and *S. platensis*-derived tetrapyrroles using an experimental model of pancreatic cancer. The anti-proliferative effects of *S. platensis* and its tetrapyrrolic components [phycocyanobilin (PCB) and chlorophyllin, a surrogate molecule for chlorophyll A] were tested on several human pancreatic cancer cell lines and xenotransplanted nude mice. The effects of experimental therapeutics on mitochondrial reactive oxygen species (ROS) production and glutathione redox status were also evaluated. Compared to untreated cells, experimental therapeutics significantly decreased proliferation of human pancreatic cancer cell lines *in vitro* in a dose-dependent manner (from 0.16 g·L-1 [*S. platensis*], 60 μM [PCB], and 125 μM [chlorophyllin], $p<0.05$). The anti-proliferative effects of *S. platensis* were also shown *in vivo*, where inhibition of pancreatic cancer growth was evidenced since the third day of treatment ($p < 0.05$). All tested compounds decreased generation of mitochondrial ROS and glutathione redox status ($p = 0.0006$; 0.016; and 0.006 for *S. platensis*, PCB, and chlorophyllin, respectively). In conclusion, *S. platensis* and its tetrapyrrolic components substantially decreased the proliferation of experimental pancreatic cancer. These data support a chemopreventive role of this edible alga. Furthermore, it seems that dietary supplementation with this alga might enhance systemic pool of tetrapyrroles, known to be higher in subjects with Gilbert syndrome.

Key words. Bilirubin. Chlorophyll. Heme oxygenase. Phycocyanin. Phycocyanobilin.

INTRODUCTION

Spirulina platensis is a blue-green freshwater alga widely used as a dietary supplement. It is rich in proteins, carotenoids, essential fatty acids, vitamin B complex, vitamin E, and minerals such as copper, manganese, magnesium, iron, selenium, and zinc.[1] *S. platensis* has garnered much attention not only because of its high nutritional value; but also, it is a source of potent antioxidants including spirulans (sulphated polysaccharides), selenocompounds, phenolic compounds, and phycobiliproteins (C-phycocyanin and allophycocyanin).[1] In fact, numerous studies have demonstrated that dietary supplementation of *S. platensis* is helpful in the prevention and treatment of atherosclerosis, diabetes, and/or cancers (for review see Gershwin, 2008[2]).

C-phycocyanin is a light-harvesting biliprotein possibly implicated in biological effects of *S. platensis*.[2] C-phycocyanin contains a covalently-linked chromophore called phycocyanobilin (PCB),[3] a linear tetrapyrrolic molecule structurally resembling biliverdin, an antioxidant bile pigment

Correspondence and reprint request: Libor Vítek, MD, PhD
Institute of Medical Biochemistry and Laboratory Diagnostics. 1st Faculty of Medicine, Charles University in Prague.
Na Bojišti 3. Praha 2, 12000. Czech Republic.
Tel.: +420 2 2496 4203. Fax: +420 2 2496 4203
E-mail: vitek@cesnet.cz

Manuscript received: November 27, 2013.
Manuscript accepted: December 12, 2013.

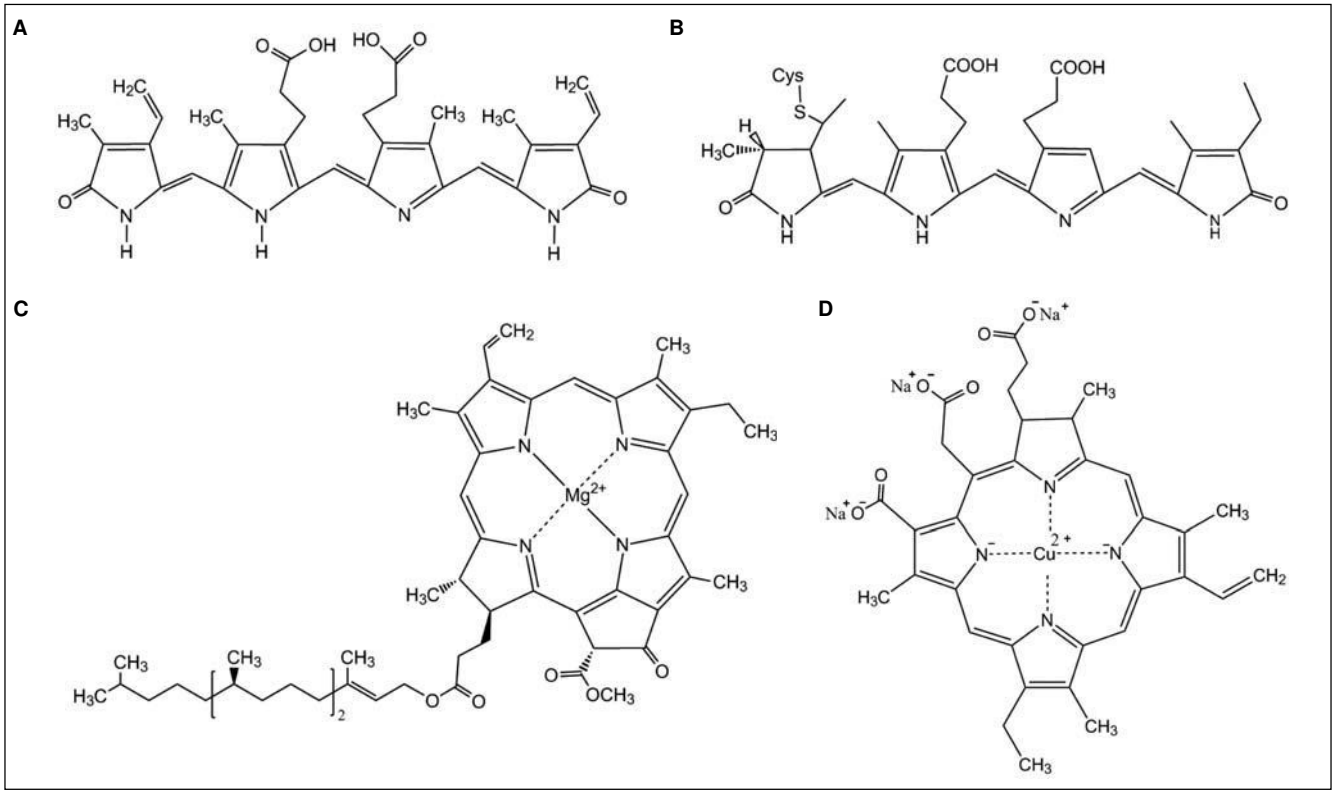

Figure 1. *Structures of tetrapyrrolic compounds of human and algal origin.* ***A.*** *Biliverdin.* ***B.*** *Phycocyanobilin.* ***C.*** *Chlorophyll A.* ***D.*** *Chlorophyllin.*

(Figure 1). PCB can be metabolized by biliverdin reductase to phycocyanorubin similarly as biliverdin is reduced to bilirubin in the human body. Bilirubin is a known major antioxidant in blood and negative associations between serum levels and numerous oxidative stress-mediated diseases including cardiovascular, certain cancer and autoimmune diseases have been published in recent years.[4-6] In fact, hyperbilirubinemic subjects with Gilbert syndrome were shown to have substantially lower risk of colon cancer,[5,7] and iatrogenic increase of serum bilirubin levels was proposed as a plausible approach to prevent oxidative stress-mediated diseases.[8] In addition, bilirubin has been reported to inhibit mitochondrial cytochrome c oxidase activity,[9] which causes cells to undergo premature apoptosis mediated through mitochondrial depolarization, caspase-3 activation and increased expression of mitochondria-associated pro-apoptotic Bax protein,[10] or even more profound changes in mitochondrial membrane integrity.[11] Simultaneously, bilirubin was demonstrated to substantially inhibit NADPH oxidase activity,[12,13] and the same inhibitory action was described also for phycocyanin and phycocyanobilin.[13]

Bilirubin is the major product of the heme catabolic pathway in the intravascular compartment, and its production is dependent on heme oxygenase activity (HMOX), the rate-limiting enzyme of this pathway. The inducible HMOX isoform (HMOX1, OMIM*141250), a member of the heat-shock protein HSP32 family, is activated by a number of oxidative stress-provoking stimuli. HMOX is also believed to be implicated in carcinogenesis, although our understanding of its exact role is still far from complete.[14] It is also important to note that various tetrapyrrolic compounds are potent modulators of HMOX1.[15]

In addition to PCB, *S. platensis* is also rich in another bioactive tetrapyrrole compound, which is chlorophyll. Despite being one of the most abundant biomolecules on Earth, only scarce data exist on the possible anti-proliferative effects of chlorophyll. These reports, nevertheless, propose the potential use of chlorophyll as a chemopreventive agent,[16] although detailed data are lacking. Chlorophylls, nonetheless, exert potent reactive oxygen species scavenging effects, as described in detail for chlorophyllin, a water-soluble analog of chlorophylls.[17] Since the cell proliferation is strongly influenced by redox signaling,[18] this antioxi-

dant action of chlorophylls might account for their presumed anti-proliferative properties.

The aim of our study was to evaluate possible anticancer effects of *S. platensis* and its tetrapyrrolic components on the model of experimental pancreatic cancer. More specifically, our focus was placed on their potential impact on the heme catabolic pathway and mitochondrial redox metabolism.

MATERIAL AND METHODS

Chemicals

S. platensis was purchased from Martin Bauer GmbH (Vestenbergsgreuth, Germany). Bilirubin and hemin were from Frontier Scientific (Logan, UT, USA), C-phycocyanin was purchased from ProZyme (Hayward, CA, USA), chlorophyllin (a water soluble, semi–synthetic derivate of chlorophyll commonly used in food industry, was employed in all *in vitro* studies as a surrogate for non-polar chlorophylls) and other chemicals were from Sigma-Aldrich (St. Louis, MO, USA).

Preparation of a water extract of *S. platensis*

Distilled water was added to freeze-dried *S. platensis* powder (30 $mL \cdot g^{-1}$ of alga). The suspension was sonicated for 15 min, incubated for 10 min at room temperature, centrifuged (8,000 x g, 30 min, 10 °C) and finally freeze-dried overnight. Prior to use, the extract was dissolved in culture medium and sterile-filtered.

PCB isolation from *S. platensis*

PCB was isolated from freeze-dried *S. platensis* according to the method of Terry.[19] Identification of PCB was confirmed by HPLC (Luna C8 column, 4.6·150 mm, 3m/100A, Phenomenex, Torrance, CA, USA; isocratic mobile phase with methanol/water/TBA, 59:40:1 w/w/w, flow rate of 0.5 $mL \cdot min^{-1}$), and mass spectrometry.

Cell lines

The following pancreatic cancer cell lines were used for the in vitro studies: PA-TU-8902 (DSMZ, Braunschweig, Germany), Mia PaCa-2 and BxPC-3 (ATCC, Manassas, VA, USA). All cell lines were maintained in a humidified atmosphere (containing 5% CO_2 at 37 °C) and in the following media supplemented with 10% fetal bovine serum (FBS): PA-TU-8902 and Mia PaCa-2 in DMEM, BxPC-3 in RPMI. Authentication of PA-TU-8902 cell line used in majority of described studies was confirmed by independent laboratory.

MTT assay

Viability of cancer cell lines was examined by MTT assay. The cells were cultured in a 96-well plate with tested therapeutics for 24 h. Then the cells were incubated for 2 h with the new medium containing MTT. The absorbance of formazan-reduction product of MTT corresponding to the relative viable cell number was measured at 545 nm with standard ELISA reader. Experimental therapeutics were found not to interfere with the reduction of MTT.

Selenium analysis

To assess possible contribution of selenium and/or selenocompounds to the biological effects of *S. platensis*, its content in the water extract of *S. platensis* used in our *in vitro* studies was determined by atomic absorption spectrometry using a standard clinical chemistry procedure.

Peroxyl radical scavenging capacity

Peroxyl radical scavenging capacity was measured fluorometrically as a proportion of antioxidant consumption relative to that of Trolox, as described previously.[20]

Determination of heme oxygenase enzyme activity

PA-TU-8902 cells were incubated for 24 h with tested therapeutics. After incubation, the cells were quickly washed with phosphate buffered saline (PBS, 0.1 M, pH 7.4), harvested, centrifuged, and each pellet was dispersed in PBS, and then sonicated. HMOX activity was determined by measurements of CO production using gas chromatography with a reduction gas analyzer (Peak Instruments, Menlo Park, CA, USA) as described previously.[21] HMOX activity was calculated as pmol CO/h/mg of protein.

Determination of mitochondrial reactive oxygen species production

The production of reactive oxygen species (ROS) in the mitochondrial matrix was determined as a

time-dependent increase in the fluorescence intensity of selective MitoSOX (Life Technologies, Pleasanton, CA, USA) dye in the cells exposed to tested therapeutics using flow cytometry (BD LSRII, BD Biosciences, San Jose, CA, USA). After 24 h, MitoSOX was added for 15 min to cells. Immediately before each measurement, cells were treated with rotenone (10 μM) to enhance the production of mitochondrial ROS. The rate of fluorescence intensity increase was determined in 1-min intervals for 16 min by flow cytometry.

Determination of GSH/GSSG

The cells exposed to tested therapeutics for 24 h were re-suspended in distilled water, and then lyzed with chloroform. The lysates were centrifuged at 1,000 x g for 5 min, upper aqueous phase containing glutathione was collected, snap-frozen in liquid nitrogen, and stored at liquid nitrogen until analysis. Samples (in 40 mM PBS, pH 7.0) were analyzed by capillary electrophoresis (voltage = 30 kV, detection at 195 nm, Agilent 7100, Agilent, Santa Clara, CA, USA) equipped with a polyimide-coated fused silica capillary (68 cm x 50 μm) as described previously.[22]

High-resolution respirometry

The respiration of intact and treated cells in the complete medium was measured with the Oroboros Oxygraph-2k (Oroboros Instruments, Innsbruck, Austria). Oxygen consumption was measured in the basal state, after treatment with oligomycin (2 mg·L^{-1}), a Complex V inhibitor used to determine the relative coupling of respiration and phosphorylation, and FCCP (5 μM), a ionophore and mitochondrial uncoupling agent used to determine maximal respiratory capacity of the cells.

Fluorescence microscopy determination of PCB and C-phycocyanin within PA-TU-8902 cells

To determine the uptake of PCB and C-phycocyanin, PA-TU-8902 cells (10^5·well^{-1}) were seeded on microscopic dishes and left to adhere overnight (16 h). Attached cells were incubated with PCB and C-phycocyanin (0.2 to 5.0 μM) dissolved in the complete phenol red-free medium at 37°C for 1, 3, 6, and 20 h. In an additional set of experiments that focused on the determination of intracellular localization of pigment uptake, cells were exposed to C-phycocyanin (0.2 μM) for 1 and 20 h, and MitoTracker® Green FM (100 nM) and LysoTracker® Green DND-26 (75 nM) (Molecular Probes, Life Technologies, Carlsbad, CA, USA) for staining of mitochondria and lysosomes, respectively.

Intracellular localization was assessed by real-time live-cell fluorescence microscopy. The images were acquired by an inverse fluorescent microscope Olympus IX-81 with a confocal unit Cell® System (Olympus, Tokyo, Japan) using high-stability 150 W xenon arc burner and EM-CCD camera C9100-02 (Hamamatsu, Ammersee, Germany).

Reverse Transcription quantitative Polymerase Chain Reaction (RT-qPCR)

PA-TU-8902 cells were incubated for 24 h before treatment. Chlorophyllin (30 μM), unconjugated bilirubin (10 μM), PCB (30 μM), and *S. platensis* extract (0.3 g·L) were added and RNA was isolated after 1 h (PerfectPure RNA Cultured Cell Kit, 5PRIME, Hamburg, Germany). Primers (sequences in table 1) were designed using Primer 3 software http://frodo.wi.mit.edu/primer3/) and synthesized by Generi Biotech (Hradec Kralove, Czech Republic). RT-qPCR were performed in 20-μL reaction volumes, containing 4 μL of 10-fold diluted cDNA template from a completed reverse transcription

Table 1. Primer sequences for RT-qPCR target genes.

	Forward primer	Reverse primer	PCR product (bp)
NOX2	GATTCTCTTGCCAGTCTGTCG	ATTCCTGTCCAGTTGTCTTCG	94
P22	CTTCACCCAGTGGTACTTTGG	GGCGGTCATGTACTTCTGTCC	130
HMOX1	GGGTGATAGAAGAGGCCAAGA	AGCTCCTGCAACTCCTCAAA	67
BLVRA	tccctctttggggagctttc	ggacccagacttgaaatggaag	180
HPRT	CACTGGCAAAACAATGCAGAC	GGGTCCTTTTCACCAGCAAG	92

NOX2: NADPH oxidase. p22: p22phox NADPH oxidase. HMOX1: heme oxygenase 1. BLVRA: biliverdin reductase A. HPRT: hypoxanthine phosphoribosyltransferase (a control gene).

reaction, 1x SYBR Green Master Mix (Applied Biosystems, Foster City, CA, USA), and 200-1000 nM of forward and reverse primers. All RT-qPCR were run on a ViiATM™ (Applied Biosystems).

In vivo experiments

In vivo studies were performed on nude mice (strain CD-1, Charles River WIGA, Sulzfeld, Germany) xenotransplanted subcutaneously with PA-TU-8902 cells (107 per mouse; n = 6 for each treatment group). After initiation of tumor growth (7-10 days after xenotransplantation), mice received oral treatment (intragastrically once daily via a gastric tube) with a placebo (water) or a water suspension of freeze-dried *S. platensis* (0.5 $g \cdot kg^{-1}$). An assessment of subcutaneous tumor size was performed by measurements of the 2 greatest perpendicular diameters, measured every 3 days with a caliper.[23] After 14 days of treatment, mice were sacrificed. Blood and tumor tissue specimens were sampled and stored at -80 °C until analyzed.

To confirm antioxidant effects of *S. platensis* treatment (10 $g \cdot kg^{-1}$ BW for 4 days), Wistar rats (n = 9) were used in a separate study using the same protocol as described above. To determine the total peroxyl scavenging activity in sera, blood was sampled from the ocular sinus prior to initiation of the feeding and from vena cava at sacrifice.

Ethics statement

All aspects of the animal studies and all protocols met the accepted criteria for the care and experimental use of laboratory animals, and were approved by the Animal Research Committee of the 1st Faculty of Medicine, Charles University in Prague (under registration No. 356/10). All procedures were performed under lege artis conditions and all efforts were made to minimize animal suffering.

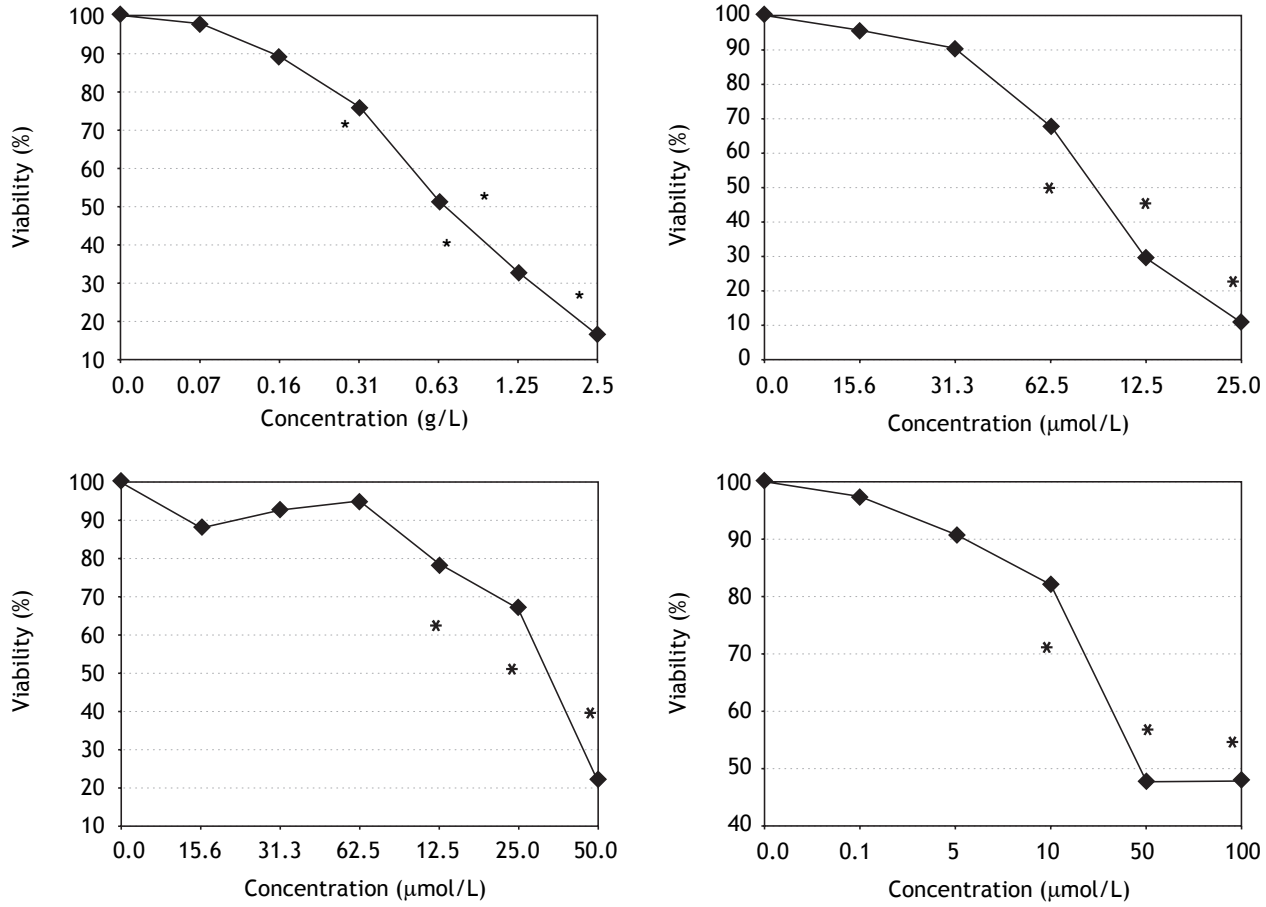

Figure 2. *Effects of S. platensis extract and related tetrapyrrolic compounds on PA-TU-8902 pancreatic cancer cell viability.* ***A.*** *S. platensis extract.* ***B.*** *PCB.* ***C.*** *Chlorophyllin.* ***D.*** *Bilirubin. Viability was measured using the MTT assay after 24 h exposure to each compound. Experiments were performed in quadruplicates, data presented as mean. *p < 0.05.*

Statistical analyses

Differences between variables were evaluated by the Mann-Whitney Rank Sum test. Group mean differences in tumor size were measured by repeated measures analysis of variance (RM ANOVA) with Holm–Šidák posthoc testing, when p-values were significant. When needed, log transform values of tumor size were used for comparisons to comply with normality and equal variance requirements. Linear regression analyses were used to compare the effects of *S. platensis* treatment on total peroxyl scavenging activity *in vitro*. Paired t-tests were used to compare the effects of *S. platensis* on total peroxyl scavenging activity *in vivo*. Depending on their normality, data are presented as the mean ± SD or the median and 25%-75% range. Differences were considered statistically significant when p-values were less than 0.05.

RESULTS

Effects of *S. platensis* extract and its tetrapyrrolic components on pancreatic cancer cell viability

All therapeutics efficiently decreased pancreatic cancer cell viability in a dose-dependent manner. The most sensitive cancer cell line was PA-TU-8902, whose viability was substantially decreased following treatment with *S. platensis* (from 0.16 g·L-1, $p < 0.05$) (Figure 2). As low as 10 μM concentrations of bilirubin (corresponding to its levels in human serum) substantially suppressed PA-TU-8902 cell viability ($p < 0.05$); whereas, doses of approximately 60 μM PCB, and 125 μM chlorophyllin were needed to reach the same effect (Figure 2). For other pancreatic cancer cell lines (Mia PaCa-2 and BxPC-3), higher concentrations of all compounds (~3 x) were required to reduce cell viability to 50% (data not shown). No selenium was detected in the *S. platensis* extract (detection limit of the method = 9 ng·mL) indicating that selenoproteins were not responsible for observed anti-proliferative effects of *S. platensis* treatment.

Based on these findings, the PA-TU-8902 cell line was used for further studies.

Effects of *S. platensis* extract and its tetrapyrrolic components on HMOX in PA-TU-8902 cells

The HMOX pathway was investigated for two reasons:

- HMOX has been reported to affect tumor cell proliferation[24] and tetrapyrrolic compounds used in our study might modulate HMOX in a feedback mechanism; and
- HMOX is a potent effector of the antioxidant defense system.

Therefore, the effects of *S. platensis* extract and its related tetrapyrrolic compounds on HMOX in the PA-TU-8902 cells were analyzed. Neither the *S. platensis* extract, PCB, nor bilirubin had any effect on HMOX activity (Figure 3) or *HMOX1* mRNA expression. However, only chlorophyllin (30 μM) significantly inhibited HMOX activity (to 51 ± 6% of control values, $p < 0.001$) (Figure 3) and mRNA expression (to 55 ± 32% of control values, $p = 0.016$, data not shown). Interestingly, the same inhibitory effect of chlorophyllin on HMOX activity was also observed for Mia PaCa-2 pancreatic cancer cells (data not shown). Expression of biliverdin reductase (*OMIM* * 109750), another important gene in the heme catabolic pathway, was not affected by any of these compounds (data not shown).

Effects of *S. platensis* extract and its tetrapyrrolic components on mitochondrial redox status of PA-TU-8902 cells

Proliferation of normal and cancer cells is strongly influenced by redox signaling.[18] Because PCB is

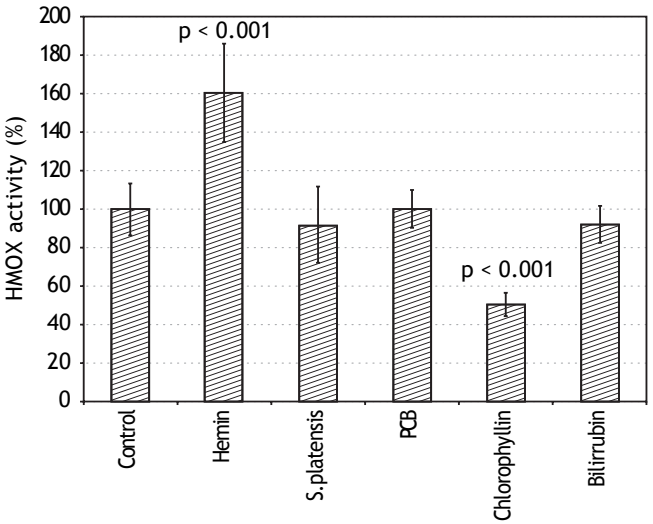

Figure 3. *Effects of* S. platensis *extract and related tetrapyrrolic compounds on HMOX enzyme activity. PA-TU-8902 pancreatic cancer cells were incubated with* S. platensis *extract (0.3 g·L^{-1}), hemin (30 μM), PCB (30 μM), chlorophyllin (30 μM), and bilirubin (10 μM) for 24 h. Heme oxygenase activity expressed as percentage of control (100%).*

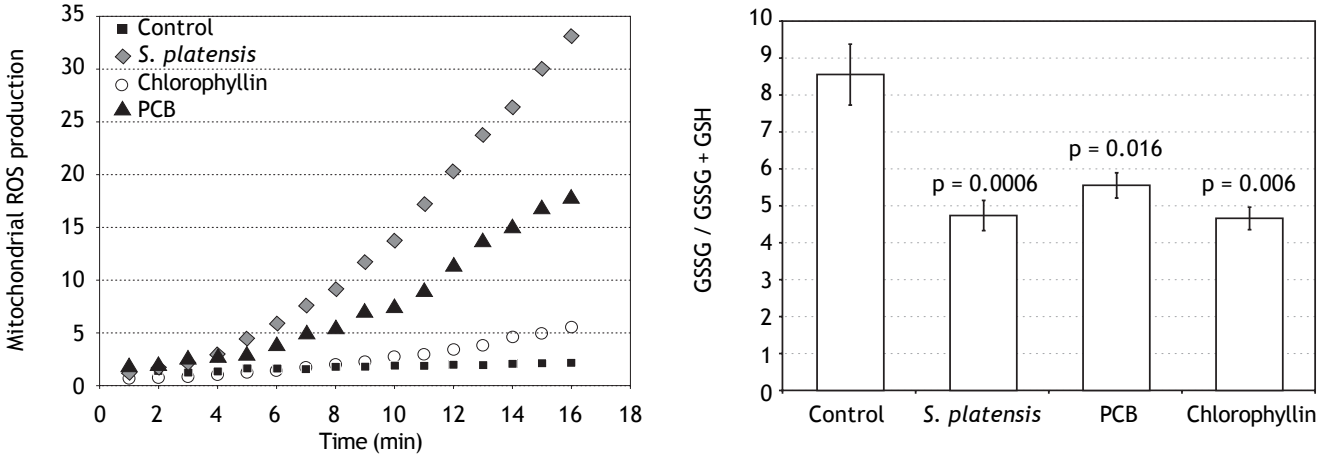

***Figure 4**. Effects of* S. platensis *and related tetrapyrrolic compounds on (**A**) mitochondrial production of ROS and (**B**) glutathione redox status. PA-TU-8902 pancreatic cancer cells were incubated with* S. platensis *extract (0.3 g·L^{-1}), PCB (50 μM), and chlorophyllin (50 μM) for 24 h. ROS: reactive oxygen species. GSH: reduced glutathione. GSSG: oxidized glutathione.*

structurally related to the potent antioxidants bilirubin and biliverdin, its effects on the cellular redox balance were investigated. The main source of intracellular free radicals under basal conditions is from a leakage of superoxide from the mitochondrial respiratory chain.[25] Even more importantly, NADPH oxidase-derived superoxide has an important function in pancreatic cancer cell proliferation due to K-ras/Rac1-dependent NADPH oxidase induction[26] and the importance of this pathway was demonstrated also for liver carcinogenesis.[27] Therefore, we were interested whether *S. platensis* and/or *S. platensis*-derived tetrapyrroles could influence mitochondrial production of ROS.

Indeed, we found that 24 h after exposure of PA-TU-8902 cells to *S. platensis* extract, PCB, and chlorophyllin resulted in significant decreases in intramitochondrial ROS production (Figure 4A), despite the fact that mRNA expressions of *NOX2* and *p22* NADPH oxidase subunits were not affected by 1 h incubation of cells with either *S. platensis* extract, PCB, or chlorophyllin (data not shown).

We then investigated whether this effect is robust enough to modify the cellular redox balance by determination of the oxidized and reduced glutathione ratio. We found that pre-incubation of cells with *S. platensis* extract, PCB, or chlorophyllin shifted the ratio towards increased reduction ($p = 0.0006$; 0.016; and 0.006, respectively) (Figure 4B).

Finally, we investigated whether a decreased leakage of mitochondrial ROS was due to direct antioxidant properties of tested therapeutics, or whether these compounds influence the ROS leakage by modulation of activity and efficiency of mitochondrial respiratory chain.[25] We measured mitochondrial respiration of the cells maintained in the complete medium in a basal state and during maximal stimulation with an uncoupling agent FCCP, and basal proton leakage during inhibition of Complex V with oligomycin. Interestingly, we found no changes in the respiration of the PA-TU-8902 cells after exposure to *S. platensis* extract, PCB, or chlorophyllin (data not shown) suggesting that decreased leakage of ROS was due to direct antioxidant properties of *S. platensis* and its tetrapyrroles, PCB, and/or chlorophyllin.

Uptake and localization of C-phycocyanin and PCB in PA-TU-8902 cells

Live cell imaging studies demonstrated that both C-phycocyanin and PCB incubated with PA-TU-8902 cells can easily enter the cells (Figure 5.1, data for PCB not shown). Accumulation of both pigments within the cells was apparent within 1 h of treatment, and gradually increased in time- and concentration-dependent manners. Localizations of C-phycocyanin and PCB in the cells were observed mainly in the form of vesicles localized in perinuclear region. The co-localization of LysoTracker Green with C-phycocyanin was seen in most of the observed vesicles within the cells (Figure 5.1). Co-localization study with a mitochondrial marker MitoTracker Green revealed that C-phycocyanin was absent in the mitochondria as shown by their typical elongated shape

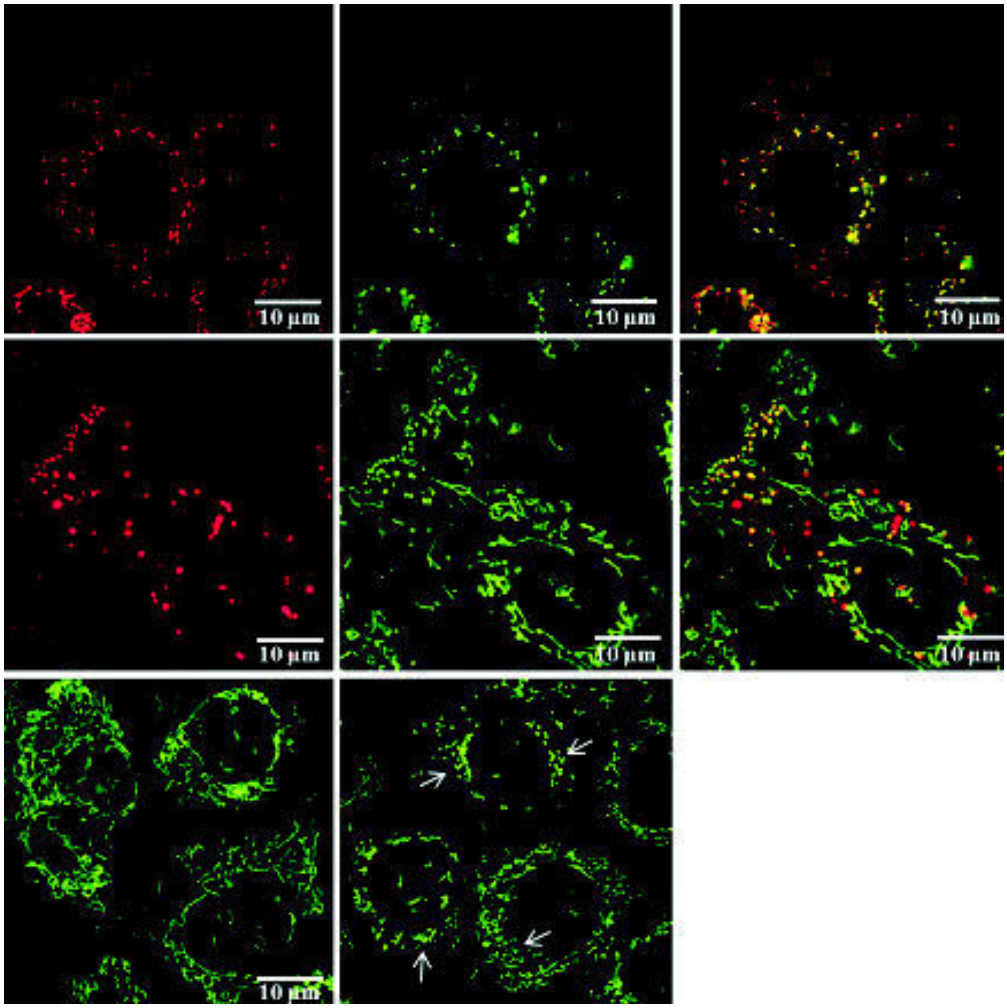

Figure 5. *C-phycocyanin uptake and its localization within PA-TU-8902 cells.*

1. *Lysosomal staining of PA-TU-8902 cells with LysoTracker Green exposed to C-phycocyanin (0.2 µM, 20 h incubation).* ***A.*** *C-Phycocyanin.* ***B.*** *LysoTracker Green.* ***C.*** *Merge of A and B.*

2. *Mitochondrial staining of PA-TU-8902 cells with MitoTracker Green exposed to C-phycocyanin (0.2 µM, 20 h incubation).* ***A.*** *C-Phycocyanin.* ***B.*** *MitoTracker Green.* ***C.*** *Merge of A and B.*

3. *Mitochondrial fragmentation in PA-TU-8902 cells exposed to C-phycocyanin (0.2 µM, 20 h incubation).* ***A.*** *Mitochondria of untreated cells stained with MitoTracker Green.* ***B.*** *Fragmented mitochondria of cells treated with C-phycocyanin (mitochondrial fragmentation depicted by arrows).*

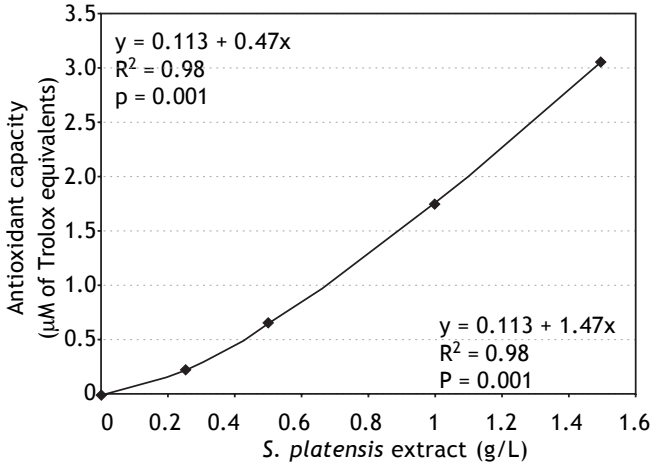

Figure 6. *Effects of* S. platensis *extract on total peroxyl scavenging activity* in vitro. *Peroxyl radical scavenging capacity was measured fluorometrically as a proportion of antioxidant consumption present in serum relative to that of Trolox (a reference and calibration antioxidant compound).*[20]

(mitochondrial network). In contrast, both dyes co-localized in aberrant-looking vesicles of mitochondrial origin (fragmented mitochondria) (Figure 5.2), disrupting the usual mitochondrial network (Figure 5.3).

Effects of *S. platensis* on total antioxidant capacity

To demonstrate whether the antioxidant effects observed on the cellular level may influence total antioxidant capacity, the total peroxyl scavenging activity was measured in *S. platensis* extracts demonstrating an approximately linear relationship between antioxidant activity and the concentration of the *S. platensis* extract (Figure 6).

Biological relevance of these findings was confirmed in our *in vivo* study, which demonstrated a significant increase (132 ± 22%, p = 0.002) in antioxidant capacity of rats fed *S. platensis* for 5 days.

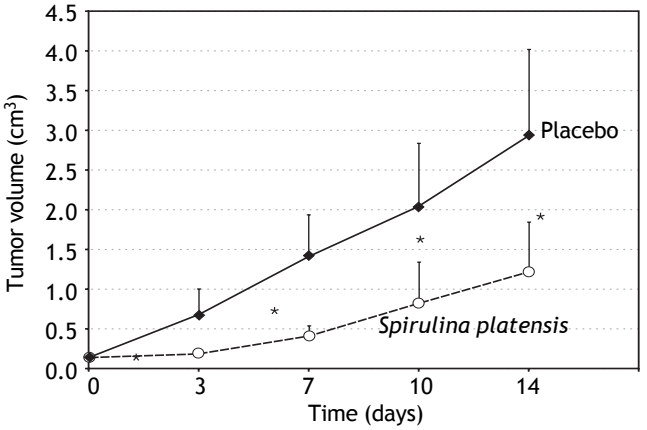

Figure 7. In vivo *anticancer effects of* S. platensis. *Athymic nu/nu mice xenotransplanted with PA-TU-8902 pancreatic cancer cells received placebo (water) or water suspension of freeze-dried* S. platensis *(0.5 g·kg^{-1}) intragastrically. Data expressed as mean ± SD. *p < 0.01.*

In vivo anticancer effects of *S. platensis*

Athymic nu/nu mice xenotransplanted with PA-TU-8902 cells, which were treated orally with *S. platensis* extract, exhibited much slower tumor progression compared to the placebo-treated mice. Tumor sizes were significantly smaller as early as the third day after initiation of the treatment ($p < 0.01$) (Figure 7).

DISCUSSION

S. platensis has been used by humans for centuries as evidenced by reports from Mexico and Central Africa.[2] Currently, it is widely used as a nutraceutical namely for the prevention of diabetes, although numerous other biological effects have been ascribed to this alga.[2] Among many potentially-bioactive substances, PCB and chlorophylls, represent compounds of particular interest due to their structural resemblance to bilirubin, a potent antioxidant, atheroprotective, and anti-proliferative agent.[24] In fact, the anticancer action of bilirubin has been attributed to its effects on mitochondria[28] as well as intracellular signalization.[29] In addition, bilirubin was found to be a widespread inhibitor of protein phosphorylation,[30] which might account for these biological properties. Importantly, these data are reflected by results from human studies demonstrating lower risk of colon[5,7] as well as lung[31] cancer in Gilbert syndrome subjects. In our study, we demonstrated that *S. platensis* and related tetrapyrroles have potent anti-proliferative effects on experimental human pancreatic cancer. We found that tested therapeutics exerted strong antioxidant effects with substantial reductions of mitochondrial ROS production, which may improve overall cellular redox status as indicated by an observed shift in glutathione redox parameters. These findings seem to parallel the inhibitory effects of bilirubin on superoxide production[32] and on overall mitochondrial metabolism.[33] In fact, pyrrole groups of bilirubin, present also in our compounds, have been suggested to compete with NADH on the active sites of mitochondrial dehydrogenases indicating possible mechanisms of these effects.[33] This conclusion is also in accord with a report by Boloor, et al., who described marked protective effects of chlorophyllin on mitochondria-induced lipid peroxidation.[34] It seems that observed anti-carcinogenic effects are mediated, at least partially, by direct inhibition of mitochondrial ROS generation.

Collectively, our data suggest that the primary target of algal tetrapyrroles is the mitochondria of the pancreatic cancer cells. This is based on the results of our topological as well as functional studies. The former observation is supported by our finding of co-localization of C-phycocyanin/PCB with fragmented mitochondria and lysosomes. It is generally believed that the observed mitochondria-related cytoplasmic vesicles result from the lysosomal apoptotic pathway mediated by mitochondria.[35] The formed vesicles might also be autophagosomes of mitochondrial origin, which after maturation, fuse with lysosomes.[36] It is of note that a similar preferential intracellular co-localization phenomenon was described for phtalocyanine, a related porphyrin-like molecule.[37] This data are also in line with the results of the functional studies. Although we did not see changes in mRNA expressions of NADPH oxidase subunits, our results on inhibition of mitochondrial ROS production are consistent with previous reports indicating that bilirubin, biliverdin, and PCB are potent inhibitors of NADPH oxidase.[12,13,38] In fact, Lanone, *et al*. showed potent inhibitory effects of bilirubin towards NADPH oxidase activity, although mRNA expressions were unchanged.[12] Mitochondrial NADPH oxidase-derived superoxide represents an important carcinogenic factor affecting redox-sensitive cell survival, cell cycle as well as multiple metabolic pathways[18,39] and this factor is implicated not only in pancreatic,[26] but also liver carcinogenesis.[27] Consistent with this data is the algal tetrapyrroles-induced improvement in glutathione redox status known to be associated with inhibition of tumor promotion.[40] Interestingly, complementary antioxidant and cytoprotective roles of glutathione and bilirubin have been reported previously.[41]

Interestingly, we also observed a marked inhibitory effect of chlorophyllin on both *HMOX1* mRNA expression and total HMOX enzyme activity, while the other tetrapyrroles did not have any effect. This inhibitory action, which is in accord with opposing effects of various metalloporphyrins on HMOX,[15] might contribute to anti-carcinogenic effects observed in our study and also, at least in part, account for chemopreventive effects of chlorophyll-rich nutrients.

One of the limitations of our study is that we have not directly identified all particular components in the *S. platensis* extract responsible for the observed biological effects, and focused only on the algal tetrapyrroles. However, it should be emphasized that exactly the same preparation, i.e. pulverized *S. platensis*, is commonly used in a global scale. Our data thus provide evidence for all the consumers on the anti-cancer potential of this alga.

In conclusion, *S. platensis*, as well as its tetrapyrrolic components, substantially decreased proliferation of pancreatic cancer. These effects were at least partially due to their potent antioxidant activity, inhibition of mitochondrial production of ROS and subsequent changes in intracellular redox status. These data support a chemopreventive role of this edible alga with promising potential for its broad use in the chemoadjuvant treatment of cancer diseases. This assumption of more generalized use of *S. platensis* in cancer chemoprevention is supported also by recent data demonstrating anti-cancer potential of this alga on liver[39] as well as breast[42] carcinogenesis. It also should be noted, that dietary supplementation with this alga might enhance systemic pool of tetrapyrroles in a more natural way, as compared to xenobiotic-induced hyperbilirubinemia approach proposed recently.[43]

FINANCIAL SUPPORT

This work was supported by grants Nos. 55210, 438911, LH11030, PRVOUK-P25/LF1/2, and RVO-VFN64165/2013 given by the Granting Agency of the Charles University in Prague, Czech Ministry of Education and Czech Ministry of Health, respectively. The granting agencies had no influence upon the collection, analysis, interpretation of data, writing of the report, nor on the decision to submit the paper for publication.

ACKNOWLEDGEMENTS

Authors thank to Drs. Pavel Coufal and Tomáš Křížek from Department of Analytical Chemistry, Faculty of Science of the Charles University in Prague for kindly providing us with capillary electrophoresis equipment, Magdalena Kadlecová and Olga Švejdová for excellent technical assistance.

REFERENCES

1. Dillon JC, Phuc AP, Dubacq JP. Nutritional value of the alga Spirulina. *World Rev Nutr Diet* 1995; 77: 32-46.
2. Gershwin ME, Belay A. Spirulina in human nutrition and health. Boca Raton: CRC Press; 2008.
3. Padyana AK, Bhat VB, Madyastha KM, Rajashankar KR, Ramakumar S. Crystal structure of a light-harvesting protein C-phycocyanin from Spirulina platensis. *Biochem Biophys Res Commun* 2001; 282: 893-8.
4. Novotny L, Vitek L. Inverse relationship between serum bilirubin and atherosclerosis in men: a meta-analysis of published studies. *Exp Biol Med* 2003; 228: 568-71.
5. Jiraskova A, Novotny J, Novotny L, Vodicka P, Pardini B, Naccarati A, Schwertner HA, et al. Association of serum bilirubin and promoter variations in HMOX1 and UGT1A1 genes with sporadic colorectal cancer. *Int J Cancer* 2012; 131: 1549-55.
6. Vitek L, Muchova L, Jancova E, Pešičková S, Tegzová D, Peterová V, Pavelka K, et al. Association of systemic lupus erythematosus with low serum bilirubin levels. *Scand J Rheumatol* 2010; 39: 480-4.
7. Zucker SD, Horn PS, Sherman KE. Serum bilirubin levels in the US population: Gender effect and inverse correlation with colorectal cancer. *Hepatology* 2004; 40: 827-35.
8. McCarty MF. «Iatrogenic Gilbert syndrome»-a strategy for reducing vascular and cancer risk by increasing plasma unconjugated bilirubin. *Med Hypotheses* 2007; 69: 974-94.
9. Malik SG, Irwanto KA, Ostrow JD, Tiribelli C. Effect of bilirubin on cytochrome c oxidase activity of mitochondria from mouse brain and liver. *BMC Res Notes* 2010;3: 162.
10. Rodrigues CM, Sola S, Brites D. Bilirubin induces apoptosis via the mitochondrial pathway in developing rat brain neurons. *Hepatology* 2002; 35: 1186-95.
11. Rodrigues CM, Sola S, Brito MA, Brites D, Moura JJ. Bilirubin directly disrupts membrane lipid polarity and fluidity, protein order, and redox status in rat mitochondria. *J Hepatol* 2002; 36: 335-41.
12. Lanone S, Bloc S, Foresti R, Almolki A, Taillé C, Callebert J, Conti M, et al. Bilirubin decreases nos2 expression via inhibition of NAD(P)H oxidase: implications for protection against endotoxic shock in rats. *FASEB J* 2005; 19: 1890-2.
13. Zheng J, Inoguchi T, Sasaki S, et al. Phycocyanin and phycocyanobilin from Spirulina platensis protect against diabetic nephropathy by inhibiting oxidative stress. *Am J Physiol Regul Integr Comp Physiol* 2013; 304: R110-R120.
14. Was H, Dulak J, Jozkowicz A. Heme oxygenase-1 in tumor biology and therapy. *Curr Drug Targets* 2010; 11: 1551-70.
15. Drummond GS, Kappas A. Prevention of neonatal hyperbilirubinemia by tin protoporphyrin IX, a potent competitive inhibitor of heme oxidation. *Proc Natl Acad Sci USA* 1981; 78: 6466-70.
16. Hayatsu H, Negishi T, Arimoto S, Hayatsu T. Porphyrins as potential inhibitors against exposure to carcinogens and mutagens. *Mutat Res* 1993; 290: 79-85.
17. Kumar SS, Devasagayam TP, Bhushan B, Verma NC. Scavenging of reactive oxygen species by chlorophyllin: an ESR study. *Free Radic Res* 2001; 35: 563-74.

18. Antico Arciuch VG, Elguero ME, Poderoso JJ, Carreras MC. Mitochondrial regulation of cell cycle and proliferation. *Antioxid Redox Signal* 2012; 16: 1150-80.
19. Terry MJ, Maines MD, Lagarias JC. Inactivation of phytochrome- and phycobiliprotein-chromophore precursors by rat liver biliverdin reductase. *J Biol Chem* 1993; 268: 26099-106.
20. Iuliano L, Piccheri C, Coppola I, Pratico D, Micheletta F, Violi F. Fluorescence quenching of dipyridamole associated to peroxyl radical scavenging: a versatile probe to measure the chain breaking antioxidant activity of biomolecules. *Biochim Biophys Acta* 2000; 1474: 177-82.
21. Vreman HJ, Stevenson DK. Heme oxygenase activity as measured by carbon monoxide production. *Anal Biochem* 1988; 168: 31-8.
22. Maeso N, Garcia-Martinez D, Ruperez FJ, Cifuentes A, Barbas C. Capillary electrophoresis of glutathione to monitor oxidative stress and response to antioxidant treatments in an animal model. *J Chromatogr B Analyt Technol Biomed Life Sci* 2005; 822: 61-9. Doi: 10.1016/j.jchromb.2005.05.015.
23. McKeage MJ, Kelland LR, Boxall FE, Valenti MR, Jones M, Goddard PM, Gwynne J, et al. Schedule dependency of orally administered bis-acetato-ammine-dichloro-cyclohexylamine-platinum(IV) (JM216) in vivo. *Cancer Res* 1994; 54: 4118-22.
24. Vitek L, Schwertner HA. The heme catabolic pathway and its protective effects on oxidative stress-mediated diseases. *Adv Clin Chem* 2007; 43: 1-57.
25. Jezek P, Hlavata L. Mitochondria in homeostasis of reactive oxygen species in cell, tissues, and organism. *Int J Biochem Cell Biol* 2005; 37: 2478-503.
26. Du J, Liu J, Smith BJ, Tsao MS, Cullen JJ. Role of Rac1-dependent NADPH oxidase in the growth of pancreatic cancer. *Cancer Gene Ther* 2011; 18: 135-43. Doi: 10.1038/cgt.2010.64.
27. Teufelhofer O, Parzefall W, Kainzbauer E, Ferk F, Freiler C, Knasmüller S, Elbling L, et al. Superoxide generation from Kupffer cells contributes to hepatocarcinogenesis: studies on NADPH oxidase knockout mice. *Carcinogenesis* 2005; 26: 319-29.
28. Keshavan P, Schwemberger SJ, Smith DLH, Babcock GF, Zucker SD. Unconjugated bilirubin induces apoptosis in colon cancer cells by triggering mitochondrial depolarization. *Int J Canc* 2004; 112: 433-45.
29. Ollinger R, Kogler P, Troppmair J, Hermann M, Wurm M, Drasche A, Königsrainer I, et al. Bilirubin inhibits tumor cell growth via activation of ERK. *Cell Cycle* 2007; 6: 3078-85.
30. Hansen TW, Mathiesen SB, Walaas SI. Bilirubin has widespread inhibitory effects on protein phosphorylation. *Pediatr Res* 1996; 39: 1072-77.
31. Horsfall LJ, Rait G, Walters K, Swallow DM, Pereira SP, Nazareth I, Petersen I. Serum bilirubin and risk of respiratory disease and death. *JAMA* 2011; 305: 691-7.
32. Nakamura H, Uetani Y, Komura M, Takada S, Sano K, Matsuo T. Inhibitory action of bilirubin on superoxide production by polymorphonuclear leukocytes. *Biol Neonate* 1987; 52: 273-8.
33. Noir BA, Boveris A, Garaza Pereira AM, Stoppani AO. Bilirubin: a multi-site inhibitor of mitochondrial respiration. *FEBS Lett* 1972; 27: 270-4.
34. Boloor KK, Kamat JP, Devasagayam TP. Chlorophyllin as a protector of mitochondrial membranes against gamma-radiation and photosensitization. *Toxicology* 2000; 155: 63-71.
35. Boya P, Andreau K, Poncet D, Zamzami N, Perfettini JL, Metivier D, Ojcius DM, et al. Lysosomal membrane permeabilization induces cell death in a mitochondrion-dependent fashion. *J Exp Med* 2003; 197: 1323-34.
36. Arstila AU, Trump BF. Studies on cellular autophagocytosis. The formation of autophagic vacuoles in the liver after glucagon administration. *Am J Pathol* 1968; 53: 687-733.
37. Rodriguez ME, Kim J, Delos Santos GB, Azizuddin K, Berlin J, Anderson VE, Kenney ME, et al. Binding to and photo-oxidation of cardiolipin by the phthalocyanine photosensitizer Pc 4. *J Biomed Opt* 2010; 15: 051604.
38. Fujii M, Inoguchi T, Sasaki S, Maeda Y, Zheng J, Kobayashi K, Takayanagi R. Bilirubin and biliverdin protect rodents against diabetic nephropathy by downregulating NAD(P)H oxidase. *Kidney Int* 2010; 78: 905-19.
39. Nazarewicz RR, Dikalova A, Bikineyeva A, Ivanov S, Kirilyuk IA, Grigor'ev IA, Dikalov SI. Does scavenging of mitochondrial superoxide attenuate cancer prosurvival signaling pathways? *Antioxid Redox Signal* 2013; 19: 344-9.
40. Perchellet JP, Perchellet EM, Orten DK, Schneider BA. Decreased ratio of reduced/oxidized glutathione in mouse epidermal cells treated with tumor promoters. *Carcinogenesis* 1986; 7: 503-6.
41. Sedlak TW, Saleh M, Higginson DS, Paul BD, Juluri KR, Snyder SH. Bilirubin and glutathione have complementary antioxidant and cytoprotective roles. *Proc Natl Acad Sci USA* 2009; 106: 5171-6.
42. Ouhtit A, Ismail MF, Osman A, Fernando A, Abdraboh ME, El-Kott AF, Azab YA, et al. Chemoprevention of rat mammary carcinogenesis by Spirulina. *Am J Pathol* 2013. Doi: 10.1016/j.ajpath.2013.10.025 [Epub ahead of print].
43. Dekker D, Dorresteijn MJ, Pijnenburg M, Heemskerk S, Rasing-Hoogveld A, Burger DM, Wagener FA, et al. The bilirubin-increasing drug atazanavir improves endothelial function in patients with type 2 diabetes mellitus. *Arterioscler Thromb Vasc Biol* 2011; 31: 458-63.

5 Discussion

Our work was focused on unknown aspects of bilirubin metabolism in the intestinal lumen as well as brain tissue with the aim to elucidate behavior of this pigment and uncover further potential biological consequences. Our further effort was directed to investigation of antiproliferative properties of the heme catabolic pathway´s products, in particular bilirubin, carbon monoxide, and bilirubin-like tetrapyrrolic compounds naturally contained in certain plants and algae.

In the project **„Reduction of bilirubin ditaurate by the intestinal bacterium *Clostridium perfringens*“** we proved that the bilirubin-reducing bacterial strain of *C. perfringens* isolated from neonatal feces is capable of reducing BDT (Vitek, Majer et al. 2006). BDT is a polar molecule due to the attachment of two taurine moieties through amid bonds. As compared with UCB, that is a non-polar substance, BDT has very different properties. It has been published that the *C. perfringens* strain is able to reduce also the natural bilirubin conjugate, bisglucuronosyl bilirubin (Vitek, Majer et al. 2006). Nevertheless, this bacterial reduction of bisglucuronosyl bilirubin is prevented by the hydrolysis of ester bond, by which, as a result, the glucuronic acids and UCB are released. Subsequently, UCB is further reduced to various reduction products (Vitek, Majer et al. 2006). In our study, we were able to demonstrate that *C. perfringens* reduced BDT to diverse taurine-conjugated urobilinoids, urobilinogen ditaurate, urobilin ditaurate and most likely mesobiliviolin ditaurate. The amid bond of BDT is probably resistant to enzymatic hydrolysis pointing to the broad substrate specificity of bilirubin-reducing enzyme(s) in the gastrointestinal tract. This may help our understanding of bilirubin intestinal metabolism, in particular bilirubin reduction in the intestinal lumen, a process, which still awaits to be described in detail. These findings, as we believe, might have impact for management of neonatal jaundice by enhancing bilirubin catabolism in the intestinal lumen, but also might help to understand the role of intestinal microflora in colonic carcinogenesis.

Potent bilirubin neurotoxicity, that can occur during severe unconjugated hyperbilirubinemia, was studied in the work named **„Bilirubin accumulation and *Cyp* mRNA**

expression in selected brain regions of jaundiced Gunn rat pups". Recent studies emphasized the importance of Bf, that can enter tissues, as protective antioxidant on one side and on the other hand under pathological conditions as neurotoxic agent. It also should be emphasized, that mechanisms causing bilirubin-induced neurotoxicity are likely to be responsible also for beneficial anti-proliferative/anticancer properties believed to be in play in the adult age. Thus, understanding of all of these processes might enable to identify the role of bilirubin in carcinogenesis as well.

As regard to bilirubin neurotoxicity, only scarce data existed on bilirubin distribution in selected brain areas during bilirubin encephalopathy, in particular due to inaccessibility of a sensitive analytical method for bilirubin determination in the tissues. Establishment and optimization of a novel sensitive HPLC method for bilirubin determination in tissues (Zelenka, Lenicek et al. 2008) enabled us to explore these kinetic data in our experimental study on neonatal hyperbilirubinemic rats. The study focused on determination of bilirubin content and mRNA expression of cytochrome P450 monooxygenases (Cyp) and ATP-binding cassette transporters (ABC) in selected brain regions of hyperbilirubinemic Gunn rat pups after sulphadimetoxine treatment. Sulphadimetoxine administration causes acute displacing of bilirubin from albumin leading to sudden increase of Bf concentrations. This experimental model is being used to study severe unconjugated hyperbilirubinemias, such as neonatal jaundice or CN syndrome. Our experimental animal study has provided important new data on the time dependency of the sudden and massive accumulation and gradual clearance of UCB in different brain regions during neonatal period. We were able to demonstrate greater and longer-lasting accumulations of UCB in the cerebellum and inferior colliculi, whose functions (in particular motor coordination and auditory functions, respectively) are impaired in sudden onset bilirubin encephalopathy (Ahlfors and Shapiro 2001). By contrast, UCB accumulation after sulphadimethoxine was limited and brief in the cortex and superior colliculi, whose functions (cognition and vision, respectively) are unimpaired in bilirubin-induced neurological damage. The spatial proximity of the superior colliculi and inferior colliculi suggests further that their markedly different kinetics and severity of UCB accumulation are unlikely to be due to differences in blood supply or blood–brain barriers, but most probably are linked to cellular mechanisms responsible for biotransformation of

UCB. This conclusion has been further supported by the relationships between expression of Cyp known to oxidize UCB and the dynamics of tissue UCB in the selected brain regions. An immediate and massive upregulation of the Cyp mRNAs and much smaller immediate upregulation of the ABC transporters in the unaffected brain regions (cortex and superior colliculi), in striking contrast to the delayed and relatively low upregulation of Cyp and ABC transporters in the affected brain regions (cerebellum and inferior colliculi). This suggests that Cyp and, presumably, UCB oxidation provide major protection against acute accumulation of UCB in the unaffected regions, with the minor role of ABC transporters originally thought to play an important role in bilirubin export from the bilirubin-overloaded cells. Because only mRNA expression was assessed, confirmation of this hypothesis will require further studies of upregulation of enzyme and transporter protein levels and activities. Our data suggest that the original concept of kernicterus, based on selective damage due to regional bilirubin accumulation in the brain, should be reassessed. Our study shows that regional modulation of Cyp may account for the differences among brain regions in severity and duration of bilirubin accumulation during sudden increases in Bf.

In the further study focused on bilirubin neurotoxicity entitled **„Beyond plasma bilirubin: The effects of phototherapy and albumin on brain bilirubin levels in Gunn rats“**, it was shown that human serum albumin effectively decreased brain bilirubin levels in phototherapy-treated Gunn rats. The decrease was obvious in both used models of chronic (like in CN syndrome patients) and acute hemolytic jaundice (model for severe neonatal hyperbilirubinemia). Our results support the use of human serum albumin (HSA) as adjunct treatment to phototherapy of unconjugated hyperbilirubinemias. HSA treatment is based on ability of HSA to effectively bind Bf within the intravascular compartment and thus it prevents its translocation into the brain and development of bilirubin-induced brain damage. The role of Bf translocation became apparent in 1950s, when sulphisoxazole-treated newborns developed kernicterus even in the presence of unusually low plasma bilirubin level (Harris, Lucey et al. 1958). It was discovered that sulphisoxazol displaced bilirubin from albumin, that first pointed to the importance of the non-albumin bound bilirubin (Odell 1959). The importance of Bf for pathophysiology of bilirubin encephalopathy was highlighted by Ahlfors et al. by the observation that auditory brainstem response screening, a

quantifiable method to evaluate the bilirubin-induced neurotoxicity, correlates with Bf rather than with total blood bilirubin concentration (Ahlfors, Amin et al. 2009). The protective impact of HSA administration has been studied in neonates, but there were still insufficient information on the efficiency as well as mechanisms of presumed beneficial effects. We first investigated the efficacy of adjunct HSA treatment in hyperbilirubinemic Gunn rats. Phototherapy decreased unconjugated hyperbilirubinemia in these animals, while HSA alone increased plasma bilirubin level. Bf and brain bilirubin concentrations were decreased by phototherapy and also by HSA administration alone. These results are in concordance with previous animal studies (Diamond and Schmid 1966). Next we investigated adjunct HSA treatment during phototherapy in Gunn rats. Animals with adjunct HSA treatment had lower Bf and, to lesser extent, brain bilirubin levels, compared with phototherapy alone. Our data support the Bf paradigm, according to which only Bf is able to move between vascular and tissue compartment. HSA could work in tandem with phototherapy by decreasing Bf in plasma and thus also its translocation into brain. This shift was reflected in our study by an increase of plasma total bilirubin during the HSA treatment, where bilirubin was photoisomerized, transported to the liver and excreted into bile. In acutely jaundiced Gunn rats neither phototherapy nor HSA treatment alone did affect the severity of hemolysis. The most striking finding was the synergistic effect of combined phototherapy and HSA treatment in this case. Adjunct HSA decreased Bf in plasma, and completely prevented the hemolysis-induced deposition of bilirubin in the brain, in contrast to phototherapy and HSA treatment alone. The failure of HSA treatment alone demonstrates the importance of phototherapy. When HSA induces bilirubin shift from tissue compartment to plasma, phototherapy is needed to convert bilirubin to its photoisomers. Without phototherapy, bilirubin would move back from plasma to tissue as the albumin levels return to baseline. We cannot exclude the possibility that non-albumin bound bilirubin is less readily converted to its photoisomers compared to the protein bound fraction. Our results not only demonstrate the benefits of adjunct HSA administration, but also raise the question on the efficacy of phototherapy during acute hemolytic jaundice. Our data show that HSA enhances the efficacy of routine phototherapy in phototherapy-treated Gunn rats, in both chronic and acute jaundice.

Potential anticancer effects of CO, another important product of the heme catabolic pathway, were studied in another study entitled **„Antiproliferative effects of carbon monoxide on pancreatic cancer“**. For a long time CO has been seen only as toxic gas, however, today it is being investigated mainly for its broad beneficial effects for human health. CO is endogenously produced by HMOX, an important stress enzyme in the human body (Ryter, Alam et al. 2006). Our *in vitro* and *in vivo* data showed that exogenously administered CO, either in the form of CORM2 or as direct CO exposure, acts as a potent inhibitor of pancreatic carcinogenesis. In fact, in mice bearing human pancreatic xenografts, CO reduced tumor volume and neovascularization, and extended their overall survival. As far as the safety issues, the CO doses used in our experiments (500 ppm of CO for 1 hr a day) were far below the lethal doses for mice, that is 2400 ppm for 4 hours (Rose, Jones et al. 1970). CO-hemoglobin levels of the CO-treated animals were even below the CO-hemoglobin concentrations, which were achieved from clinically relevant CO dosages, using a FDA-approved CO-inhalation device for human use (Motterlini and Otterbein 2010). We showed that CO inhibited Akt (serin/threonin protein kinase B) phosphorylation *in vitro*, which was reflected by decreased neovascularization of the tumor tissue, as observed in our CORM2-treated mice. Akt kinase activation is common in pancreatic cancer (Schlieman, Fahy et al. 2003); this pathway is critical for ischemic and VEGF-mediated angiogenesis (Ackah, Yu et al. 2005) and its inhibition has been associated with cancer cell sensitization to apoptotic therapy (Fahy, Schlieman et al. 2003). CO seems to contribute to suppression of carcinogenesis by several mechanisms, as shown e.g. in CO-induced inhibition of photocarcinogenesis (Allanson and Reeve 2007) or migration of hepatoblastoma HepG2 cells (Zou, Zhang et al. 2011). CO released from CORM3 was also shown to interfere with the p38 MAPK signaling pathway in endothelial cells (Bergstraesser, Hoeger et al. 2012), which is consistent with our data demonstrating CO-induced inhibition of Akt phosphorylation in pancreatic cancer cells. Furthermore, CO, a potent activator of guanylate cyclase (Brune and Ullrich 1987), may also modulate cellular proliferation via increased cGMP production (Pilz and Casteel 2003). Additionally, for the first time we could report pharmacokinetic data of CO inhaled by the experimental mice demonstrating a clinically significant CO distribution within the various organs and tissues including subcutaneously xenografted tumours, even after a prolonged period of time. Consistent with this data, we have also validated the

efficient distribution of CO within pancreatic cancer cells exposed to the CORM2 molecule. This kinetic data supports the idea that CO might possibly be used in clinical settings. Our data point to the antiproliferative nature of CO in relatively low, but clinically relevant and applicable doses, which may genuinely have chemotherapeutic or chemoadjuvant potential against certain cancers.

Also our last study was focused on potential anticancer effects of bilirubin and bilirubin-like tetrapyrrolic molecules. In this study entitled **„Anti-cancer effects of blue-green alga *Spirulina platensis*, a natural source of bilirubin-like tetrapyrrolic compounds**", a blue-green alga *S. platensis* was used as a source of bilirubin-resembling compounds and its antioxidant and anticancer impact on experimental pancreatic cancer was studied in our paper. *S. platensis* is a strongly blue-green colored microalga, that is commonly consumed in central Africa or Mexico for centuries (Borowitzka 2009) and is widely used as a food supplement nowadays. Among many potentially bioactive substances, PCB and chlorophyll represented compounds of our interest due to their structural resemblance to bilirubin, a potent antioxidant, atheroprotective, and antiproliferative agent (Vitek and Schwertner 2007). The anticancer impact of bilirubin has been attributed to its effects on mitochondria (Keshavan, Schwemberger et al. 2004), note that the same effects are believed to be responsible for bilirubin neurotoxicity in severe neonatal jaundice (Rodrigues, Sola et al. 2002), as well as intracellular signalization (Ollinger, Kogler et al. 2007). In addition, bilirubin was found to be an inhibitor of protein phosphorylation (Hansen, Mathiesen et al. 1996), which might account for its biological properties. In our study, we demonstrated that *S. platensis* and related tetrapyrroles have potent antiproliferative effects on experimental human pancreatic cancer. We found that tested therapeutics exerted strong antioxidant effects with substantial reduction of mitochondrial ROS production, which may improve overall cellular redox status as indicated by an observed shift in glutathione redox parameters. These findings seem to parallel the inhibitory effects of bilirubin on superoxide production and on overall mitochondrial metabolism (Noir, Boveris et al. 1972, Nakamura, Uetani et al. 1987). Even more, our topological as well as functional studies suggest that the primary target of algal tetrapyrroles is mitochondria of the pancreatic cells. This observation is supported by co-localization of C-phycocyanin with fragmented mitochondria and

lysosomes. It is generally believed that the observed mitochondria-related cytoplasmic vesicles result from the lysosomal apoptotic pathway mediated by mitochondria (Boya, Andreau et al. 2003). The formed vesicles might also be autophagosomes of mitochondrial origin, which after maturation, fuse with lysosomes (Arstila and Trump 1968). It is of note that a similar preferential intracellular co-localization phenomenon was described for phtalocyanine, a related porphyrin-like molecule (Rodriguez, Kim et al. 2010). This data are also in line with the results of the functional studies. Our results on inhibition of mitochondrial ROS production are consistent with previous reports indicating that bilirubin, biliverdin, and PCB are potent inhibitors of NADPH oxidase (Lanone, Bloc et al. 2005, Fujii, Inoguchi et al. 2010, Zheng, Inoguchi et al. 2013). Mitochondrial NADPH oxidase-derived superoxide represents an important carcinogenic factor affecting redox-sensitive cell survival, cell cycle as well as multiple metabolic pathways (Antico Arciuch, Elguero et al. 2012, Nazarewicz, Dikalova et al. 2013) and this factor is implicated not only in pancreatic (Du, Liu et al. 2011) but also liver carcinogenesis (Teufelhofer, Parzefall et al. 2005). Consistent with this data is the algal tetrapyrrole-induced improvement in glutathione redox status known to be associated with inhibition of tumor promotion (Perchellet, Perchellet et al. 1986). Interestingly, complementary antioxidant and cytoprotective roles of glutathione and bilirubin have been reported previously (Sedlak, Saleh et al. 2009). We also observed a marked inhibitory effect of chlorophyllin on both mRNA expression and total HMOX enzyme activity, while the other tetrapyrroles did not have any effect. This inhibitory action, which is in accord with opposing effects of various metalloporphyrins on HMOX (Drummond and Kappas 1981), might contribute to anticarcinogenic effects observed in our study and also, at least in part, account for chemopreventive effects of chlorophyll-rich nutrients. One of the limitations of our study is that we have not directly identified all particular components in the *S. platensis* extract responsible for the observed biological effects, and focused only on the algal tetrapyrroles. However, it should be emphasized that exactly the same preparation, i.e. pulverized *S. platensis*, is commonly used in common nutraceutical practice. Importantly, our data are consistent with results from human studies showing lower risk of colon (Zucker, Horn et al. 2004, Jiraskova, Novotny et al. 2012) as well as lung (Horsfall, Rait et al. 2011) cancer in Gilbert syndrome subjects.

In conclusion of this study, *S. platensis*, as well as its tetrapyrrolic components, substantially decreased proliferation of pancreatic cancer. These effects were at least partially due to their potent antioxidant activity, inhibition of mitochondrial production of ROS and subsequent changes in intracellular redox status. These data support a chemopreventive role of this edible alga with promising potential for its broad use in the chemoadjuvant treatment of cancer diseases. This assumption of more generalized use of *S. platensis* in cancer chemoprevention is supported also by recent data demonstrating anti-cancer potential of this alga on liver (Nazarewicz, Dikalova et al. 2013) as well as breast carcinogenesis (Ouhtit, Ismail et al. 2014). It also should be noted, that dietary supplementation with this alga might enhance systemic pool of tetrapyrroles in a more natural way, as compared to xenobiotic-induced hyperbilirubinemia approach proposed recently (Dekker, Dorresteijn et al. 2011).

6 Summary

1. In our work **„Reduction of bilirubin ditaurate by the intestinal bacterium Clostridium perfringens“** products of this enzymatic process mediated by bilirubin-reducing strain of *C. perfringens* were identified and characterized. It was demonstrated that BDT is reduced without previous amid bond hydrolysis. The conversion rate was substantial, although not as efficient compared to UCB. Based on comparison with bilirubin reduction products and synthetic urobilinogen ditaurate standards, three BDT reduction products were identified: urobilinogen ditaurate, urobilin ditaurate and most likely mesobiliviolin ditaurate. Our results demonstrate very broad enzymatic substrate specificity of bilirubin reducing enzyme(s) and may help in understanding of bilirubin metabolism in the intestinal lumen by intestinal microflora. These findings, as we believe, might have impact for management of neonatal jaundice by enhancing bilirubin catabolism in the intestinal lumen, but also might help to understand the role of intestinal microflora in colonic carcinogenesis.
2. Our study focused on UCB neurotoxicity entitled **„Bilirubin accumulation and *Cyp* mRNA expression in selected brain regions of jaundiced Gunn rat pups“** uniquely describes very important UCB distribution and mRNA expression of cytochrome P450

monooxygenases and ABC transporters within different brain areas (cortex, superior colliculi, inferior colliculi, cerebellum) of experimental animal model of severe neonatal jaundice. The most sensitive cerebral areas for UCB accumulation were cerebellum and inferior colliculi (parts of the brain responsible for motor coordination and auditory functions). In contrast to cortex and superior colliculi where the UCB accumulation was limited and brief. Interestingly there was massive and immediate upregulation of Cyps and immediate ABC transporters expression in UCB unaffected brain regions (cortex, superior colliculi). In distinctive contrast to the delayed and relatively small upregulation of Cyps and ABC transporters in the affected brain regions (cerebellum and inferior colliculi). It seems that the close relationship in distinct brain regions between the extent of UCB accumulation and induction of Cyp mRNA plays an important role in protecting selected brain areas from bilirubin neurotoxicity. It is believed that the mechanisms causing bilirubin-induced neurotoxicity are likely to be responsible also for beneficial anti-proliferative/anticancer properties.

3. Data presented in the other paper focused on bilirubin neurotoxicity entitled **„Beyond plasma bilirubin: The effects of phototherapy and albumin on brain bilirubin levels in Gunn rats“** support adjunct albumin treatment for severe unconjugated hyperbilirubinemia. Human albumin was administered to chronic (a model for CN syndrome) and acute hemolytic (a model for severe neonatal jaundice) moderate hyperbilirubinemic Gunn rats with phototherapy. Our study confirmed importance of Bf for pathogenesis of bilirubin neurotoxicity, secondly, albumin treatment was demonstrated to enhance the efficacy of phototherapy leading to significantly decreased plasma Bf and brain bilirubin. Our results support the feasibility of adjunct albumin treatment in patients with CN syndrome or neonatal jaundice.
4. Data presented in our paper **„Antiproliferative effects of carbon monoxide on pancreatic cancer“** highlight potential anticancer impact of CO, an important gaseous molecule originating from heme catabolism. In our study, CO released from CORM or in the form of inhaled gas significantly inhibited proliferation of human pancreatic cancer cells. CO decreased substantially Akt (serin/threonin protein kinase B)

phosphorylation in the cancer cells. Athymic mice with xenotransplanted pancreatic tumor treated with CO had doubled the survival rates with significant inhibition of tumor proliferation and lower density of microvascular net formation. Interestingly, mice exposed to CO led to an almost 3-fold increase in CO content in tumor tissue grown subcutaneously. Additionally, our study reports for the first time the pharmacokinetic data of CO inhaled by experimental animals demonstrating a clinically important CO distribution within the various organs and tissue of the mice body. Results of this work point to the potential chemotherapeutic/chemoadjuvant use of CO in pancreatic cancer treatment.

5. Our work presented in the paper **„Anti-cancer effects of blue-green alga *Spirulina platensis*, a natural source of bilirubin-like tetrapyrrolic compounds**" describes antiproliferative effects of edible blue-green algae *S. platensis* and its tetrapyrroles (PCB and chlorophyllin, a surrogate molecule for chlorophyll A) on experimental pancreatic cancer. *In vitro,* a decrease of human pancreatic cancer cell lines´ viability was demonstrated in a dose-dependent manner. The antiproliferative effects of *S. platensis* were also shown *in vivo* in a xenograft mouse model. All tested compounds decreased generation of mitochondrial ROS and modulated glutathione redox status. These data support a chemopreventive role of this edible alga.

7 Souhrn

1. V naší práci **„Reduction of bilirubin ditaurate by the intestinal bacterium *Clostridium perfringens*"** jsme identifikovali produkty, které vznikly bakteriální, enzymatickou redukcí BDT. Byl použit nepatogenní kmen střevních bakterií *C. perfringens*, který mimo jiné také redukuje UCB. Ukázali jsme, že BDT je překvapivě redukováno bez předchozího hydrolytického odštěpení taurínů, i když rychlost konverze BDT ve srovnání s UCB byla snížená. Na základě srovnání s redukčními produkty UCB a syntetického standardu urobilinogenu ditaurátu jsme identifikovali následující produkty: urobilin ditaurát, urobilinogen ditaurát a pravděpodobě mesobiliviolin ditaurát. Naše výsledky poukazují na širokou substrátovou specifitu enzymu/ů schopných redukce UCB a také mohou pomoci porozumět bakteriálnímu

metabolismu bilirubinu ve střevním lumen s možným klinickým dopadem, včetně ochranného vlivu UCB na zažívací trakt.

2. Ve studii **„Bilirubin accumulation and *Cyp* mRNA expression in selected brain regions of jaundiced Gunn rat pups“** zaměřené na neurotoxické působení UCB jsme využili zvířecího modelu těžkých hyperbilirubinémií, jako jsou např. CN syndrome či patologická novorozenecká žloutenka. V této práci jsme zkoumali distribuci UCB a také expresi mRNA cytochrom P450 monooxigenás (Cyp) a ABC transportérů v různých částech mozku (kortex, colliculus superior, colliculus inferior a cerebellum). UCB se nejvíce akumuloval v cerebellu a také v colliculu inferior, což jsou části mozku zodpovědné za koordinaci pohybů a sluch, zatímco v kortexu a colliculu superior byla koncentrace UCB značně omezená. Je zajímavé, že výrazné a okamžité zvýšení exprese mRNA u Cyp a mírné zvýšení exprese mRNA u ABC transportérů bylo zaznamenáno v UCB nepostižených částech mozku, t.j. kortexu a colliculu superior, v porovnání se zpožděným a nepatrným zvýšením exprese v UCB postižených částech, cerebellu a colliculu inferior. Vypadá to tedy, že uzký vztah mezi obsahem UCB a zvýšením exprese mRNA u Cyp hraje důležitou roli v ochraně určitých částí mozku před neurotoxickými účinky UCB.
3. Data publikovaná v dalším článku **„Beyond plasma bilirubin: The effects of phototherapy and albumin on brain bilirubin levels in Gunn rats“** také zaměřeném na neurotoxický vliv UCB podporují podávání albuminu jako doplňku při léčbě, fototerapii, těžkých nekonjugovaných hyperbilirubinemií. I v této práci byl použit zvířecí model- hyperbilirubinemičtí Gunnovi potkani s chronickou (model pro CN syndrom) a akutní hemolytickou (model závažné novorozenecké žloutenky) hyperbilirubinemií. Potkanům byl podáván lidský albumin a byli léčeni fototerapií. Podávání albuminu zvyšovalo účinky fototerapie a tím došlo k poklesu Bf v krvi a také v mozku. Tato práce jen potvrzuje význam Bf v patogenezi neurotoxického vlivu bilirubinu a poukazuje na proveditelnost doplňkové léčby albuminem při fototerapii pacientů s CN syndromem či novorozeneckou žloutenkou.
4. Práce **„Antiproliferative effects of carbon monoxide on pancreatic cancer“** poukazuje na potenciální antiproliferační účinky CO, což je důležitá molekula vznikající při odbourání hemu. V naší studii byl použit CO uvolněný z CORM nebo

plynný CO. V obou případech CO významně inhiboval růst buněk lidského adenokarcinomu pankreatu a výrazně snižoval fosforylaci Akt (serin/threonin protein kinase B) v nádorových buňkách. Athymické myši nesoucí xenotransplantovaný nádor adenokarcinomu pankreatu, které byly léčeny CO, měly menší nádory s menší hustotou mikrovaskulární sítě a také doba přežití byla dvojnásobná v porovnání s kontrolní-neléčenou skupinou. Překvapivě u myší vystavených CO byl obsah CO v nádorové tkáni třikrát vyšší než v kontrolní skupině. Naše práce poprvé popisuje distribuci CO v různých orgánech myši a také farmakokinetiku CO v myších po jeho inhalaci. Výsledky práce poukazují na potenciální chemoterapeutické využití CO v léčbě rakoviny pankreatu.

5. Náš poslední článek **„Anti-cancer effects of blue-green alga *Spirulina platensis*, a natural source of bilirubin-like tetrapyrrolic compounds**" popisuje antiproliferační účinky jedlé, intenzivně modro-zelené mikrořasy *S. platensis* a v ní obsažených tetrapyrolů (PCB a chlorophyllinu, stabilního derivátu chlorofylu) na experimentální adenokarcinom pankreatu. *In vitro* jsme pozorovali pokles viability lidských nádorových linií adenokarcinomu pankreatu v závislosti na koncentraci sledovaných působků. Antiproliferační vliv *S. platensis* jsme prokázali také *in vivo* na modelu athymických myší, které byly xenotransplantovány nádorovou linií lidského adenokarcinomu pankreatu. Všechny testované látky snižovaly mitochondriální produkci ROS a ovlivňovaly redox statut buněk na úrovni glutathionu. Publikovaná data podporují chemopreventivní roli této jedlé mikrořasy.

8 List of abbreviations

ABC- ATP-binding cassette

ATP- adenosine triphosphate

AhR- aryl hydrocarbon receptor

BDT- bilirubin ditaurate

BHT- 2,6-di-tert-butyl-4-methylphenol

Bf- free bilirubin

BLVRA- biliverdin reductase

BV- biliverdin

CN- Crigler-Najjar

CO- carbon monoxide

CORM- CO-releasing molecule

CoA- coenzyme A

DMSO- dimethyl sulphoxide

DJS- Dubin-Johnson syndrome

GS- Gilbert syndrome

HMOX- heme oxygenase

HPLC- high performance liquid chromatography

HPRT- hypoxanthine phosphoribosyl transferase

MAPK- mitogen-activated phosphokinase

MRP- multidrug resistance-related polypeptide

MTT- 3-(4,5-dimethylthiazol-2-yl)-2,5-diphenol tetrazolium bromide

NAD- nicotinamide adenine dinucleotide

NADP- nicotinamide adenine dinucleotide phosphate

NOX2- NADPH oxidase 2

OATPs- Organic Anion Transport Polypeptides

p22- p22phox NADPH oxidase

PCB- phycocyanobilin

ROS- reactive oxygen species

RS- Rotor syndrome

RT-PCR - Real time polymerase chain reaction

TCA- trichloracetic acid

TLC- thin layer chromatography

UCB- unconjugated bilirubin

UGT1A1- UDP-glucuronosyl transferase

UDP- uridin-diphosphate

VEGFA- vascular endothelial growth factor A

9 References

Ackah, E., J. Yu, S. Zoellner, Y. Iwakiri, C. Skurk, R. Shibata, N. Ouchi, R. M. Easton, G. Galasso, M. J. Birnbaum, K. Walsh and W. C. Sessa (2005). "Akt1/protein kinase Balpha is critical for ischemic and VEGF-mediated angiogenesis." J Clin Invest **115**(8): 2119-2127.

Aft, R. L. and G. C. Mueller (1983). "Hemin-mediated DNA strand scission." J Biol Chem **258**(19): 12069-12072.

Ahlfors, C. E., S. B. Amin and A. E. Parker (2009). "Unbound bilirubin predicts abnormal automated auditory brainstem response in a diverse newborn population." J Perinatol **29**(4): 305-309.

Ahlfors, C. E. and S. M. Shapiro (2001). "Auditory brainstem response and unbound bilirubin in jaundiced (jj) Gunn rat pups." Biol Neonate **80**(2): 158-162.

Allanson, M. and V. E. Reeve (2007). "Carbon monoxide signalling reduces photocarcinogenesis in the hairless mouse." Cancer Immunol Immunother **56**(11): 1807-1815.

Amersi, F., R. Buelow, H. Kato, B. Ke, A. J. Coito, X. D. Shen, D. Zhao, J. Zaky, J. Melinek, C. R. Lassman, J. K. Kolls, J. Alam, T. Ritter, H. D. Volk, D. G. Farmer, R. M. Ghobrial, R. W. Busuttil and J. W. Kupiec-Weglinski (1999). "Upregulation of heme oxygenase-1 protects genetically fat Zucker rat livers from ischemia/reperfusion injury." J Clin Invest **104**(11): 1631-1639.

Antico Arciuch, V. G., M. E. Elguero, J. J. Poderoso and M. C. Carreras (2012). "Mitochondrial regulation of cell cycle and proliferation." Antioxid Redox Signal **16**(10): 1150-1180.

Arstila, A. U. and B. F. Trump (1968). "Studies on cellular autophagocytosis. The formation of autophagic vacuoles in the liver after glucagon administration." Am J Pathol **53**(5): 687-733.

Baranano, D. E., M. Rao, C. D. Ferris and S. H. Snyder (2002). "Biliverdin reductase: a major physiologic cytoprotectant." Proc Natl Acad Sci U S A **99**(25): 16093-16098.

Beale, S. I. and J. Cornejo (1983). "Biosynthesis of phycocyanobilin from exogenous labeled biliverdin in Cyanidium caldarium." Arch Biochem Biophys **227**(1): 279-286.

Bergstraesser, C., S. Hoeger, H. Song, L. Ermantraut, M. Hottenrot, T. Czymai, M. Schmidt, M. Goebeler, N. Ponelies, C. Stich, R. Loesel, G. Molema, M. Seelen, W. van Son, B. A. Yard and N. Rafat (2012). "Inhibition of VCAM-1 expression in endothelial cells by CORM-3: the role of the ubiquitin-proteasome system, p38, and mitochondrial respiration." Free Radic Biol Med **52**(4): 794-802.

Berk, P. D., R. B. Howe, J. R. Bloomer and N. I. Berlin (1969). "Studies of bilirubin kinetics in normal adults." J Clin Invest **48**(11): 2176-2190.

Bhutani, V. K. and L. Johnson (2009). "Kernicterus in the 21st century: frequently asked questions." J Perinatol **29 Suppl 1**: S20-24.

Bhutani, V. K. and R. J. Wong (2013). "Bilirubin neurotoxicity in preterm infants: risk and prevention." J Clin Neonatol **2**(2): 61-69.

Bhutani, V. K., A. Zipursky, H. Blencowe, R. Khanna, M. Sgro, F. Ebbesen, J. Bell, R. Mori, T. M. Slusher, N. Fahmy, V. K. Paul, L. Du, A. A. Okolo, M. F. de Almeida, B. O. Olusanya, P. Kumar, S. Cousens and J. E. Lawn (2013). "Neonatal hyperbilirubinemia and Rhesus disease of the newborn: incidence and impairment estimates for 2010 at regional and global levels." Pediatr Res **74 Suppl 1**: 86-100.

Borowitzka, M. (2009). "M. E. Gershwin, A. Belay (eds). Spirulina in human nutrition and health." Journal of Applied Phycology **21**(6): 747-748.

Boya, P., K. Andreau, D. Poncet, N. Zamzami, J. L. Perfettini, D. Metivier, D. M. Ojcius, M. Jaattela and G. Kroemer (2003). "Lysosomal membrane permeabilization induces cell death in a mitochondrion-dependent fashion." J Exp Med **197**(10): 1323-1334.

Braggins, P. E., G. M. Trakshel, R. K. Kutty and M. D. Maines (1986). "Characterization of two heme oxygenase isoforms in rat spleen: comparison with the hematin-induced and constitutive isoforms of the liver." Biochem Biophys Res Commun **141**(2): 528-533.

Brouard, S., L. E. Otterbein, J. Anrather, E. Tobiasch, F. H. Bach, A. M. Choi and M. P. Soares (2000). "Carbon monoxide generated by heme oxygenase 1 suppresses endothelial cell apoptosis." J Exp Med **192**(7): 1015-1026.

Brune, B. and V. Ullrich (1987). "Inhibition of platelet aggregation by carbon monoxide is mediated by activation of guanylate cyclase." Mol Pharmacol **32**(4): 497-504.

Buchler, J. W. (1975). Static coordination chemistry of metalloporphyrins. Porphyrins and Metalloporhyrins. Amsterodam, Elsevier.

Dashwood, R., T. Negishi, H. Hayatsu, V. Breinholt, J. Hendricks and G. Bailey (1998). "Chemopreventive properties of chlorophylls towards aflatoxin B1: a review of the antimutagenicity and anticarcinogenicity data in rainbow trout." Mutat Res **399**(2): 245-253.

Dekker, D., M. J. Dorresteijn, M. Pijnenburg, S. Heemskerk, A. Rasing-Hoogveld, D. M. Burger, F. A. Wagener and P. Smits (2011). "The bilirubin-increasing drug atazanavir improves endothelial function in patients with type 2 diabetes mellitus." Arterioscler Thromb Vasc Biol **31**(2): 458-463.

Diamond, I. and R. Schmid (1966). "Experimental bilirubin encephalopathy. The mode of entry of bilirubin-14C into the central nervous system." J Clin Invest **45**(5): 678-689.

Donaldson, M. S. (2004). "Nutrition and cancer: a review of the evidence for an anti-cancer diet." Nutr J **3**: 19.

Drummond, G. S. and A. Kappas (1981). "Prevention of neonatal hyperbilirubinemia by tin protoporphyrin IX, a potent competitive inhibitor of heme oxidation." Proc Natl Acad Sci U S A **78**(10): 6466-6470.

Du, J., J. Liu, B. J. Smith, M. S. Tsao and J. J. Cullen (2011). "Role of Rac1-dependent NADPH oxidase in the growth of pancreatic cancer." Cancer Gene Ther **18**(2): 135-143.

Eaton, J. W. and M. Qian (2002). "Molecular bases of cellular iron toxicity." Free Radic Biol Med **32**(9): 833-840.

Fahy, B. N., M. Schlieman, S. Virudachalam and R. J. Bold (2003). "AKT inhibition is associated with chemosensitisation in the pancreatic cancer cell line MIA-PaCa-2." Br J Cancer **89**(2): 391-397.

Floyd, R. A. and J. M. Carney (1993). "The role of metal ions in oxidative processes and aging." Toxicol Ind Health **9**(1-2): 197-214.

Foresti, R., C. J. Green and R. Motterlini (2004). "Generation of bile pigments by haem oxygenase: a refined cellular strategy in response to stressful insults." Biochem Soc Symp(71): 177-192.

Frei, B., R. Stocker and B. N. Ames (1988). "Antioxidant defenses and lipid peroxidation in human blood plasma." Proc Natl Acad Sci U S A **85**(24): 9748-9752.

Fujii, M., T. Inoguchi, S. Sasaki, Y. Maeda, J. Zheng, K. Kobayashi and R. Takayanagi (2010). "Bilirubin and biliverdin protect rodents against diabetic nephropathy by downregulating NAD(P)H oxidase." Kidney Int **78**(9): 905-919.

Furchgott, R. F. and D. Jothianandan (1991). "Endothelium-dependent and -independent vasodilation involving cyclic GMP: relaxation induced by nitric oxide, carbon monoxide and light." Blood Vessels **28**(1-3): 52-61.

Gibbs, P. E., C. Tudor and M. D. Maines (2012). "Biliverdin reductase: more than a namesake - the reductase, its Peptide fragments, and biliverdin regulate activity of the three classes of protein kinase C." Front Pharmacol **3**: 31.

Gies, H. P. and C. R. Roy (1990). "Bilirubin phototherapy and potential UVR hazards." Health Phys **58**(3): 313-320.

Hansen, T. W., S. B. Mathiesen and S. I. Walaas (1996). "Bilirubin has widespread inhibitory effects on protein phosphorylation." Pediatr Res **39**(6): 1072-1077.

Hardy, K. R. and S. R. Thom (1994). "Pathophysiology and treatment of carbon monoxide poisoning." J Toxicol Clin Toxicol **32**(6): 613-629.

Harris, R. C., J. F. Lucey and J. R. Maclean (1958). "Kernicterus in premature infants associated with low concentrations of bilirubin in the plasma." Pediatrics **21**(6): 875-884.

Horsfall, L. J., G. Rait, K. Walters, D. M. Swallow, S. P. Pereira, I. Nazareth and I. Petersen (2011). "Serum bilirubin and risk of respiratory disease and death." JAMA **305**(7): 691-697.

Inguaggiato, P., L. Gonzalez-Michaca, A. J. Croatt, J. J. Haggard, J. Alam and K. A. Nath (2001). "Cellular overexpression of heme oxygenase-1 up-regulates p21 and confers resistance to apoptosis." Kidney Int **60**(6): 2181-2191.

Jackson, J. C. (1997). "Adverse events associated with exchange transfusion in healthy and ill newborns." Pediatrics **99**(5): E7.

Jahanshahifard, S., M. Ahmadpour-Kacho and Y. Z. Pasha (2012). "Effects of phototherapy on cytokines' levels and white blood cells in term neonate with hyperbilirubinemia." J Clin Neonatol **1**(3): 139-142.

Jansen, P. L. (1999). "Diagnosis and management of Crigler-Najjar syndrome." Eur J Pediatr **158 Suppl 2**: S89-94.

Jansen, T. and A. Daiber (2012). "Direct Antioxidant Properties of Bilirubin and Biliverdin. Is there a Role for Biliverdin Reductase?" Front Pharmacol **3**: 30.

Jiraskova, A., J. Novotny, L. Novotny, P. Vodicka, B. Pardini, A. Naccarati, H. A. Schwertner, J. A. Hubacek, L. Puncocharova, Z. Smerhovsky and L. Vitek (2012). "Association of serum bilirubin and promoter variations in HMOX1 and UGT1A1 genes with sporadic colorectal cancer." Int J Cancer **131**(7): 1549-1555.

Jubert, C., J. Mata, G. Bench, R. Dashwood, C. Pereira, W. Tracewell, K. Turteltaub, D. Williams and G. Bailey (2009). "Effects of chlorophyll and chlorophyllin on low-dose aflatoxin B(1) pharmacokinetics in human volunteers." Cancer Prev Res (Phila) **2**(12): 1015-1022.

Kapitulnik, J. and F. J. Gonzalez (1993). "Marked endogenous activation of the CYP1A1 and CYP1A2 genes in the congenitally jaundiced Gunn rat." Mol Pharmacol **43**(5): 722-725.

Kawashima, A., Y. Oda, A. Yachie, S. Koizumi and I. Nakanishi (2002). "Heme oxygenase-1 deficiency: the first autopsy case." Hum Pathol **33**(1): 125-130.

Keenan, W. J., K. K. Novak, J. M. Sutherland, D. A. Bryla and K. L. Fetterly (1985). "Morbidity and mortality associated with exchange transfusion." Pediatrics **75**(2 Pt 2): 417-421.

Kennedy, G. Y. (1975). "Porphyrins in invertebrates." Ann N Y Acad Sci **244**: 662-673.

Kennedy, G. Y. and H. G. Vevers (1976). "A survey of avian eggshell pigments." Comp Biochem Physiol B **55**(1): 117-123.

Keshavan, P., S. J. Schwemberger, D. L. Smith, G. F. Babcock and S. D. Zucker (2004). "Unconjugated bilirubin induces apoptosis in colon cancer cells by triggering mitochondrial depolarization." Int J Cancer **112**(3): 433-445.

Kjartansson, S., K. Hammarlund and G. Sedin (1992). "Insensible water loss from the skin during phototherapy in term and preterm infants." Acta Paediatr **81**(10): 764-768.

Kodíček, M. (2004). Biochemické pojmy- výkladový slovník. Praha, VŠCHT-Praha**:** 171.

Kotal, P. and J. Fevery (1991). "Quantitation of urobilinogen in feces, urine, bile and serum by direct spectrophotometry of zinc complex." Clin Chim Acta **202**(1-2): 1-9.

Kutty, R. K. and M. D. Maines (1981). "Purification and characterization of biliverdin reductase from rat liver." J Biol Chem **256**(8): 3956-3962.

Lanone, S., S. Bloc, R. Foresti, A. Almolki, C. Taille, J. Callebert, M. Conti, D. Goven, M. Aubier, B. Dureuil, J. El-Benna, R. Motterlini and J. Boczkowski (2005). "Bilirubin decreases nos2 expression via inhibition of NAD(P)H oxidase: implications for protection against endotoxic shock in rats." FASEB J **19**(13): 1890-1892.

Lee, B. C. (1995). "Quelling the red menace- heme capture by bacteria." Molecular Microbiology **18**(3): 383-390.

Lenicek, M., D. Duricova, O. Hradsky, P. Dusatkova, A. Jiraskova, M. Lukas, P. Nachtigal and L. Vitek (2014). "The relationship between serum bilirubin and Crohn's disease." Inflamm Bowel Dis **20**(3): 481-487.

Lerner-Marmarosh, N., J. Shen, M. D. Torno, A. Kravets, Z. Hu and M. D. Maines (2005). "Human biliverdin reductase: a member of the insulin receptor substrate family with serine/threonine/tyrosine kinase activity." Proc Natl Acad Sci U S A **102**(20): 7109-7114.

Maines, M. D. (1997). "The heme oxygenase system: a regulator of second messenger gases." Annu Rev Pharmacol Toxicol **37**: 517-554.

Maines, M. D. (2003). "Bile pigments: newcomers to the cell signaling arena." Toxicol Sci **71**(1): 9-10.

Maines, M. D. (2005). "New insights into biliverdin reductase functions: linking heme metabolism to cell signaling." Physiology (Bethesda) **20**: 382-389.

Maisels, M. J. (1988). "Neonatal jaundice." Semin Liver Dis **8**(2): 148-162.

McCarty, M. F. (2007). "''Iatrogenic Gilbert syndrome''--a strategy for reducing vascular and cancer risk by increasing plasma unconjugated bilirubin." Med Hypotheses **69**(5): 974-994.

McDonagh, A. F. and F. Assisi (1972). "The ready isomerization of bilirubin IX- in aqueous solution." Biochem J **129**(3): 797-800.

McDonagh, A. F., L. A. Palma and R. Schmid (1981). "Reduction of biliverdin and placental transfer of bilirubin and biliverdin in the pregnant guinea pig." Biochem J **194**(1): 273-282.

McQuistan, T. J., M. T. Simonich, M. M. Pratt, C. B. Pereira, J. D. Hendricks, R. H. Dashwood, D. E. Williams and G. S. Bailey (2012). "Cancer chemoprevention by dietary chlorophylls: a 12,000-animal dose-dose matrix biomarker and tumor study." Food Chem Toxicol **50**(2): 341-352.

Meshnick, S. R., K. P. Chang and A. Cerami (1977). "Heme lysis of the bloodstream forms of Trypanosoma brucei." Biochem Pharmacol **26**(20): 1923-1928.

Meyer, T. C. (1956). "A study of serum bilirubin levels in relation to kernikterus and prematurity." Arch Dis Child **31**(156): 75-80.

Mohammadi Asl, J., M. A. Tabatabaiefar, H. Galehdari, K. Riahi, M. H. Masbi, Z. Zargar Shoshtari and F. Rahim (2013). "UGT1A1 gene mutation due to Crigler-Najjar syndrome in Iranian patients: identification of a novel mutation." Biomed Res Int **2013**: 342371.

Moscowitz, A., M. Weimer, D. A. Lightner, Z. J. Petryka, E. Davis and C. J. Watson (1971). "The in vitro conversion of bile pigments to the urobilinoids by a rat clostridia species as compared with the human fecal flora. 3. Natural d-urobilin, synthetic i-urobilin, and synthetic i-urobilinogen." Biochem Med **4**(2): 149-164.

Mosmann, T. (1983). "Rapid colorimetric assay for cellular growth and survival: application to proliferation and cytotoxicity assays." J Immunol Methods **65**(1-2): 55-63.

Motterlini, R., J. E. Clark, R. Foresti, P. Sarathchandra, B. E. Mann and C. J. Green (2002). "Carbon monoxide-releasing molecules: characterization of biochemical and vascular activities." Circ Res **90**(2): E17-24.

Motterlini, R. and L. E. Otterbein (2010). "The therapeutic potential of carbon monoxide." Nat Rev Drug Discov **9**(9): 728-743.

Muramoto, T., T. Kohchi, A. Yokota, I. Hwang and H. M. Goodman (1999). "The Arabidopsis photomorphogenic mutant hy1 is deficient in phytochrome chromophore biosynthesis as a result of a mutation in a plastid heme oxygenase." Plant Cell **11**(3): 335-348.

Nakagami, T., K. Toyomura, T. Kinoshita and S. Morisawa (1993). "A beneficial role of bile pigments as an endogenous tissue protector: anti-complement effects of biliverdin and conjugated bilirubin." Biochim Biophys Acta **1158**(2): 189-193.

Nakamura, H., Y. Uetani, M. Komura, S. Takada, K. Sano and T. Matsuo (1987). "Inhibitory action of bilirubin on superoxide production by polymorphonuclear leukocytes." Biol Neonate **52**(5): 273-278.

Nazarewicz, R. R., A. Dikalova, A. Bikineyeva, S. Ivanov, I. A. Kirilyuk, I. A. Grigor'ev and S. I. Dikalov (2013). "Does scavenging of mitochondrial superoxide attenuate cancer prosurvival signaling pathways?" Antioxid Redox Signal **19**(4): 344-349.

Nicholas, R. E. and C. Rimington (1951). "Isolation of unequivocal uroporphyrin III; a further study of turacin." Biochem J **50**(2): 194-201.

Noir, B. A., A. Boveris, A. M. Garaza Pereira and A. O. Stoppani (1972). "Bilirubin: a multi-site inhibitor of mitochondrial respiration." FEBS Lett **27**(2): 270-274.

Nose, K. (2000). "Role of reactive oxygen species in the regulation of physiological functions." Biol Pharm Bull **23**(8): 897-903.

O'Carra, P., R. F. Murphy and S. D. Killilea (1980). "The native forms of the phycobilin chromophores of algal biliproteins. A clarification." Biochem J **187**(2): 303-309.

Odell, G. B. (1959). "Studies in kernicterus. I. The protein binding of bilirubin." J Clin Invest **38**(5): 823-833.

Ollinger, R., P. Kogler, J. Troppmair, M. Hermann, M. Wurm, A. Drasche, I. Konigsrainer, A. Amberger, H. Weiss, D. Ofner, F. H. Bach and R. Margreiter (2007). "Bilirubin inhibits tumor cell growth via activation of ERK." Cell Cycle **6**(24): 3078-3085.

Onishi, S., K. Isobe, S. Itoh, N. Kawade and S. Sugiyama (1980). "Demonstration of a geometric isomer of bilirubin-IX alpha in the serum of a hyperbilirubinaemic newborn infant and the mechanism of jaundice phototherapy." Biochem J **190**(3): 533-536.

Ostrow, J. D., L. Pascolo and C. Tiribelli (2003). "Reassessment of the unbound concentrations of unconjugated bilirubin in relation to neurotoxicity in vitro." Pediatr Res **54**(6): 926.

Otterbein, L. E., F. H. Bach, J. Alam, M. Soares, H. Tao Lu, M. Wysk, R. J. Davis, R. A. Flavell and A. M. Choi (2000). "Carbon monoxide has anti-inflammatory effects involving the mitogen-activated protein kinase pathway." Nat Med **6**(4): 422-428.

Otterbein, L. E. and A. M. Choi (2000). "Heme oxygenase: colors of defense against cellular stress." Am J Physiol Lung Cell Mol Physiol **279**(6): L1029-1037.

Otterbein, L. E., L. L. Mantell and A. M. Choi (1999). "Carbon monoxide provides protection against hyperoxic lung injury." Am J Physiol **276**(4 Pt 1): L688-694.

Otterbein, L. E., B. S. Zuckerbraun, M. Haga, F. Liu, R. Song, A. Usheva, C. Stachulak, N. Bodyak, R. N. Smith, E. Csizmadia, S. Tyagi, Y. Akamatsu, R. J. Flavell, T. R. Billiar, E. Tzeng, F. H. Bach, A. M. Choi and M. P. Soares (2003). "Carbon monoxide suppresses arteriosclerotic lesions associated with chronic graft rejection and with balloon injury." Nat Med **9**(2): 183-190.

Ouhtit, A., M. F. Ismail, A. Othman, A. Fernando, M. E. Abdraboh, A. F. El-Kott, Y. A. Azab, S. H. Abdeen, R. L. Gaur, I. Gupta, S. Shanmuganathan, Y. M. Al-Farsi, H. Al-Riyami and M. H. Raj (2014). "Chemoprevention of rat mammary carcinogenesis by spirulina." Am J Pathol **184**(1): 296-303.

Owens, D. and J. Evans (1975). "Population studies on Gilbert's syndrome." J Med Genet **12**(2): 152-156.

Pandey, N., S. Gupta, R. K. Yadav and K. Sarvottam (2013). "Physiological jaundice: role in oxidative stress." IJCRR **5**(19): 69-80.

Perchellet, J. P., E. M. Perchellet, D. K. Orten and B. A. Schneider (1986). "Decreased ratio of reduced/oxidized glutathione in mouse epidermal cells treated with tumor promoters." Carcinogenesis **7**(3): 503-506.

Peyton, K. J., S. V. Reyna, G. B. Chapman, D. Ensenat, X. M. Liu, H. Wang, A. I. Schafer and W. Durante (2002). "Heme oxygenase-1-derived carbon monoxide is an autocrine inhibitor of vascular smooth muscle cell growth." Blood **99**(12): 4443-4448.

Phelan, D., G. M. Winter, W. J. Rogers, J. C. Lam and M. S. Denison (1998). "Activation of the Ah receptor signal transduction pathway by bilirubin and biliverdin." Archives of Biochemistry and Biophysics **357**(1): 155-163.

Pilz, R. B. and D. E. Casteel (2003). "Regulation of gene expression by cyclic GMP." Circ Res **93**(11): 1034-1046.

Pirone, C., J. M. Quirke, H. A. Priestap and D. W. Lee (2009). "Animal pigment bilirubin discovered in plants." J Am Chem Soc **131**(8): 2830.

Poland, R. L. and G. B. Odell (1971). "Physiologic jaundice: the enterohepatic circulation of bilirubin." N Engl J Med **284**(1): 1-6.

Ponka, P. (1999). "Cell biology of heme." Am J Med Sci **318**(4): 241-256.

Radhakrishnan, N., S. P. Yadav, A. Sachdeva, P. K. Pruthi, S. Sawhney, T. Piplani, T. Wada and A. Yachie (2011). "Human heme oxygenase-1 deficiency presenting with hemolysis, nephritis, and asplenia." J Pediatr Hematol Oncol **33**(1): 74-78.

Radu, P. and J. Atsmon (2001). "Gilbert's syndrome--clinical and pharmacological implications." Isr Med Assoc J **3**(8): 593-598.

Richardson, D. R., D. S. Kalinowski, S. Lau, P. J. Jansson and D. B. Lovejoy (2009). "Cancer cell iron metabolism and the development of potent iron chelators as anti-tumour agents." Biochim Biophys Acta **1790**(7): 702-717.

Rodrigues, C. M., S. Sola, R. E. Castro, P. A. Laires, D. Brites and J. J. Moura (2002). "Perturbation of membrane dynamics in nerve cells as an early event during bilirubin-induced apoptosis." J Lipid Res **43**(6): 885-894.

Rodriguez, M. E., J. Kim, G. B. Delos Santos, K. Azizuddin, J. Berlin, V. E. Anderson, M. E. Kenney and N. L. Oleinick (2010). "Binding to and photo-oxidation of cardiolipin by the phthalocyanine photosensitizer Pc 4." J Biomed Opt **15**(5): 051604.

Rose, C. S., R. A. Jones, L. J. Jenkins, Jr. and J. Siegel (1970). "The acute hyperbaric toxicity of carbon monoxide." Toxicol Appl Pharmacol **17**(3): 752-760.

Rothschild, M. A., A. Bauman, R. S. Yalow and S. A. Berson (1955). "Tissue distribution of I131 labeled human serum albumin following intravenous administration." J Clin Invest **34**(9): 1354-1358.

Ryter, S. W., J. Alam and A. M. Choi (2006). "Heme oxygenase-1/carbon monoxide: from basic science to therapeutic applications." Physiol Rev **86**(2): 583-650.

Ryter, S. W. and R. M. Tyrrell (2000). "The heme synthesis and degradation pathways: role in oxidant sensitivity. Heme oxygenase has both pro- and antioxidant properties." Free Radic Biol Med **28**(2): 289-309.

Sakai, T., K. Watanabe and H. Kawatsu (1987). "Occurrence of ditaurobilirubin, bilirubin conjugated with two moles of taurine, in the gallbladder bile of yellowtail, Seriola quinqueradiata." J Biochem **102**(4): 793-796.

Sampietro, M. and A. Iolascon (1999). "Molecular pathology of Crigler-Najjar type I and II and Gilbert's syndromes." Haematologica **84**(2): 150-157.

Sarkar, D., A. Sharma and G. Talukder (1994). "Chlorophyll and chlorophyllin as modifiers of genotoxic effects." Mutat Res **318**(3): 239-247.

Sato, K., J. Balla, L. Otterbein, R. N. Smith, S. Brouard, Y. Lin, E. Csizmadia, J. Sevigny, S. C. Robson, G. Vercellotti, A. M. Choi, F. H. Bach and M. P. Soares (2001). "Carbon monoxide generated by heme oxygenase-1 suppresses the rejection of mouse-to-rat cardiac transplants." J Immunol **166**(6): 4185-4194.

Sedlak, T. W., M. Saleh, D. S. Higginson, B. D. Paul, K. R. Juluri and S. H. Snyder (2009). "Bilirubin and glutathione have complementary antioxidant and cytoprotective roles." Proc Natl Acad Sci U S A **106**(13): 5171-5176.

Shapiro, S. M. (2005). "Definition of the clinical spectrum of kernicterus and bilirubin-induced neurologic dysfunction (BIND)." J Perinatol **25**(1): 54-59.

Schlieman, M. G., B. N. Fahy, R. Ramsamooj, L. Beckett and R. J. Bold (2003). "Incidence, mechanism and prognostic value of activated AKT in pancreas cancer." Br J Cancer **89**(11): 2110-2115.

Schluchter, W. M. and A. N. Glazer (1997). "Characterization of cyanobacterial biliverdin reductase. Conversion of biliverdin to bilirubin is important for normal phycobiliprotein biosynthesis." J Biol Chem **272**(21): 13562-13569.

Schmitt, T. H., W. A. Frezzatti, Jr. and S. Schreier (1993). "Hemin-induced lipid membrane disorder and increased permeability: a molecular model for the mechanism of cell lysis." Arch Biochem Biophys **307**(1): 96-103.

Sieg, A., L. Arab, G. Schlierf, A. Stiehl and B. Kommerell (1987). "[Prevalence of Gilbert's syndrome in Germany]." Dtsch Med Wochenschr **112**(31-32): 1206-1208.

Sinal, C. J. and J. R. Bend (1997). "Aryl hydrocarbon receptor-dependent induction of cyp1a1 by bilirubin in mouse hepatoma hepa 1c1c7 cells." Mol Pharmacol **52**(4): 590-599.

Sirota, L., R. Straussberg, N. Gurary, D. Aloni and H. Bessler (1999). "Phototherapy for neonatal hyperbilirubinemia affects cytokine production by peripheral blood mononuclear cells." Eur J Pediatr **158**(11): 910-913.

Sticova, E. and M. Jirsa (2013). "New insights in bilirubin metabolism and their clinical implications." World J Gastroenterol **19**(38): 6398-6407.

Stocker, R., Y. Yamamoto, A. F. McDonagh, A. N. Glazer and B. N. Ames (1987). "Bilirubin is an antioxidant of possible physiological importance." Science **235**(4792): 1043-1046.

Telezhkin, V., S. P. Brazier, S. Cayzac, C. T. Müller, D. Riccardi and P. J. Kemp (2009). Hydrogen Sulfide Inhibits Human BKCa Channels. Arterial Chemoreceptors. C. Gonzalez, C. Nurse and C. Peers, Springer Netherlands. **648:** 65-72.

Terry, M. J. (2002). Biosynthesis and Analysis of Bilins. Heme, Chlorophyll, and Bilins: Methods and Protocols. M. W. Alison G. Smith**:** 273-291.

Terry, M. J., M. D. Maines and J. C. Lagarias (1993). "Inactivation of phytochrome- and phycobiliprotein-chromophore precursors by rat liver biliverdin reductase." J Biol Chem **268**(35): 26099-26106.

Teufelhofer, O., W. Parzefall, E. Kainzbauer, F. Ferk, C. Freiler, S. Knasmuller, L. Elbling, R. Thurman and R. Schulte-Hermann (2005). "Superoxide generation from Kupffer cells contributes to hepatocarcinogenesis: studies on NADPH oxidase knockout mice." Carcinogenesis **26**(2): 319-329.

Townsend, C. L. and R. L. Maynard (2002). "Effects on health of prolonged exposure to low concentrations of carbon monoxide." Occup Environ Med **59**(10): 708-711.

Tukey, R. H. and C. P. Strassburg (2000). "Human UDP-glucuronosyltransferases: metabolism, expression, and disease." Annu Rev Pharmacol Toxicol **40**: 581-616.

Ulstrom, R. A. and E. Eisenklam (1964). "The enterohepatic shunting of bilirubin in the newborn infant. I. Use of oral activated charcoal to reduce normal serum bilirubin values." J Pediatr **65**: 27-37.

Valko, M., D. Leibfritz, J. Moncol, M. T. Cronin, M. Mazur and J. Telser (2007). "Free radicals and antioxidants in normal physiological functions and human disease." Int J Biochem Cell Biol **39**(1): 44-84.

van de Steeg, E., V. Stranecky, H. Hartmannova, L. Noskova, M. Hrebicek, E. Wagenaar, A. van Esch, D. R. de Waart, R. P. Oude Elferink, K. E. Kenworthy, E. Sticova, M. al-Edreesi, A. S. Knisely, S. Kmoch, M. Jirsa and A. H. Schinkel (2012). "Complete OATP1B1 and OATP1B3 deficiency causes human Rotor syndrome by interrupting conjugated bilirubin reuptake into the liver." J Clin Invest **122**(2): 519-528.

Van Praagh, R. (1961). "Diagnosis of kernicterus in the neonatal period." Pediatrics **28**(6): 870-876.

Vitek, L. (2012). "The role of bilirubin in diabetes, metabolic syndrome, and cardiovascular diseases." Front Pharmacol **3**: 55.

Vitek, L., P. Kotal, M. Jirsa, J. Malina, M. Cerna, D. Chmelar and J. Fevery (2000). "Intestinal colonization leading to fecal urobilinoid excretion may play a role in the pathogenesis of neonatal jaundice." J Pediatr Gastroenterol Nutr **30**(3): 294-298.

Vitek, L., F. Majer, L. Muchova, J. Zelenka, A. Jiraskova, P. Branny, J. Malina and K. Ubik (2006). "Identification of bilirubin reduction products formed by Clostridium perfringens isolated from human neonatal fecal flora." J Chromatogr B Analyt Technol Biomed Life Sci **833**(2): 149-157.

Vitek, L. and J. D. Ostrow (2009). "Bilirubin chemistry and metabolism; harmful and protective aspects." Curr Pharm Des **15**(25): 2869-2883.

Vitek, L. and H. A. Schwertner (2007). "The heme catabolic pathway and its protective effects on oxidative stress-mediated diseases." Adv Clin Chem **43**: 1-57.

Wagener, F. A., H. D. Volk, D. Willis, N. G. Abraham, M. P. Soares, G. J. Adema and C. G. Figdor (2003). "Different faces of the heme-heme oxygenase system in inflammation." Pharmacol Rev **55**(3): 551-571.

Wang, R. (2002). "Two's company, three's a crowd: can H2S be the third endogenous gaseous transmitter?" The FASEB Journal **16**(13): 1792-1798.

Warren, M. J. and A. I. Scott (1990). "Tetrapyrrole assembly and modification into the ligands of biologically functional cofactors." Trends Biochem Sci **15**(12): 486-491.

Watchko, J. F. and M. J. Maisels (2003). "Jaundice in low birthweight infants: pathobiology and outcome." Arch Dis Child Fetal Neonatal Ed **88**(6): F455-458.

Watson, C. J. (1953). "The direct preparation of crystalline urobilin from bilirubin." J Biol Chem **200**(2): 691-696.

Wegiel, B. and L. E. Otterbein (2012). "Go green: the anti-inflammatory effects of biliverdin reductase." Front Pharmacol **3**: 47.

Willoughby, D. A., A. R. Moore, P. R. Colville-Nash and D. Gilroy (2000). "Resolution of inflammation." Int J Immunopharmacol **22**(12): 1131-1135.

Xiong, T., J. Tang and D. Z. Mu (2012). "[Side effects of phototherapy for neonatal hyperbilirubinemia]." Zhongguo Dang Dai Er Ke Za Zhi **14**(5): 396-400.

Xu, Y. Q. and Z. K. Ding (2003). "Biliverdin reductase from the liver of Atlantic salmon (Salmo salar)." Biochemistry (Mosc) **68**(6): 639-643.

Yamaguchi, T., Y. Komoda and H. Nakajima (1994). "Biliverdin-IX alpha reductase and biliverdin-IX beta reductase from human liver. Purification and characterization." J Biol Chem **269**(39): 24343-24348.

Yamaguchi, T. and H. Nakajima (1995). "Changes in the composition of bilirubin-IX isomers during human prenatal development." Eur J Biochem **233**(2): 467-472.

Yang, L., S. Quan and N. G. Abraham (1999). "Retrovirus-mediated HO gene transfer into endothelial cells protects against oxidant-induced injury." Am J Physiol **277**(1 Pt 1): L127-133.

Zelenka, J., M. Lenicek, L. Muchova, M. Jirsa, M. Kudla, P. Balaz, M. Zadinova, J. D. Ostrow, R. J. Wong and L. Vitek (2008). "Highly sensitive method for quantitative determination of bilirubin in biological fluids and tissues." J Chromatogr B Analyt Technol Biomed Life Sci **867**(1): 37-42.

Zhao, R., G. Y. Xu, Z. Z. Liu, J. Y. Li and N. Yang (2006). "A study on eggshell pigmentation: biliverdin in blue-shelled chickens." Poult Sci **85**(3): 546-549.

Zheng, J., T. Inoguchi, S. Sasaki, Y. Maeda, M. F. McCarty, M. Fujii, N. Ikeda, K. Kobayashi, N. Sonoda and R. Takayanagi (2013). "Phycocyanin and phycocyanobilin from Spirulina platensis protect against diabetic nephropathy by inhibiting oxidative stress." Am J Physiol Regul Integr Comp Physiol **304**(2): R110-120.

Zheng, J., D. A. Nagda, S. A. Lajud, S. Kumar, A. Mouchli, O. Bezpalko, B. W. O'Malley, Jr. and D. Li (2014). "Biliverdin's regulation of reactive oxygen species signalling leads to potent inhibition of proliferative and angiogenic pathways in head and neck cancer." Br J Cancer.

Zou, C., H. Zhang, Q. Li, H. Xiao, L. Yu, S. Ke, L. Zhou, W. Liu, W. Wang, H. Huang, N. Ma, Q. Liu, X. Wang, W. Zhao, H. Zhou and X. Gao (2011). "Heme oxygenase-1: a molecular brake on hepatocellular carcinoma cell migration." Carcinogenesis **32**(12): 1840-1848.

Zucker, S. D., P. S. Horn and K. E. Sherman (2004). "Serum bilirubin levels in the U.S. population: gender effect and inverse correlation with colorectal cancer." Hepatology **40**(4): 827-835.

Zuckerbraun, B. S., T. R. Billiar, S. L. Otterbein, P. K. Kim, F. Liu, A. M. Choi, F. H. Bach and L. E. Otterbein (2003). "Carbon monoxide protects against liver failure through nitric oxide-induced heme oxygenase 1." J Exp Med **198**(11): 1707-1716.